R-07-27

Sensitivity analysis and development of calibration methodology for near-surface hydrogeology model of Forsmark

Maria Aneljung, Lars-Göran Gustafsson
DHI Water & Environment AB

April 2007

Svensk Kärnbränslehantering AB
Swedish Nuclear Fuel
and Waste Management Co
Box 5864
SE-102 40 Stockholm Sweden
Tel 08-459 84 00
+46 8 459 84 00
Fax 08-661 57 19
+46 8 661 57 19

ISSN 1402-3091
SKB Rapport R-07-27

Sensitivity analysis and development of calibration methodology for near-surface hydrogeology model of Forsmark

Maria Aneljung, Lars-Göran Gustafsson
DHI Water & Environment AB

April 2007

Summary

The hydrological modelling system MIKE SHE has been used to describe near-surface groundwater flow, transport mechanisms and the contact between ground- and surface water at the Forsmark site. The surface water system at Forsmark is described with the 1D modelling tool MIKE 11, which is fully and dynamically integrated with MIKE SHE. In spring 2007, a new data freeze will be available and a process of updating, rebuilding and calibrating the MIKE SHE model will start, based on the latest data set. Prior to this, it is important to gather as much knowledge as possible on calibration methods and to define critical calibration parameters and areas within the model.

In this project, an optimization of the numerical description and an initial calibration of the MIKE SHE model described in /Bosson and Berglund 2006/ has been made, and an updated base case has been defined. Data from 5 surface water level monitoring stations, 4 surface water discharge monitoring stations and 32 groundwater level monitoring stations (SFM soil boreholes) has been used for model calibration and evaluation.

The base case simulations generally show a good agreement between calculated and measured water levels and discharges, indicating that the total runoff from the area is well described by the model. Moreover, with two exceptions (SFM0012 and SFM0022) the base case results show very good agreement between calculated and measured groundwater head elevations for boreholes installed below lakes. The model also shows a reasonably good agreement between calculated and measured groundwater head elevations or depths to phreatic surfaces in many other points. The following major types of calculation-measurement differences can be noted:

- Differences in groundwater level amplitudes due to transpiration processes.
- Differences in absolute mean groundwater head, due to differences between borehole casing levels and the interpolated DEM.
- Differences in absolute mean head elevations, due to local errors in hydraulic conductivity values.
- Differences in the aquifer refilling process subsequent to dry periods, for example a too slow refill when the groundwater table rises after dry summers. This may be due to local deviations in the applied pF-curves in the unsaturated zone description.
- Differences in near-surface groundwater elevations. For example, the calculated groundwater level reaches the ground surface during the fall and spring at locations where the measured groundwater depth is just below the ground surface. This may be due to the presence of near-surface high-conductive layers.

A sensitivity analysis has been made on calibration parameters. For parameters that have “global” effects, such as the hydraulic conductivity in the saturated zone, the analysis was performed using the “full” model. For parameters with more local effects, such as parameters influencing the evapotranspiration and the net recharge, the model was scaled down to a column model, representing two different type areas.

The most important conclusions that can be drawn from the sensitivity analysis are the following:

- The results indicate that the horizontal hydraulic conductivity generally should be increased at topographic highs, and reduced at local depressions in the topography.
- The results indicate that no changes should be made to the vertical hydraulic conductivity at locations where the horizontal conductivity has been increased, and that the vertical conductivity generally should be decreased where the horizontal conductivity has been decreased.

- The vegetation parameters that have the largest infuence on the total groundwater recharge are the root mass distribution and the crop coefficient.
- The unsaturated zone parameter that have the largest influence on the total groundwater recharge is the effective porosity given in the pF-curve. In addition, the shape of the pF-curve above the water content at field capacity is also of great importance.
- The general conclusion is that the surrounding conditions have large effects on water-flow conditions near the ground surface, for instance if a borehole is located to a groundwater recharge- or discharge area. For example, SFM0017 is located near Lake Eckarfjärden, which is a groundwater discharge area. Hence, this borehole has a large catchment area. On the other hand, SFM0010 is installed at a topographic high in the upstream part of the model area. Therefore, it is to a larger extent affected by local conditions around the borehole.
- The bottom boundary condition has a small influence on the conditions at individual boreholes, since local conditions determine the extents of groundwater recharge and discharge areas at Forsmark.

Based on the results and the findings of the base case simulations and the sensitivity analysis, a method is suggested to perform future model calibrations.

Sammanfattning

Modellsystemet MIKE SHE har använts för att beräkna och beskriva den ytnära hydrologin i Forsmark. Ytvattensystemen har beskrivits i det endimensionella verktyget MIKE 11 vilket är helt integrerat med grundvattenmodellen i MIKE SHE. Under år 2007 kommer en ny ”datafrys” att levereras, varefter SKB påbörjar arbetet med att uppdatera och kalibrera den existerande grundvattenmodellen. Innan kalibreringsarbetet med nya data påbörjas är det önskvärt att samla så mycket kunskap som möjligt kring kalibreringsmetodik och att definiera kritiska modellparametrar och områden inom modellavgränsningen.

I detta projekt har MIKE SHE-modellen beskriven i /Bosson och Berglund 2006/ bearbetats. Den numeriska modellen har optimerats och en inledande kalibrering har genomförts. Ett basfall (”base case”) har definierats och utvärderats. Data från fem ytvattennivåstationer, fyra flödesstationer och 32 grundvattenrör har använts i kalibreringen och utvärderingen av modellen.

Basfallsberäkningarna visade en generellt god överensstämmelse mellan beräknade och uppmätta vattennivåer och flöden och den totala avrinningen från modellområdet beskrivs väl i modellen. Resultaten visade även att grundvattenrör under sjöarna i området generellt har en mycket god överensstämmelse mellan beräknade och uppmätta grundvattentryck. Modellen visade också en relativt god överensstämmelse mellan beräknade och uppmätta grundvattentryck eller djup till grundvattenytan i många övriga punkter. Ett antal olika typer av avvikelser i grundvattenobservationerna kunde konstateras:

- Avvikelser i amplitud beroende på avdunstningsprocesser.
- Avvikelser i medelnivå beroende på avvikelser mellan nivå på borrhål och den interpolerade modelltopografin.
- Avvikelser i medelnivå på grund av lokala avvikelser i hydrauliska konduktiviteter.
- Avvikelser i uppfyllnadsprocessen i akvifären efter torrperioder, exempelvis en alltför långsam stigning av grundvattentrycken efter torra somrar. Detta kan möjligen bero på lokala avvikelser i pF-kurvans utseende i den omättade zonen.
- Avvikelser i de ytnära grundvattennivåerna vilket resulterar exempelvis i grundvatten ovanför marknivån i vissa punkter. Detta kan vara orsakat av ett ytnära högkonduktivt lager som inte är beskrivet i modellen.

En känslighetsanalys har även genomförts på parametrar som är aktuella i ett kalibreringsskede. För de parametrar som har en global effekt, såsom hydrauliska konduktiviteter i den mättade zonen, har simuleringarna genomförts i fullskalemodellen. För parametrar som påverkar mer lokalt, såsom avdunstningsparametrar och parametrar för den omättade zonen, har den fulla modellen skalats ner till en encells kolonnmodell över två olika typområden.

De viktigaste resultaten från känslighetsanalysen listas nedan:

- Resultaten visar att den horisontella konduktiviteten i den mättade zonen generellt bör höjas vid höjder i topografin och minskas i svackor.
- Resultaten indikerar också att inga ändringar bör göras för den vertikala konduktiviteten i de fall där den horisontella konduktiviteten har höjts. Där den horisontella konduktiviteten har minskats ger det däremot en positiv effekt att även minska den vertikala konduktiviteten.
- De vegetationsparametrar som påverkar infiltrationen till grundvatten i störst utsträckning är fördelningen av växternas rotmassa (A_{root}) och den så kallade ”crop coefficient” som direkt påverkar den potentiella avdunstningen.

- De parametrar för den omättade zonen som påverkar infiltrationen till grundvatten i störst utsträckning är den effektiva porositeten, som anges i pF-kurvan. pF-kurvans form vid högre vatteninnehåll än vid fältkapaciteten är också av stor betydelse.
- En generell slutsats från känslighetsanalysen är att de omgivande tryckförhållandena i området i stor utsträckning påverkar de lokala förhållandena, dvs. om ett borrhål ligger i ett generellt in- eller utströmningsområde. Exempelvis borrhål SFM0017 ligger i ett utströmningsområde nära Eckarfjärden och påverkas i hög grad av omgivande tryckförhållanden och är därmed relativt okänsligt för lokala parametrar. SFM0010 ligger däremot på en höjd och påverkas i betydligt större grad av lokala parametrar.
- De regionala tryckförhållandena från det djupare berget och modellens tryckförhållande i bottenranden har visat sig ha mycket liten effekt på de lokala tryckförhållandena inom modellområdet. Istället är förhållanden inom modellens eget avrinningsområde som påverkar in- och utströmningsförhållandena i området.

En metodik för kalibrering av framtida modellversioner har sammanställts baserat på resultaten från basfallssimuleringarna och känslighetsanalysen.

Contents

1 Introduction

SKB performs site investigations and risk analyses for localisation of a deep repository for high level radioactive waste. The site investigations are performed at two sites: Forsmark in the municipality of Östhammar and Simpevarp in the municipality of Oskarshamn. The hydrological modelling system MIKE SHE is used to describe near-surface groundwater flow, transport mechanisms and the contact between ground- and surface water at both sites. The surface water systems are described with the one-dimensional modelling tool MIKE 11, which is fully and dynamically integrated with MIKE SHE.

For the Forsmark site, MIKE SHE is used to describe the near-surface hydrology in a regional catchment. The model area is 37.6 km^2 and covers the main parts of the regional model area that has been defined for the land part of the area. Previous MIKE SHE models of Forsmark have not been calibrated or otherwise compared with site specific measurements, mainly due to lack of measurements and continuous data series.

The present MIKE SHE model for Forsmark is based on the data freeze Forsmark 1.2 (dated 31st of July 2004). In spring 2007, a new data freeze will be available and a process of updating, rebuilding and calibrating the MIKE SHE model based on these new data will start. Prior to this step, it is important to gather as much knowledge as possible on calibration methods, and to define critical calibration parameters and areas within the model.

The main purposes of the project presented in this report are to:

- make a systematic comparison between model results and site specific data,
- calibrate the model against site specific data and describe a calibration methodology to be used in coming model versions,
- make a sensitivity analysis on critical parameters.

2 The MIKE SHE modelling tool

The modelling tool used in the analysis is MIKE SHE, developed by DHI (Danish Hydraulic Institute). MIKE SHE is a dynamic, physically based, modelling tool that describes the main processes in the land phase of the hydrological cycle.

2.1 Overview of the modelling tool

The precipitation can either be intercepted by leaves or fall to the ground. The water on the ground surface can infiltrate, evaporate or form overland flow. Once the water has infiltrated the soil, it enters the unsaturated zone. In the unsaturated zone, it can either be extracted by roots and leave the system as transpiration, or it can percolate down to the saturated zone. MIKE SHE is fully integrated with a channel-flow code, MIKE 11. The exchange of water between the two modelling tools takes place during the whole simulation, i.e. the two programs run simultaneously.

MIKE SHE is developed primarily for modelling of groundwater flow in porous media. However, in the present modelling the bedrock is also included. The bedrock is parameterised by use of data from the Forsmark 1.2 groundwater flow model developed using the DarcyTools code /SKB 2004/. In DarcyTools, a discrete fracture network (DFN) is used as a basis for

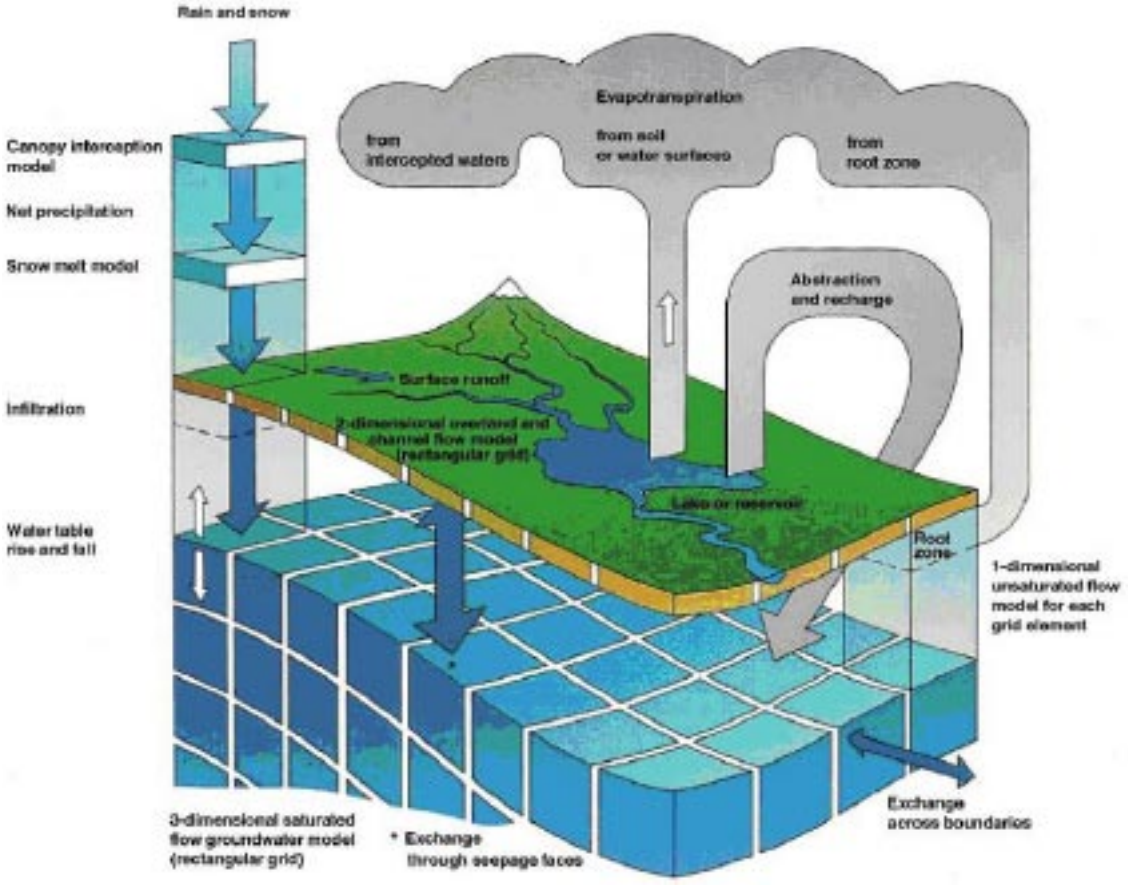

Figure 2-1. *Overview of the model structure and the processes included in MIKE SHE /DHI 2007/.*

generating hydrogeological properties for a continuum model /Svensson et al. 2004/. Thus, hydrogeological parameters can be imported directly to the corresponding elements in the MIKE SHE model.

MIKE SHE consists of the following model components:

- Precipitation (rain or snow).
- Evapotranspiration, including canopy interception, which is calculated according to the principles of /Kristensen and Jensen 1975/.
- Overland flow, which is calculated with a 2D finite difference diffusive wave approximation of the Saint-Venant equations, using the same 2D mesh as the groundwater component. Overland flow interacts with rivers, the unsaturated zone, and the saturated (groundwater) zone.
- Channel flow, which is described through the river modelling component, MIKE 11, which is a modelling system for river hydraulics. MIKE 11 is a dynamic, 1D modelling tool for the design, management and operation of river and channel systems. MIKE 11 supports any level of complexity and offers simulation tools that cover the entire range from simple Muskingum routing to high-order dynamic wave formulations of the Saint-Venant equations.
- Unsaturated water flow, which in MIKE SHE is described as a vertical soil profile model that interacts with both the overland flow (through ponding) and the groundwater model (the groundwater table is the lower boundary condition for the unsaturated zone). MIKE SHE offers three different modelling approaches, including a simple 2-layer root-zone mass balance approach, a gravity flow model, and a full Richards's equation model.
- Saturated (groundwater) flow, which allows for 3D flow in a heterogeneous aquifer, with conditions shifting between unconfined and confined. The spatial and temporal variations of the dependent variable (the hydraulic head) are described mathematically by the 3D Darcy equation and solved numerically by an iterative implicit finite difference technique.

For a detailed description of the processes included in MIKE SHE and MIKE 11, see /Werner et al. 2005/ and /DHI 2007/.

2.2 Modification of the code in release 2007

The code used in this project is software release version 2007. In this version, the communication between the river network in MIKE 11 and the overland component in MIKE SHE has been improved. Instead of communication using so called flood codes, where water levels from MIKE 11 are transferred to MIKE SHE, the two-way communication is described with a so called overbank spilling option.

If flooding is allowed via overbank spilling, river water is allowed to spill onto the MIKE SHE model as overland flow. The overbank spilling option treats the river bank as a weir. When the overland flow water level or the river water level is above the left or right bank elevation, water will spill across the bank based on the weir formula:

$$Q = \Delta x \cdot C \cdot (H_{us} - H_w)^k \cdot \left[1 - \left(\frac{H_{ds} - H_w}{H_{us} - H_w}\right)^k\right]^{0.385}$$

where Q is the flow across the weir, Δx is the cell width, C is the weir coefficient, H_{us} and H_{ds} refer to the height of water on the upstream and downstream side of the weir, respectively, H_w is the height of the weir, and k is a head exponent.

If water levels are such that water is flowing to the river, overland flow to the river is added to MIKE 11 as lateral inflow. If the water level in the river is higher than the level of ponded water, river water will spill onto the MIKE SHE cell and become part of the overland flow. If the

upstream water depth over the weir approaches zero, the flow over the weir becomes undefined. Therefore, the calculated flow is reduced to zero linearly when the upstream height goes below a threshold.

The communication between the river network and the groundwater aquifer is calculated in the same way as for previous versions of the code. The exchange flow between a saturated zone grid cell and a river link is calculated as a conductance multiplied by the head difference between the river and the grid cell. The conductance between the grid cell and the river link depends on the conductivity of both the river bed and the aquifer material /DHI 2007/.

3 Input data changes compared to Forsmark 1.2

The input data to the MIKE SHE model include data on topography, land use, geology, hydrogeology and meteorology. Most of the input data used for the present modelling are described in /Bosson and Berglund 2006/, such as topography and lake bathymetries, geological layers and lenses, hydraulic properties of the geological units and calculation layers. Data types that are changed compared to /Bosson and Berglund 2006/ are listed in chapter 3.1 to 3.4.

3.1 Meteorology

The MIKE SHE modelling uses data on temperature, precipitation and potential evapotranspiration. Data are available between 1st of May 2003 to 31st of July 2005. The meteorological input data are taken from two local meteorological stations, Högmasten and Storskäret, see Figure 3-1.

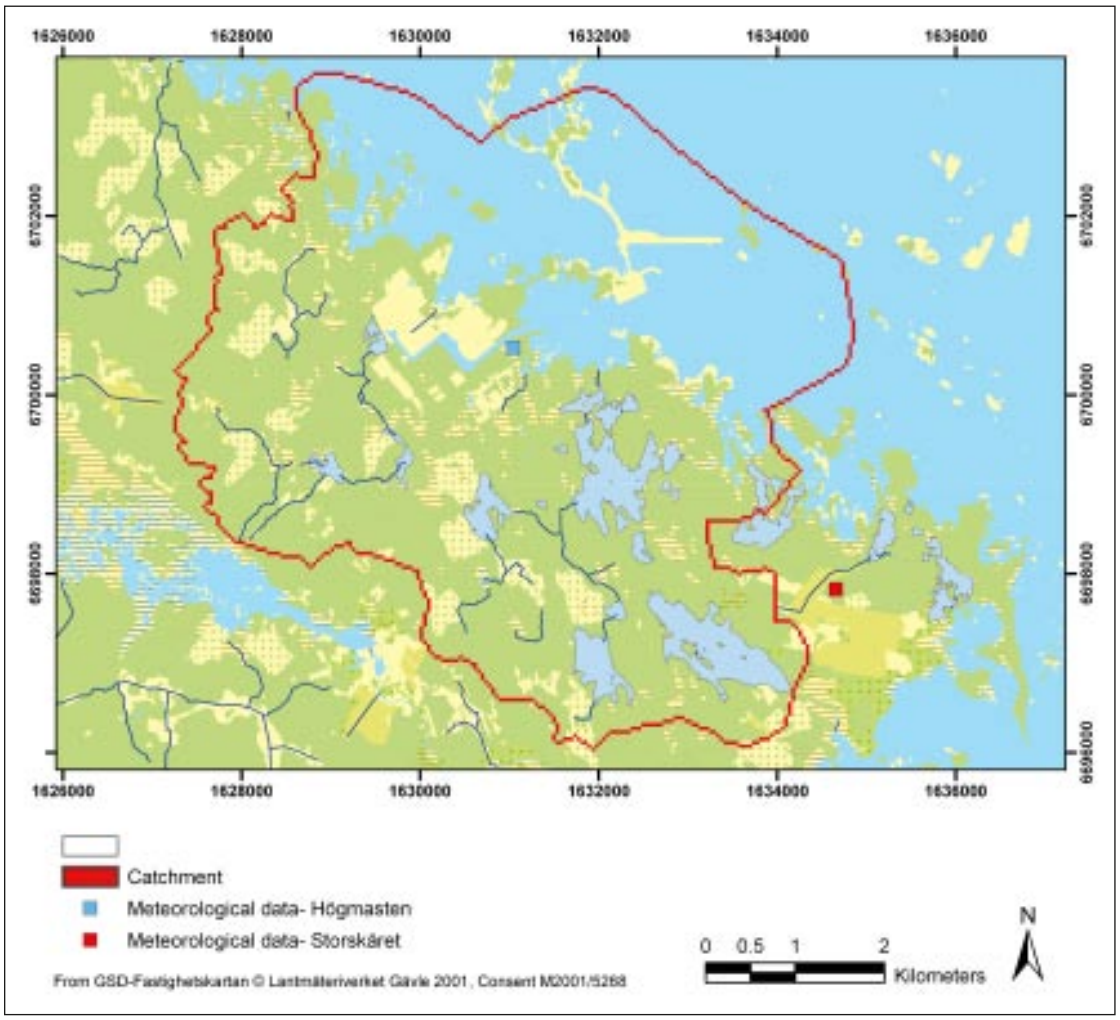

Figure 3-1. *Position of the two meteorological stations at Högmasten and Storskäret. The red line indicates the boundary of the model area.*

The precipitation is described as net precipitation including snow melt, and is calculated as a mean value of the two meteorological stations. When data are missing from one station, they are replaced by data from the other. When data are missing for both stations, multiple regression analysis on overlapping data periods with the meteorological stations at Lövsta, Örskär and Östhammar has been used to calculate a theoretical precipitation for the area.

The corrected raw precipitation data have been combined with results from an air-temperature dependent snow routine. The content of the snow storage melts at a rate defined by the degree-day coefficient, multiplied with the uncorrected temperature from the meteorological stations. The degree-day coefficient has been calibrated against measurements of snow cover and is set to 1.23 mm/day/°C /Juston et al. 2006/. The result is a daily time series of estimated site-average ground surface inflow, see Figure 3-2.

The potential evapotranspiration was calculated with the Penman-equation according to /Eriksson 1981/ using data from the local station Högmasten. An error was discovered in the potential evapotranspiration time series calculated by SMHI, resulting in an overestimation of the actual values (P-O Johansson, personal communication). Due to the errors in the calculated data series, the potential evapotranspiration was as an approximation reduced with 10%, see Figure 3-3.

The temperature input to MIKE SHE is used to calculate the effect of snow melt and snow cover. When applying the site-average ground surface inflow as net precipitation input to the model, the snow melt is included in the input data. The measured temperature has therefore only been used when calculating the applied ground surface inflow.

The total net precipitation for the simulation period, 15th of May 2003 – 31st of July 2005, is 1,275 mm, and the potential evapotranspiration 1,178 mm. Table 3-1 shows the annual values for May 2003–May 2004 and May 2004–May 2005.

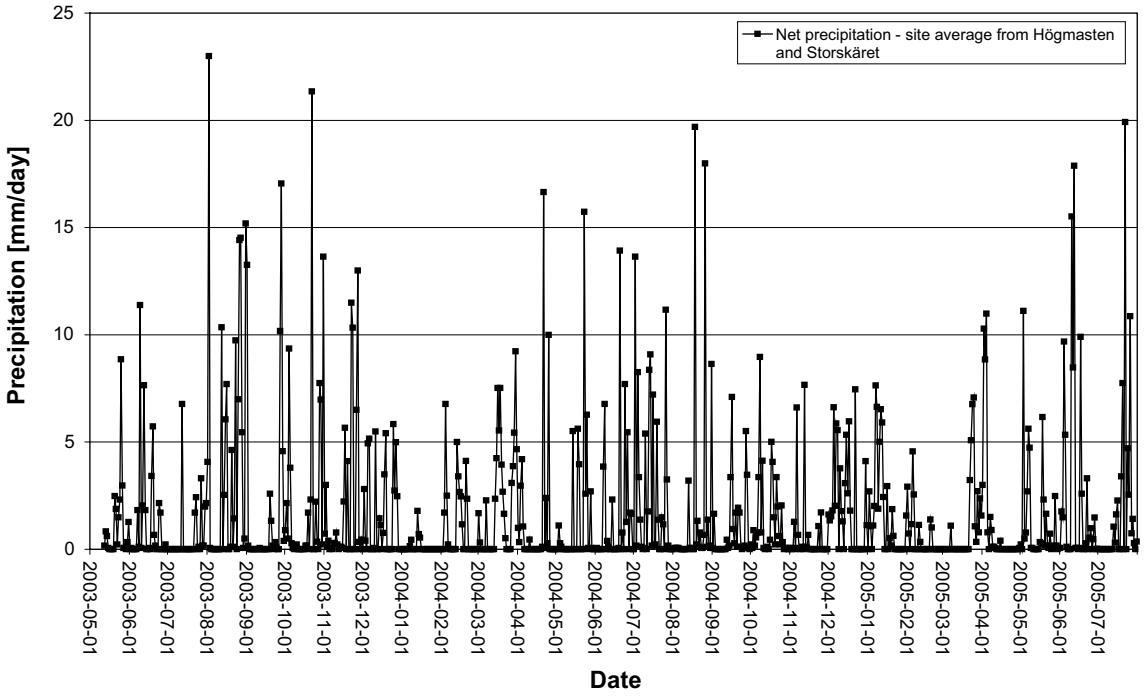

Figure 3-2. *Site average net precipitation including snow melt.*

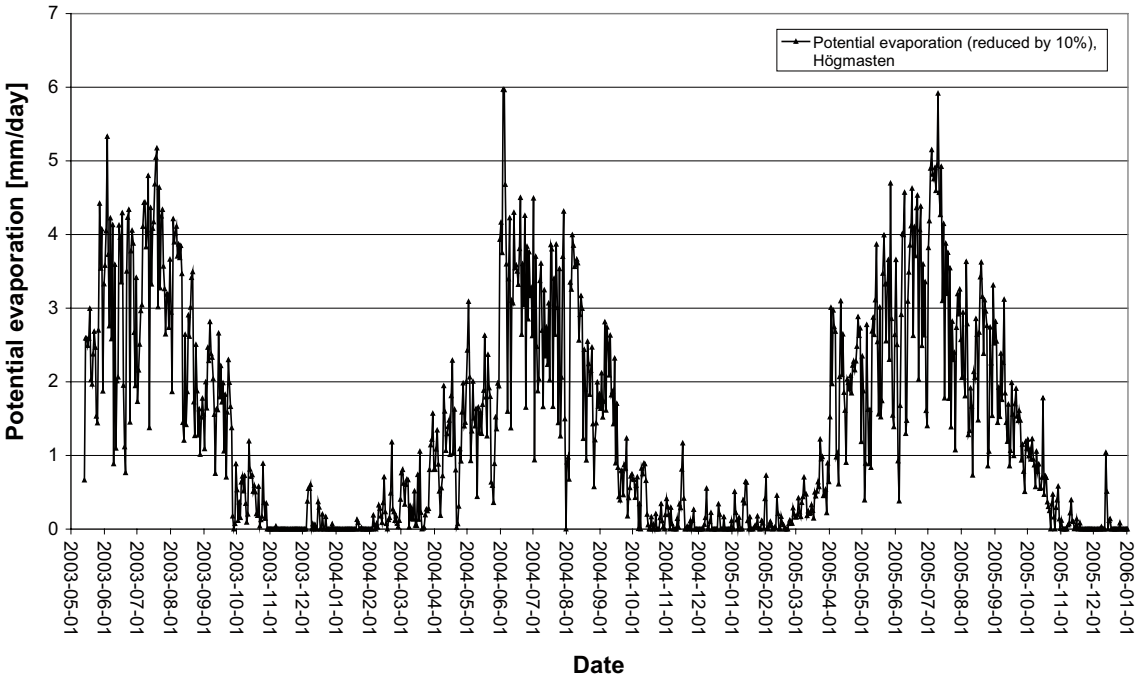

Figure 3-3. *Potential evapotranspiration from the local station at Högmasten.*

Table 3-1. Annual net precipitation and potential evapotranspiration.

Period	Net precipitation (mm)	Potential evapo-transpiration (mm)
May 2003–April 2004	587	472
May 2004–April 2005	536	457

3.2 Unsaturated zone

Coarse till is the dominating type of Quaternary deposits in the area, and accordingly also in the unsaturated zone description. Figure 3-4 shows the distribution of Quaternary deposits in the unsaturated zone, as described in the Forsmark 1.2 model /Bosson and Berglund 2006/.

Field studies indicate that the coarse till in the area has different properties at different depths /Lundin et al. 2005/. The uppermost 50 cm of the soil profile has a higher total porosity, but also a lower capacity of retaining water than the underlying soil (i.e. a higher specific yield). The variations of pF-curves used in the model update are based on local knowledge of the area (P-O Johansson, personal communication). The uppermost 50 cm of the coarse till applied in the model has a total porosity of 0.38, and a hydraulic conductivity at full saturation of $3 \cdot 10^{-5}$ m/s. The relation between the moisture potential, pF, and the moisture content is shown in Figure 3-5.

In the model description, the underlying 0.5 to 2 m below ground surface has a total porosity of 0.22 and a hydraulic conductivity of $1.5 \cdot 10^{-6}$ m/s. The air entry level is at 30 cm (corresponding to pF 1.5). The relation between the moisture potential, pF, and moisture content is shown in Figure 3-6.

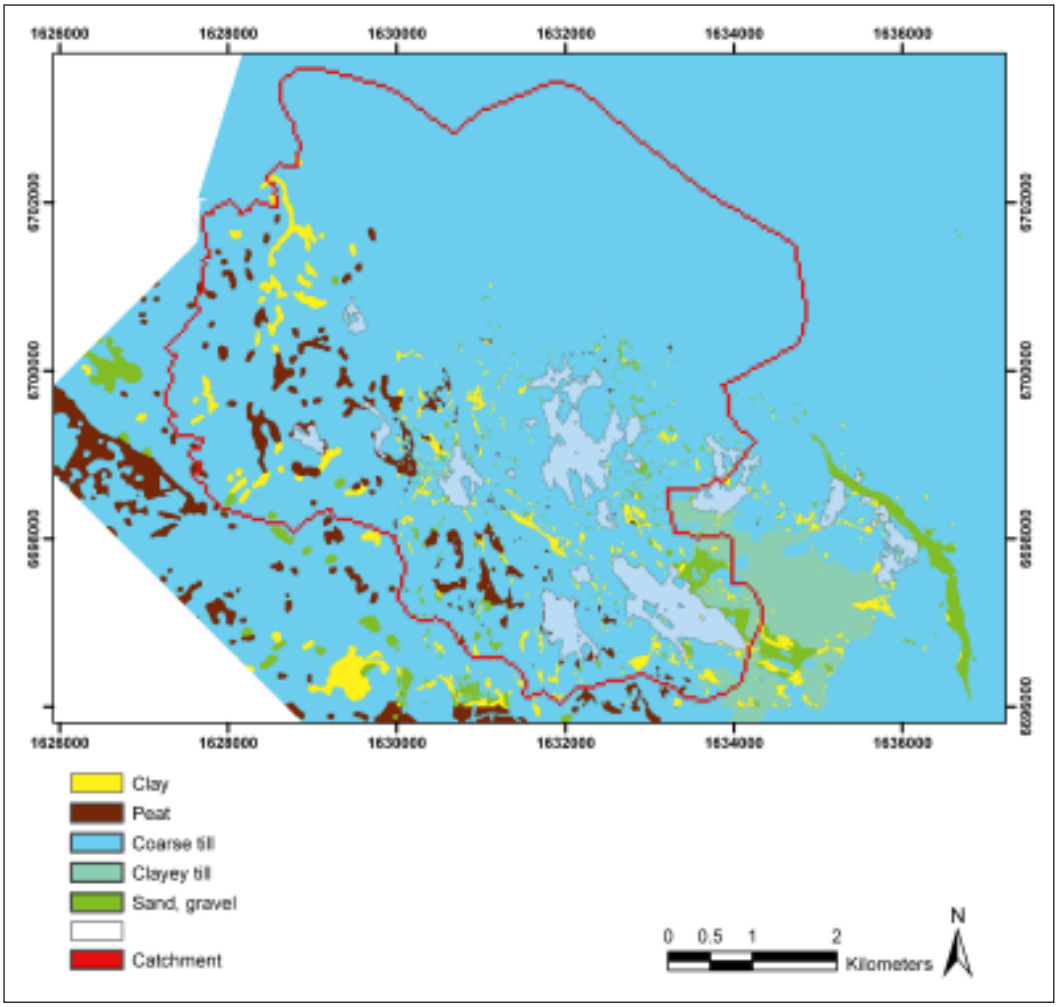

Figure 3-4. *Distribution of Quaternary deposits in the model. The red line indicates the boundary of the model area.*

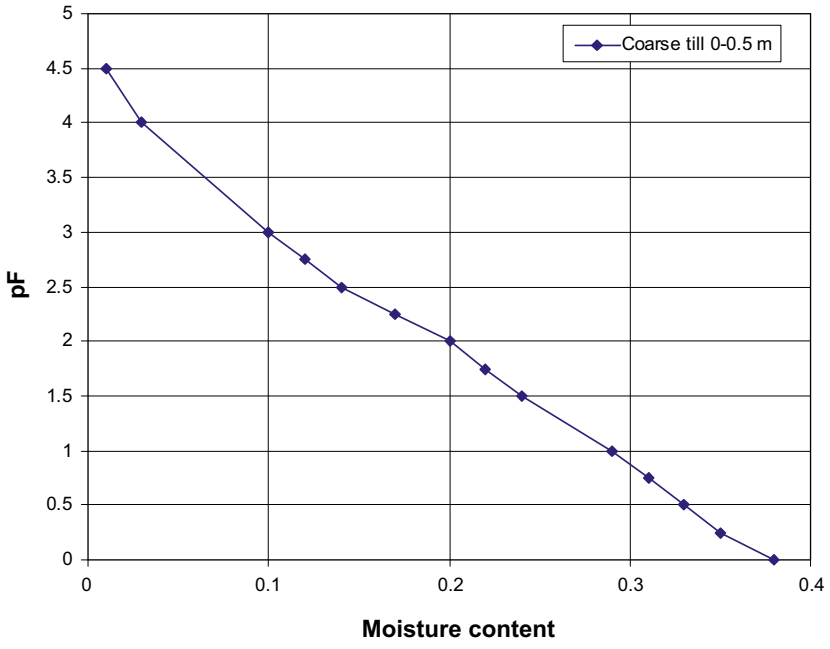

Figure 3-5. *Relation between moisture potential, pF, and moisture content for the uppermost 50 cm of a coarse till soil profile.*

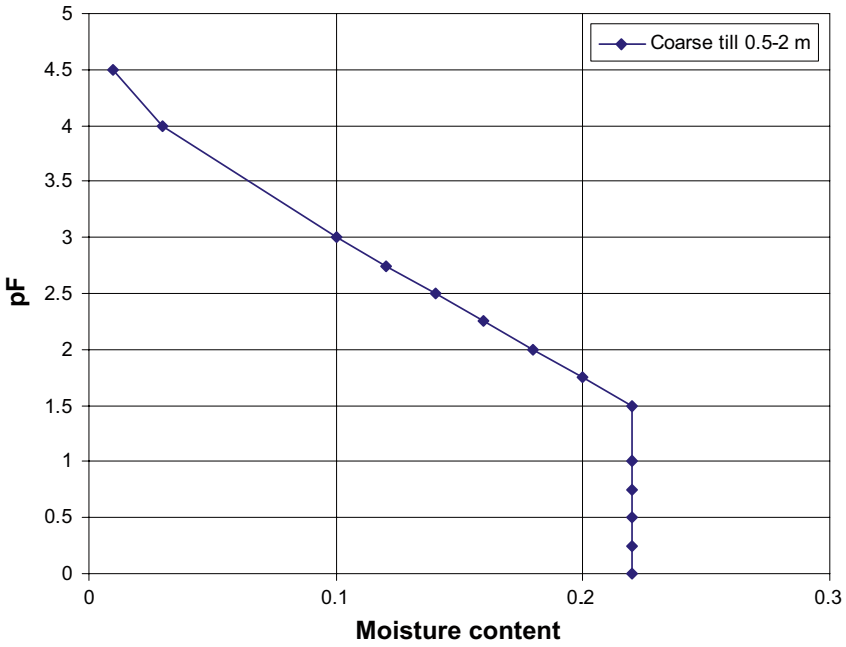

Figure 3-6. *Relation between moisture potential, pF, and moisture content for coarse till 50 to 200 cm below the surface.*

The description of the fine till included in the soil profile under the Quaternary deposits type clayey till is also described with an air entry level at 30 cm (corresponding to pF 1.5). The total porosity is 0.275 and the saturated hydraulic conductivity is $1.5 \cdot 10^{-7}$ m/s. The relation between the moisture potential, pF, and the moisture content is shown in Figure 3-7.

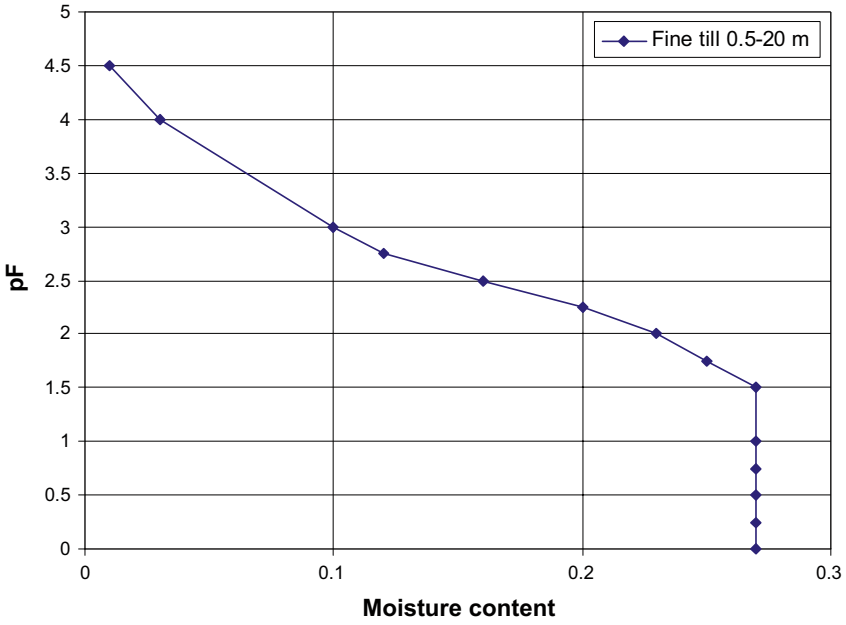

Figure 3-7. *Relation between moisture potential, pF, and moisture content for fine till 0.5 to 20 m below the surface for the Quaternary deposit clayey till.*

3.3 Stream and lake data

Data on lake thresholds and bathymetry levels from the data freeze 1.2 have been used to update the description of the surface water system in MIKE 11. Figure 3-8 shows the positions and ID codes of the lakes in the area, whereas Table 3-2 shows data on lake thresholds and bottom elevations, obtained from the SICADA database.

Table 3-2. Data on lakes in the area.

ID code	Name	Mean water level (m.a.s.l., metres above sea level)	Maximum depth (m)	Mean depth (m)	Threshold elevation (m.a.s.l., metres above sea level)
AFM000010	Eckarfjärden	5.37	2.12	0.91	5.15
AFM000048	Labboträsket	3.56	1.07	0.27	2.65
AFM000049	Lillfjärden	–0.07	0.89	0.29	–0.35
AFM000050	Bolundsfjärden	0.64	1.81	0.61	0.28
AFM000051	Fiskarfjärden	0.54	1.86	0.37	0.28
AFM000052	Bredviken	–0.12	1.72	0.74	–0.26
AFM000073	Gunnarsbo – Lillfjärden (south)	1.60	2.22	0.70	1.92
AFM000074	Norra Bassängen	0.56	0.88	0.31	0.19
AFM000081	Märrbadet	0.00	1.01	0.36	–0.29
AFM000084	Simpviken	–0.29	1.81	0.54	–0.32
AFM000086	Tallsundet	0.13	0.80	0.23	–0.23
AFM000087	Graven	0.65	0.35	0.12	0.44
AFM000088	Fräkengropen	1.35	0.79	0.19	
AFM000089	Vambörsfjärden	1.14	0.98	0.43	1.02
AFM000090	Stocksjön	2.92	0.82	0.22	2.70
AFM000091	Puttan	0.63	1.29	0.37	0.48
AFM000093	Kungsträsket	2.60	0.54	0.20	2.31
AFM000094	Gällsboträsket	1.91	1.51	0.17	1.47
AFM000095	Gunnarsboträsket	5.81	1.29	0.51	5.68
AFM000096	Gunnarsbo – Lillfjärden (north)	1.64	0.90	0.30	1.07

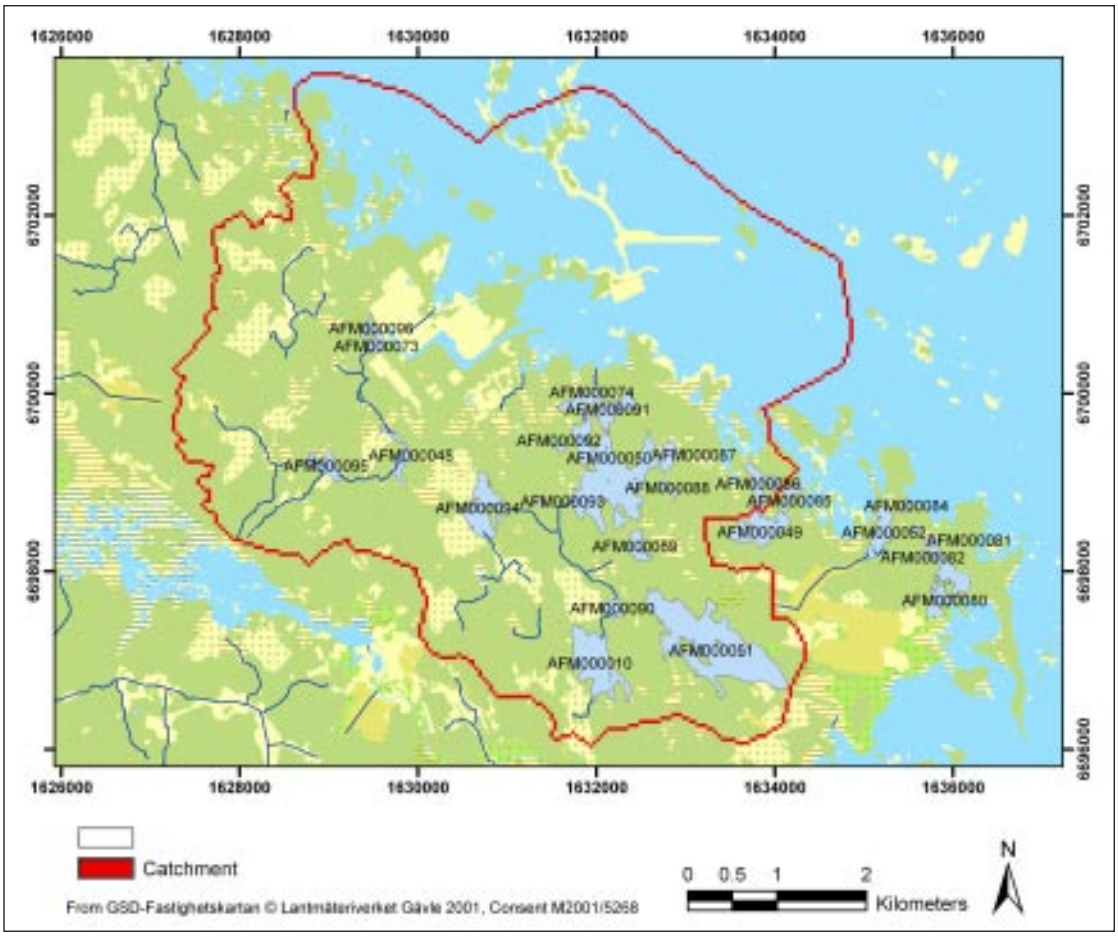

Figure 3-8. *Positions and ID codes of lakes in the Forsmark area. The red line indicates the boundary of the model area.*

3.4 Calibration data

Data from 5 surface water level monitoring stations, 4 surface water discharge monitoring stations and 32 groundwater level monitoring stations (SFM soil boreholes) have been used for model calibration and evaluation. The observations are mainly located within the candidate area, with no or only a few points in the north-western part of the model catchment.

Groundwater measurements in the bedrock are in general too disturbed by drilling to be useful as calibration data, and are therefore not used in this project. Figure 3-9 shows positions of the different monitoring data observations within the model area. Although it can not be seen in Figure 3-9, lakes contain observation points for both lake water levels and groundwater levels below the lakes.

Figure 3-9. *Positions of monitoring points used for model calibration. In the lakes, both surface water levels and groundwater levels are measured. The surface water monitoring stations are located at the same locations as some SFM boreholes and are therefore not visible in the figure. The red line indicates the boundary of the model area.*

4 Initial calibration to define a base case

As mentioned previously, the current modelling is based on the MIKE SHE version 1.2 "Open repository", described in /Bosson and Berglund 2006/. The model area is 37.6 km^2 and covers the main parts of the regional model area that has been defined for the land part of the area, see Figure 3-1. The horizontal model resolution is 40 m. The simulation period is 2003-05-15 to 2005-07-31. The simulations use a so called hot start, which constitutes the initial conditions for the base case. Hot start data are stored monthly, and data from 2005-05-04 were used as initial conditions for the base case and sensitivity simulations described in chapters 4–6.

4.1 Updates of the numerical description

A number of updates have been made to the model in order to improve the numerical solution, the overland solver stability and the temporal discretization of the model. The results of the optimizations of time steps and model control parameters are shown in Table 4-1. In time step optimization, a reasonable compromise between actual simulation times and numerical stability must be reached. A background concerning time steps of different model components and model control parameters is given in /DHI 2007/.

Table 4-1. Time steps and model control parameters. OL = overland flow, SZ = saturated zone, UZ = unsaturated zone, and ET = evapotranspiration.

Parameter	Value
Initial timestep	1 h
Maximum allowed OL, UZ, ET time step	2 h
Maximum allowed SZ timestep	6 h
MIKE 11 time step	10 s
Maximum allowed OL iterations	50
OL iteration stop criteria	1e-5
Water depth threshold for OL	0.001 m
Maximum profile water balance error, UZ/SZ coupling	0.001 m
Maximum allowed UZ iterations	50
Iteration stop criteria	0.002
Timestep reduction control: Maximum water balance error in one node (fraction)	0.03
Maximum allowed SZ iterations	80
Maximum head change per SZ iteration	0.05 m
Maximum SZ residual error	0.005 m/d
Saturated thickness threshold	0.05 m

The communication between the stream network in MIKE 11 and the overland component in MIKE SHE has been a source of numerical instability in previous model versions; this instability also increases computation times. When updating the numerical description of the model, the flood code communication between MIKE 11 and the overland component in MIKE SHE was changed to the so called overbank spilling option described above (see section 2.2). The result is a considerably more stable overland solution in MIKE SHE.

In order to reduce computational times, the number of computational layers in the Quaternary deposits was reduced from three to two layers. The top layer follows the lowest layers of the lake sediments and the sea bottom where such are present; elsewhere the layer thickness is set to 2 m. The second calculation layer in the Quaternary deposits follows the geological layer Z3, see /Bosson and Berglund 2006/. The calculation layers were originally defined to obtain a fine description of the lake sediments. The minimum thickness of each calculation layer was set to 1 m, which resulted in calculation layer 1 being 1 m for most of the area. Increasing the thickness to 2 m, the transpiration processes are allowed to be active deeper in the soil profile. Underneath lakes with lake sediments, the transpiration process is generally not active and the changes in calculation layers have little or no effect. Changing the vertical computational layers, the hydraulic properties for each layer are recalculated as an arithmetic mean value with respect to the thickness of each geological unit that is a part of the calculation layer. It should be noted that the geological layers and units are not changed compared to the original input data.

Figures 4-1 and 4-2 shows the effect of reducing the number of calculation layers in a lake borehole (SFM0015) and a borehole located on a hilltop in the model topography (SFM0010). It is notable that there are only minor changes in the calculated head elevation in SFM0015 underneath Lake Eckarfjärden, but considerable differences between the results for SFM0010, which is located on a hilltop. The reduction of calculation layers generally showed better agreement between calculated and observed data (lake boreholes are not affected), and also a more realistic variation of head elevations. This is mainly due to transpiration processes being active at larger depths.

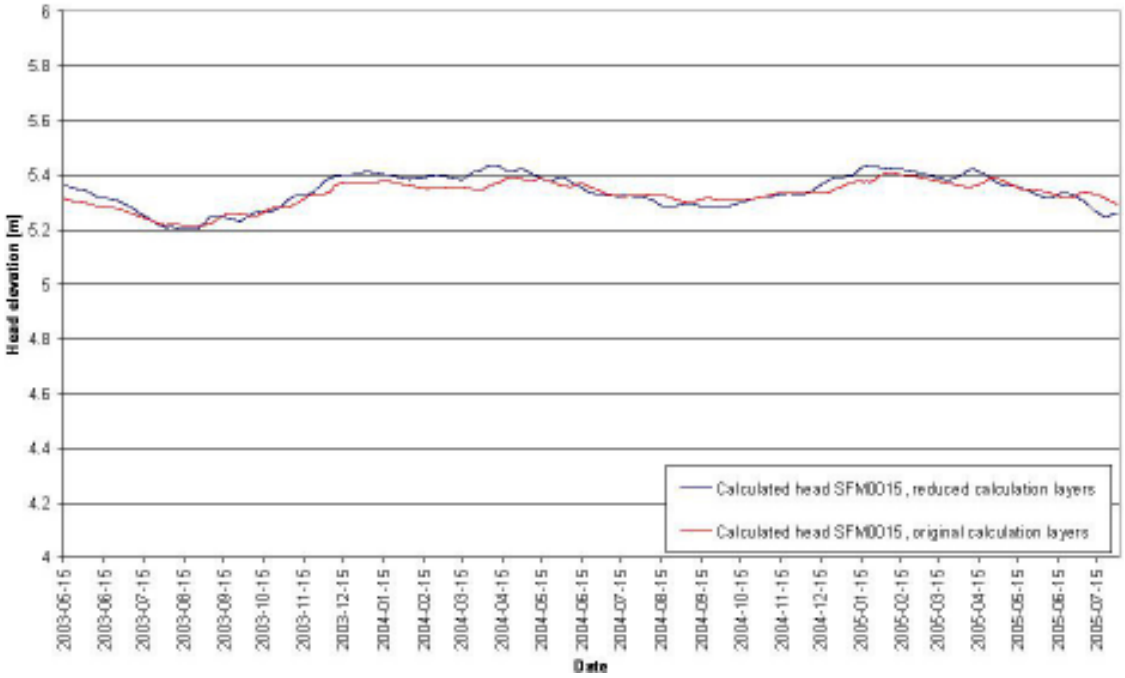

Figure 4-1. *Comparison of the effect of reducing the number of soil calculation layers at a lake borehole, SFM0015.*

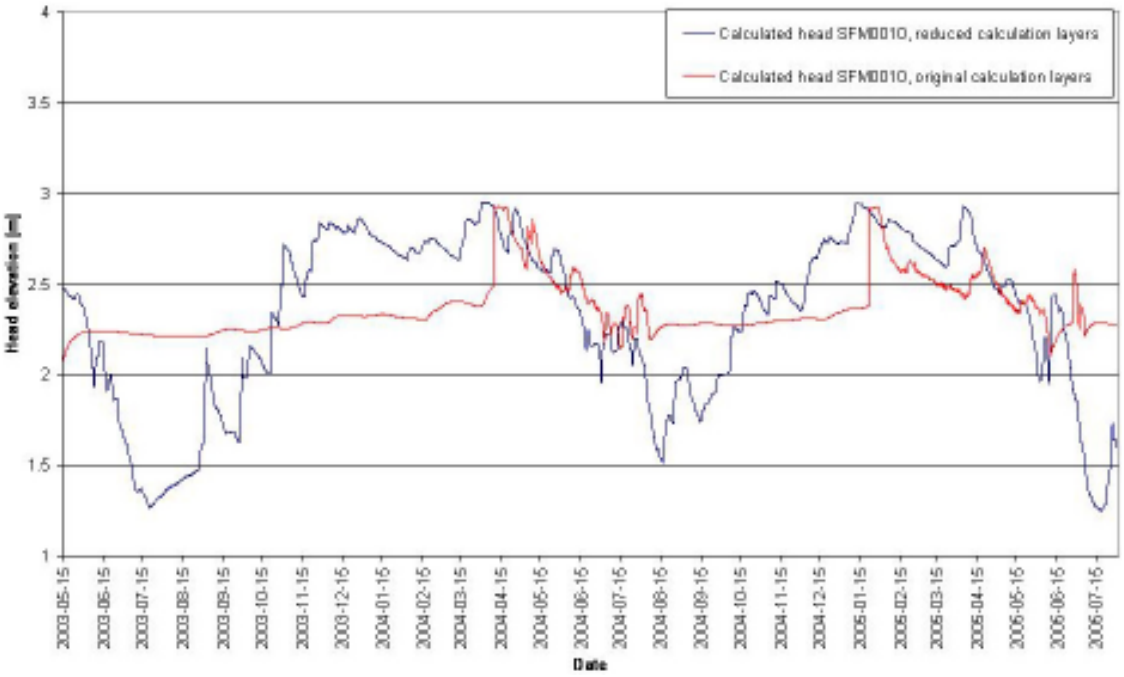

Figure 4-2. *Comparison of the effect of reducing the number of soil calculation layers at a hilltop borehole, SFM0010.*

4.2 Initial calibration

An initial calibration of model parameters and model input was made in order to define a base case for the area. As described in the following, the calibration involved a number of steps. Initial simulations showed a lack of runoff from the overland component to the surface water system, specifically during snowmelt events. A comparison between measured and calculated snow cover data also indicated that the air temperature data that were used not properly could resolve snow melt runoff in the model. To correct this, the MIKE SHE snow melt routine was turned off, and the precipitation data were replaced with a daily time series of estimated site-average ground surface inflow, as described in section 3.1.

The initial simulations also pointed out parts of the model area with obvious input data errors. In particular, updates were made concerning lake thresholds, bank levels and seabed elevations in the MIKE 11 stream network model (see Table 3-2). Moreover, it was observed that boreholes located close to the sea were affected by the internal boundary condition in the sea, where a fixed head of 0 metre above sea level was defined in the Forsmark 1.2 model. This resulted in very small amplitudes of the groundwater head variations in the vicinity of the sea. The fixed head boundary condition in the internal sea boundary in the uppermost MIKE SHE calculation layer and in MIKE 11 was therefore replaced with measured time-varying sea water levels, measured at station PFM010038. Remaining boundary conditions have not been changed compared to Forsmark 1.2; the bottom boundary condition is a fixed head elevation with input from the regional DarcyTools model /Bosson and Berglund 2006/. The horizontal boundaries are set as no-flow boundaries. The exception is at the boundary in the sea, where a fixed head of 0 metre above sea level is applied in and below layer 2.

The Manning number in MIKE 11 has been roughly calibrated against measured data for a part of the system upstream of Lake Bolundsfjärden. The Manning number was calibrated to be as low as 3 $m^{1/3}/s$ in the upper parts of branch Fm_2_9_10, downstream of Lake Eckarfjärden. For the remaining branches in MIKE 11, the calibrated Manning number of 3 $m^{1/3}/s$ resulted in too high water levels. Therefore, a Manning number of 10 $m^{1/3}/s$ was used for the remaining branches. The leakage coefficient in MIKE 11, which affects the conductance used in calculation of the flow exchange between the stream network and the saturated zone, is set to a high value ($1 \cdot 10^{-5}$ m/s). Thus, the leakage coefficient is not limiting the contact between groundwater and surface water.

The overland Manning number in MIKE SHE was decreased from 10 $m^{1/3}/s$ to 5 $m^{1/3}/s$, which is regarded to be more realistic. Figure 4-3 shows the effect of reducing the Manning number on the discharge at PFM005764. In the larger time scale, the effect is negligible, but peak values are slightly lower using the updated Manning number.

With respect to the access to more detailed data on the coarse and fine till description in the unsaturated zone, the pF-curves and hydraulic conductivities have been changed compared to the Forsmark 1.2 modelling. Moreover, the properties for the uppermost 50 cm of the till soil profiles have also been altered (see section 3.2).

The simulation time for the base case was totally c. 10 hours. The most time consuming components in the model are the overland flow (nearly 4.5 hours), the MIKE 11 river network (just over 3 hours), and the saturated zone (c. 2.5 hours).

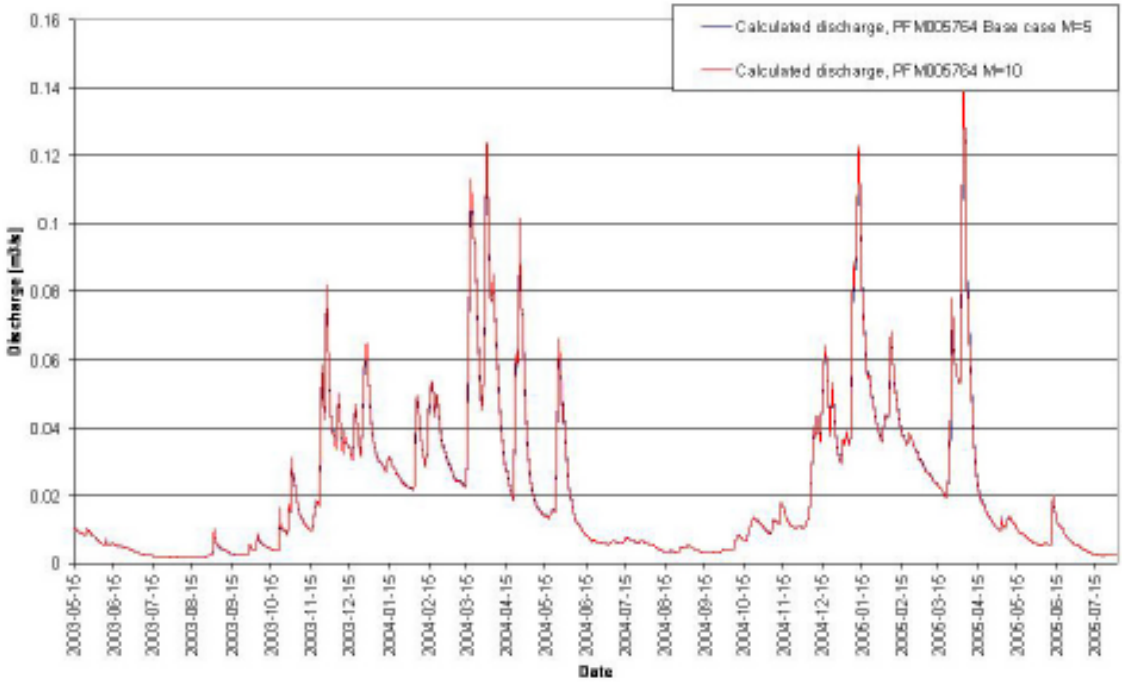

Figure 4-3. *Comparison of calculated discharge at PFM005764, located upstream of Bolundsfjärden, using overland Manning numbers equal to 10 $m^{1/3}/s$ and 5 $m^{1/3}/s$.*

4.3 Summary of model updates compared to Forsmark 1.2

The updates of the model compared to the previous model version 1.2 “Open repository”, as described in chapters 2.2, 3 and 4.1–4.2 can be summarized as follows:

Updates of the numerical model:

- Optimization of time steps and model control parameters.
- New model code for the coupling between the stream network in MIKE 11 and the overland component in MIKE SHE.
- Reduction in computational layers, now using 2 computational soil layers instead of 3.

Updates to physical model parameters:

- Updates in meteorological input data, using net precipitation including snowmelt; the snow melt routine in MIKE SHE was deactivated.
- Updates of the physical description of the stream network and lakes, including lake thresholds, bottom levels, and Manning numbers.
- Reduction of the Manning number in the overland component.
- Updates of the unsaturated zone description of coarse and fine till, including revised pF-curves and hydraulic conductivities.

5 Base case results

In this chapter, base case results are presented in terms of groundwater recharge and discharge areas, comparison between measured and calculated head elevations at a number of observation points, and total water balance over the land part of the model domain.

5.1 Groundwater recharge and discharge areas

The model results show discharge areas in and around the lakes and the sea. Figure 5-1 shows the difference between the calculated groundwater level and head elevations in calculation layer 7, indicating the strength of recharge and discharge areas during winter (2003-12-31). As can be seen in this figure, discharge areas are during winter mainly found around the lakes in the area. A comparison between groundwater levels and head elevations in bedrock layer 7 (located c. 30–40 m below sea level) gives indications of regional-scale recharge-discharge patterns, whereas a comparison between groundwater levels and head elevations closer to the ground surface would show near-surface recharge-discharge patterns.

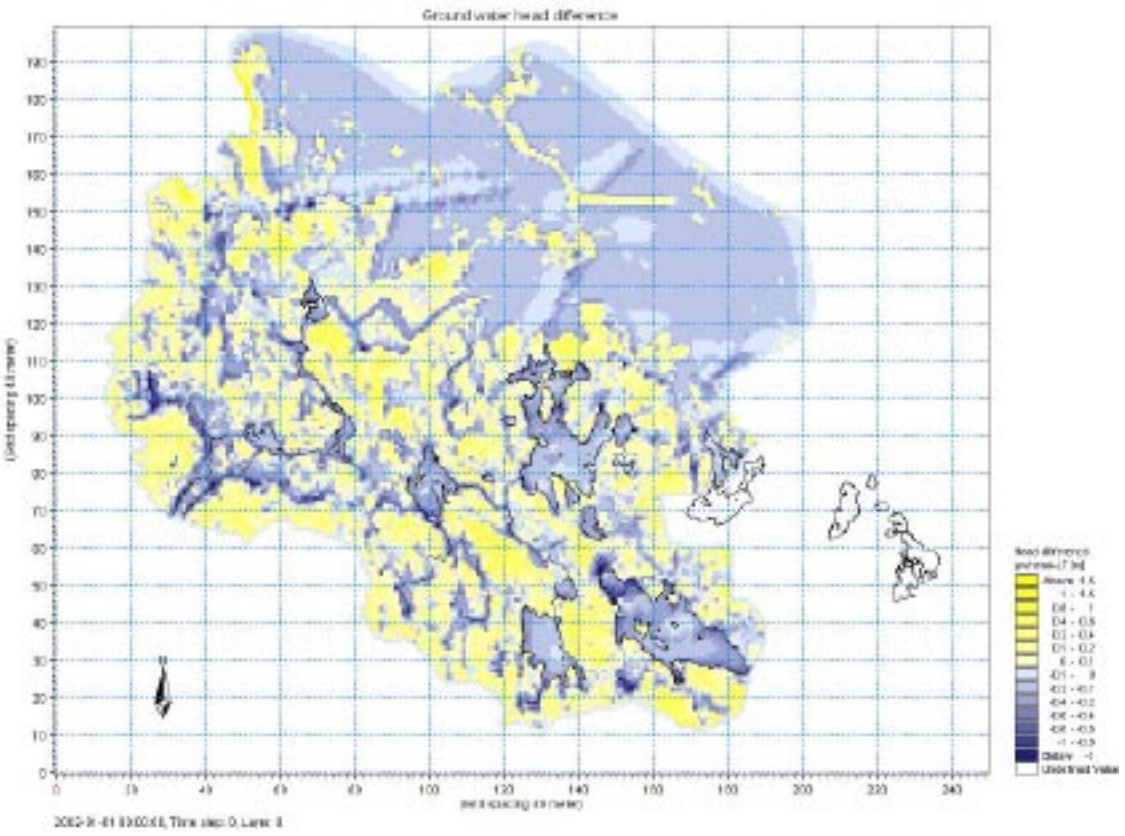

Figure 5-1. *Recharge and discharge areas during winter (2003-12-31). Yellow colours show the strength of recharge areas, and the light to dark blue the strength of discharge areas.*

Figure 5-2 shows the difference between calculated groundwater level and head elevations in calculation layer 7, indicating the strength of recharge and discharge areas during summer (2004-08-02). The summer period is characterized by weaker recharge areas and larger discharge areas.

Around the shorelines, the conditions can vary between weak recharge and discharge areas. For instance, in SFM0016, located just north of Eckarfjärden, there is a discharge area during summer and a recharge area during fall and winter.

The dry summer of 2003 yielded an exceptional decrease in head in the upper soil layers, which is observed in both measured and calculated head data. Figure 5-3 shows a comparison between head elevations in the uppermost soil layer L1, the first bedrock layer L3, in layer L7 and the second lowest bedrock layer, L9. The figure shows the variation of recharge and discharge conditions during the simulation period. In layer L1, the head elevation reaches the ground surface, resulting in a straight line during the fall and spring. Figures 5-4 and 5-5 show corresponding head elevations and temporal variations in recharge/discharge conditions for SFM0010 and SFM0030.

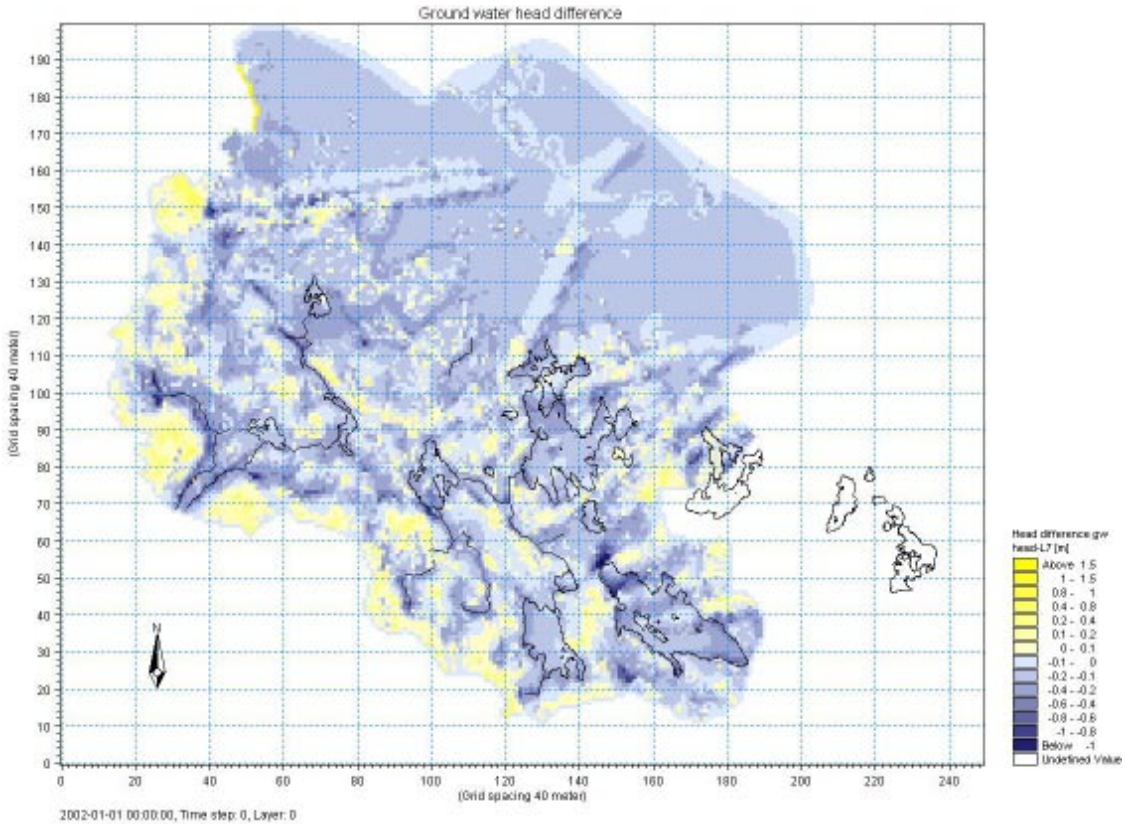

Figure 5-2. *Recharge and discharge areas during summer (2004-08-02). Yellow colours show the strength of recharge areas, and light to dark blue the strength of discharge areas.*

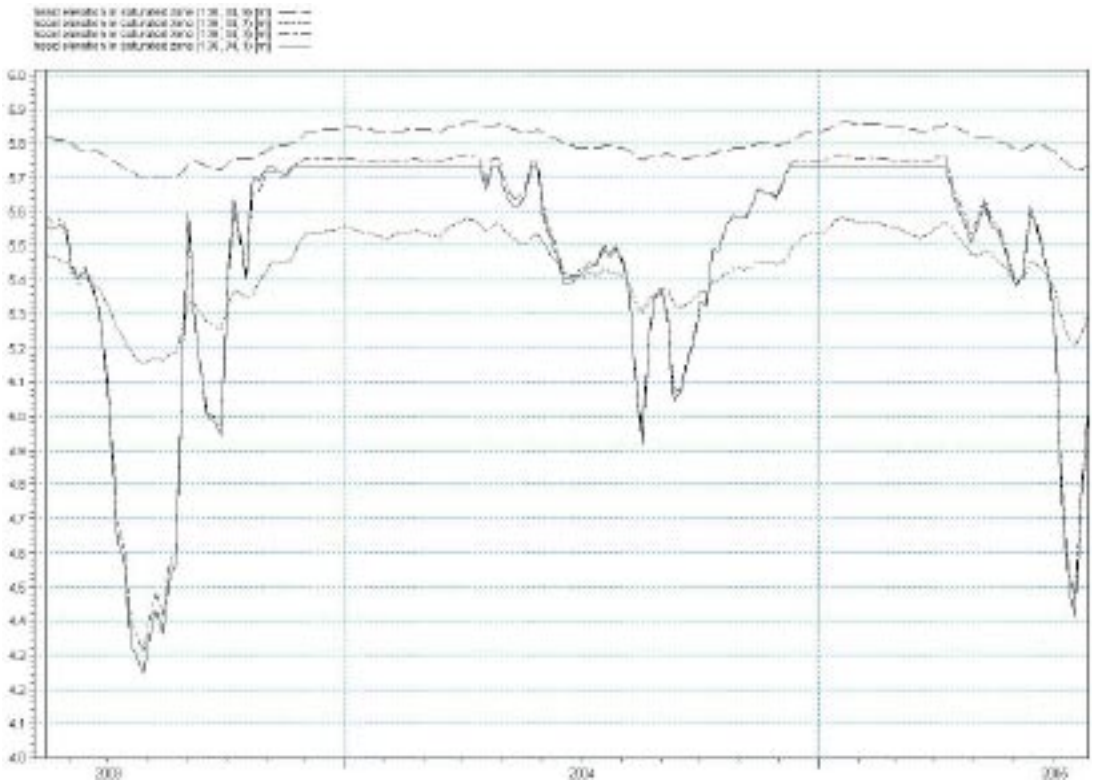

Figure 5-3. *Calculated head elevations in calculation layers L1 (marked with a solid line), L3 (marked with a dash-dot line), L7 (marked with a dot line) and L9 (marked with a dashed line) at SFM0016, located close to the northern shore of Lake Eckarfjärden.*

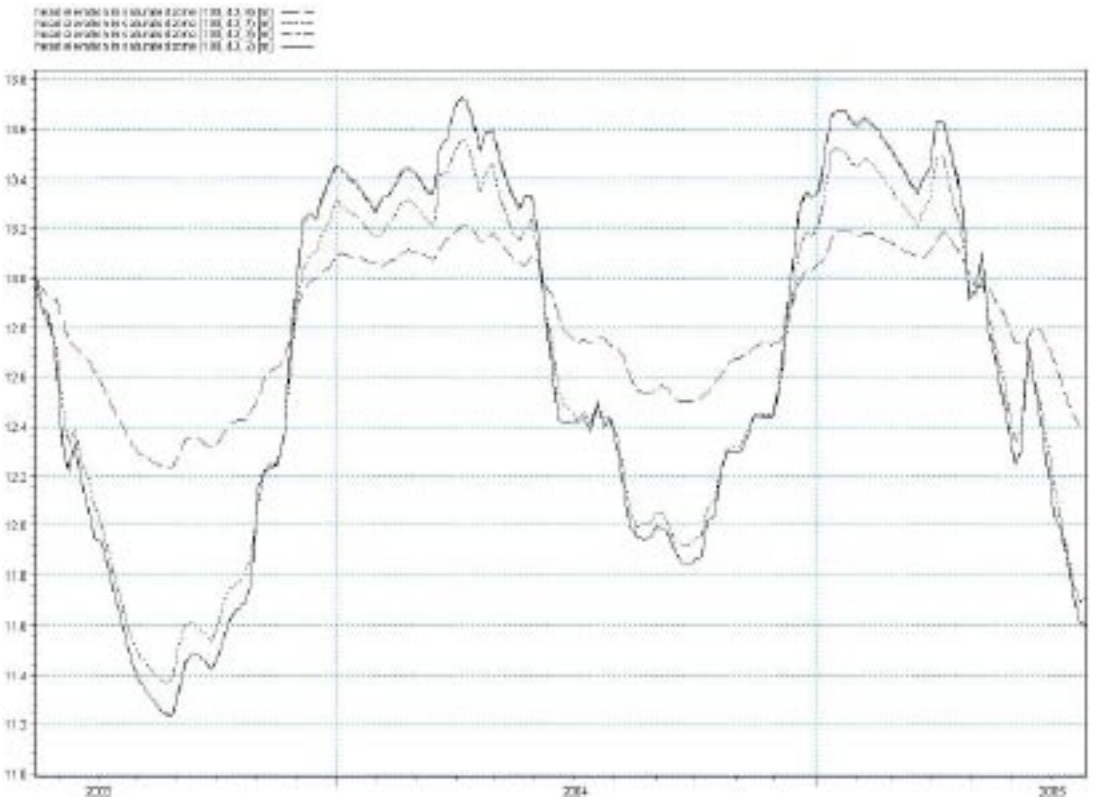

Figure 5-4. *Calculated head elevations in calculation layers L2 (marked with a solid line), L3 (marked with a dash-dot line), L7 (marked with a dot line) and L9 (marked with a dashed line) at SFM0010, located in the upstream part of the model area.*

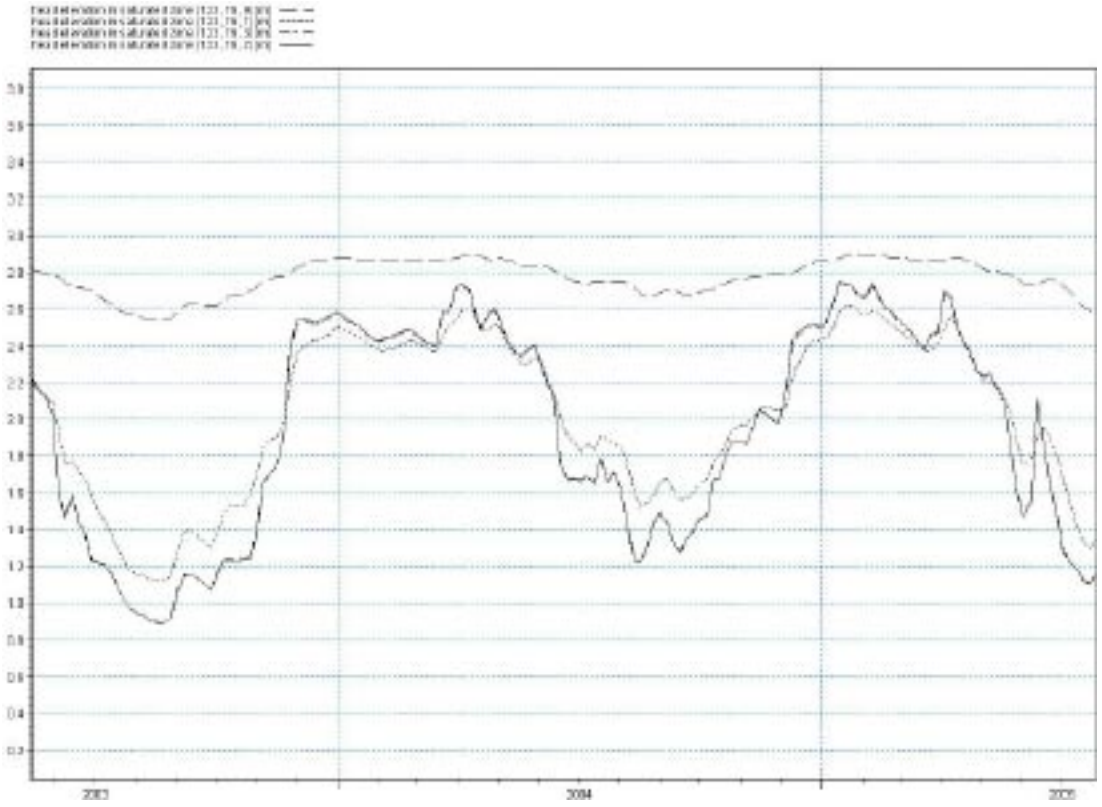

Figure 5-5. *Calculated head elevations in calculation layers L2 (marked with a solid line), L3 (marked with a dash-dot line), L7 (marked with a dot line) and L9 (marked with a dashed line) at SFM0030, located close to the inlet to Lake Bolundsfjärden.*

5.2 Surface water levels and surface water discharge

The locations of the monitoring points used in the evaluation of the base case are shown in Figure 5-6. Generally, there is good agreement between measured and calculated water levels and discharges. Figure 5-7 shows a comparison between measured and calculated water levels in the lakes Eckarfjärden, Fiskarfjärden, Gällsboträsket and Bolundsfjärden. Calculated water levels are somewhat higher compared to measurements during the summer. For Lake Bolundsfjärden, the calculated water level is slightly lower during the winter and slightly higher during the summer. In general, measured data demonstrate a slower response to changes in the water levels compared to the simulations.

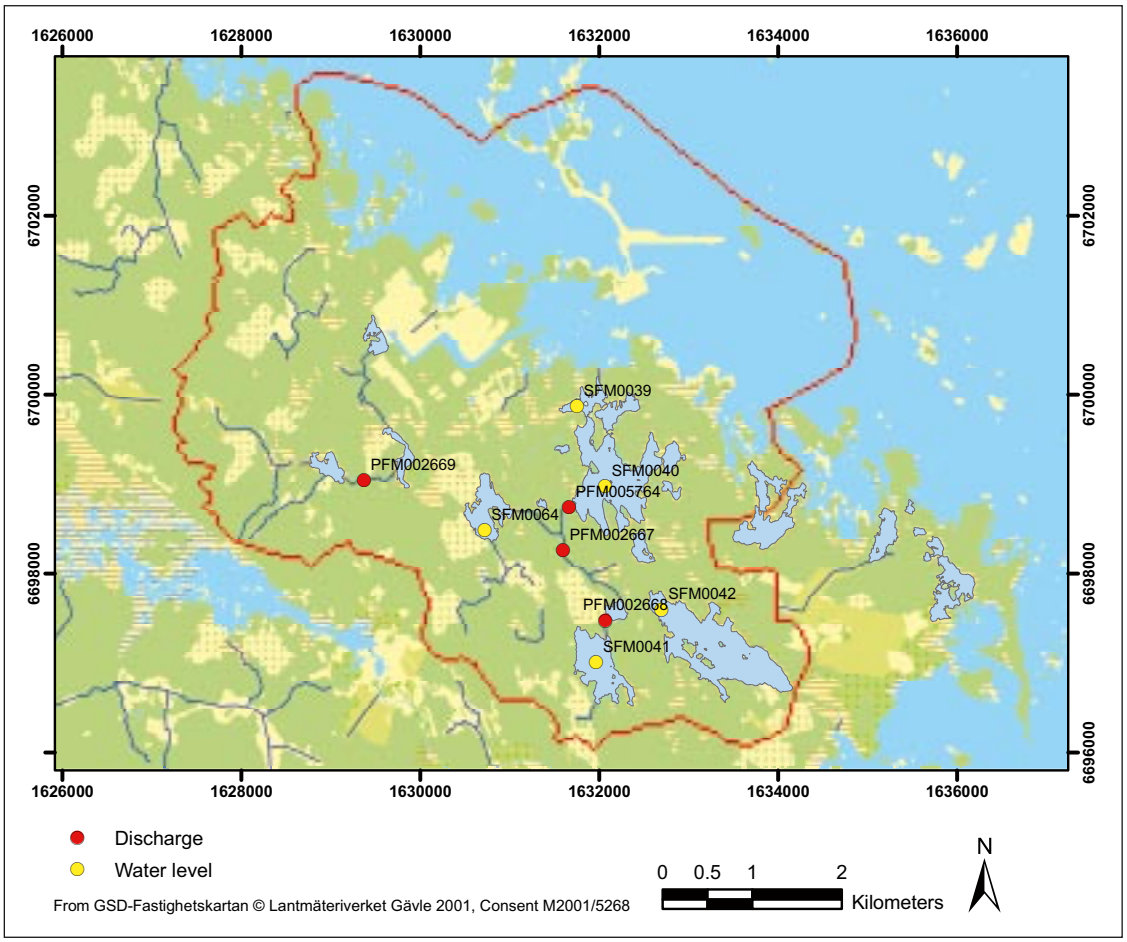

Figure 5-6. *Locations of the monitoring points used for model calibration and evaluation in terms of surface water runoff. The red line indicates the boundary of the model area.*

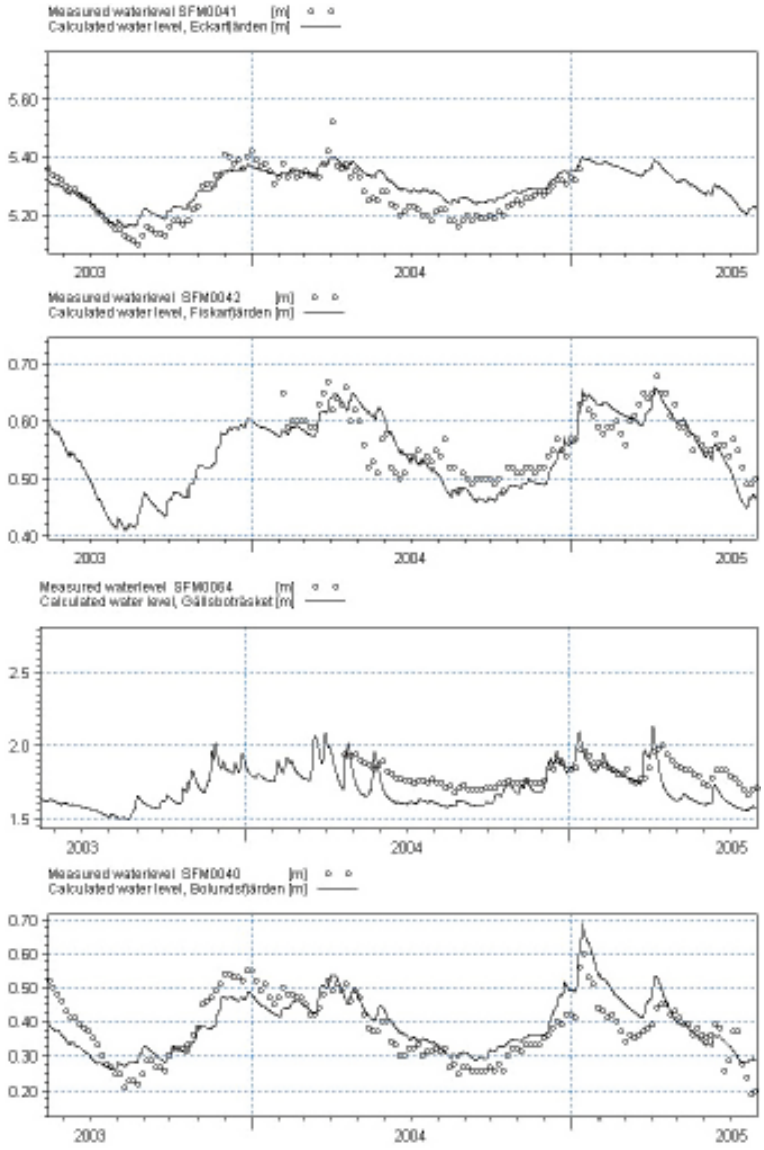

Figure 5-7. *Comparison between measured and calculated water levels in the lakes Eckarfjärden, Fiskarfjärden, Gällsboträsket and Bolundsfjärden.*

Figure 5-8 shows a comparison between measured and calculated discharges in PFM002668 (downstream Lake Eckarfjärden), PFM002667 (downstream Lake Stocksjön), PFM002669 (downstream Lake Gunnarsboträsket) and PFM005764 (upstream Lake Bolundsfjärden). The model shows a relatively good agreement in terms of the sizes of peak discharges. However, calculations generally show a quicker response compared to measurements, i.e. calculations show too fast and narrow peaks of the discharge. Larger values of storage parameters might be appropriate to solve this.

The runoff from snow-melt events is also generally too small. Thus, the errors are larger during the period January through April. This could be a result of the correction of the precipitation data used to calculate the net precipitation. The precipitation is corrected with respect to wind on a yearly basis (around 11%), and is likely not corrected for type of precipitation (snow or rain). The precipitation during snow events is generally underestimated, and it is not unusual that a correction up to 20% is applied on snow precipitation.

The poorest agreement is in PFM002668 downstream Lake Eckarfjärden, where the calculated discharge is considerably lower than measurements. However, there are uncertainties regarding

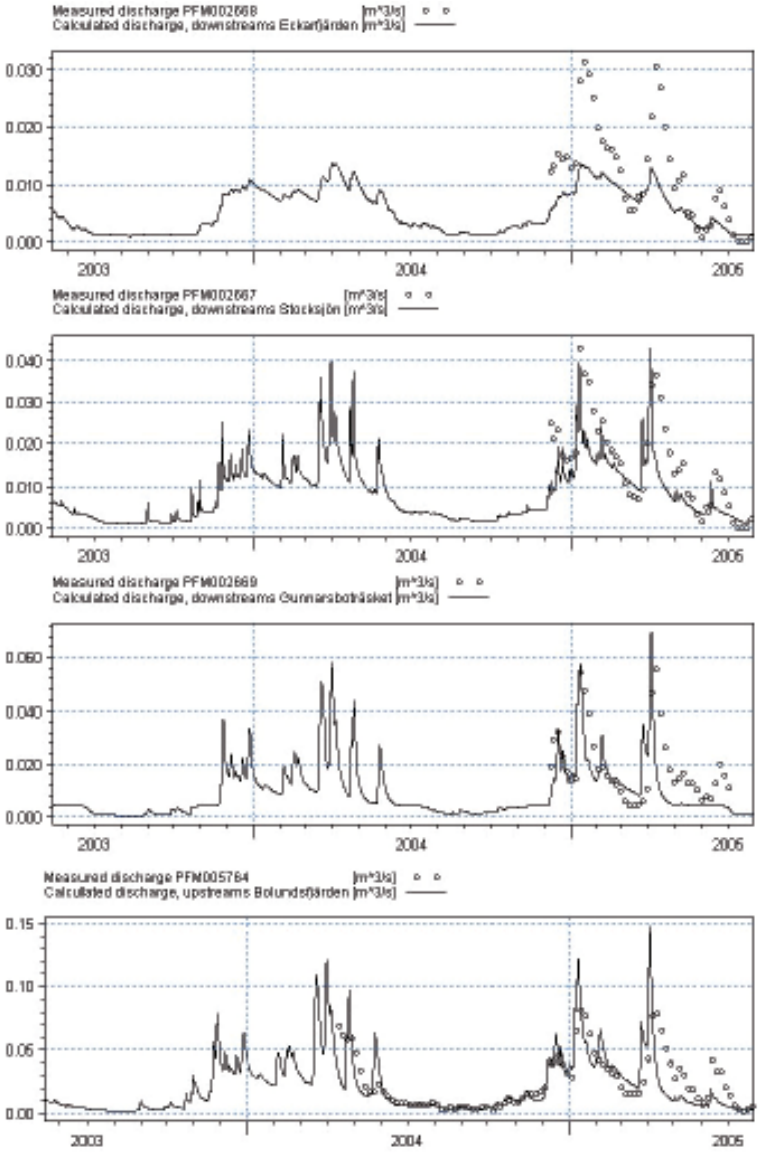

Figure 5-8. *Comparison between measured and calculated discharge at PFM002668 (downstream Lake Eckarfjärden), PFM002667 (downstream Lake Stocksjön), PFM002669 (downstream Lake Gunnarsboträsket) and PFM005764 (upstream Lake Bolundsfjärden).*

the measured data at this point, and no efforts have been made to calibrate the model with respect to PFM002668. The best agreement is noted at PFM005764, located upstream Lake Bolundsfjärden.

Figures 5-9 to 5-12 show the accumulated observed and simulated discharges for PFM002668 (downstream Eckarfjärden), PFM002667 (downstream Stocksjön), PFM002669 (downstream Gunnarsboträsket) and PFM005764 (upstream Bolundsfjärden). The runoff error is largest at PFM002668 in the upstream part of the model area, with c. 40% too small calculated runoff. There are uncertainties in the size of the actual sub-catchment of this point, and possibly some of the runoff to PFM002669 instead should be drained to Lake Eckarfjärden. The error decreases further downstream, and is around 11% upstream of Lake Bolundsfjärden considering the whole period with measurements. This period includes the low-flow season in the summer and fall of 2004, during which the model accurately calculates the runoff. The error increases for all boreholes during the snow period, for which there possibly is a lack of precipitation in the model due to the correction of raw precipitation data.

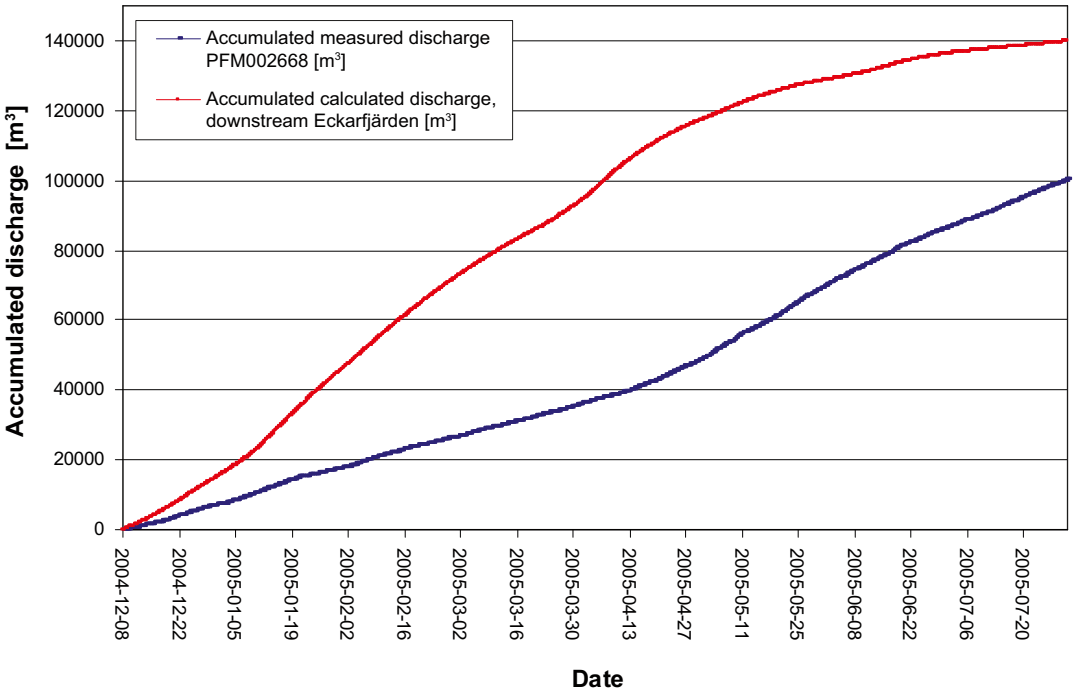

Figure 5-9. *Accumulated discharge (m^3) between 2004-12-08 and 2005-07-31 at PFM002668, downstream Lake Eckarfjärden.*

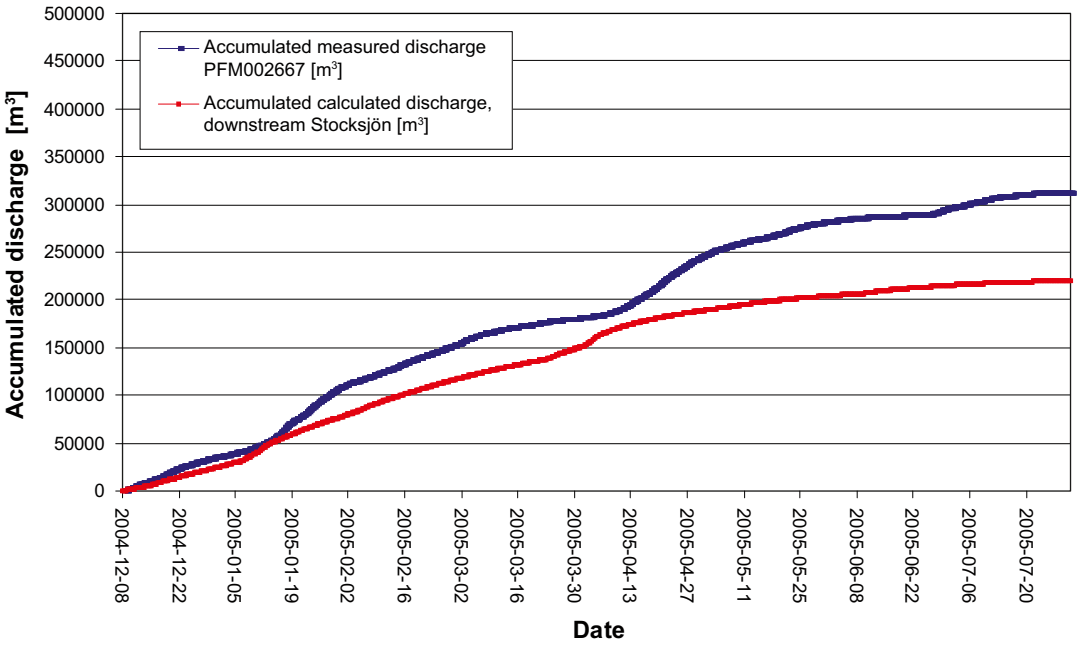

Figure 5-10. *Accumulated discharge (m^3) between 2004-12-08 and 2005-07-31 at PFM002667, downstream Lake Stocksjön.*

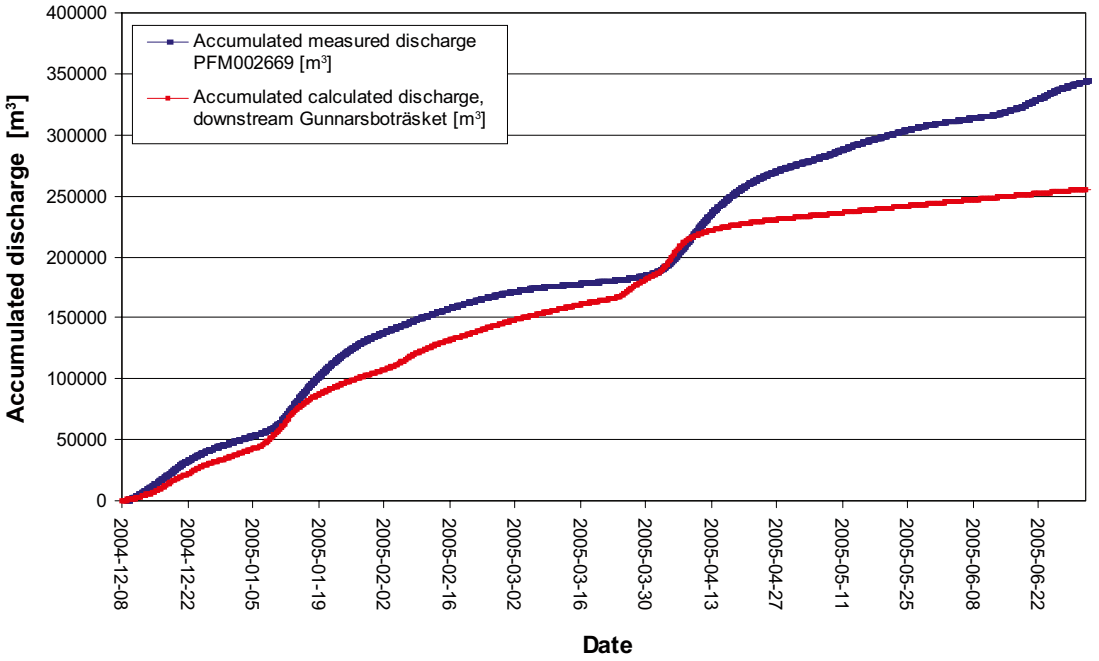

Figure 5-11. *Accumulated discharge (m³) between 2004-12-08 and 2005-07-31 at PFM002669, downstream Lake Gunnarsboträsket.*

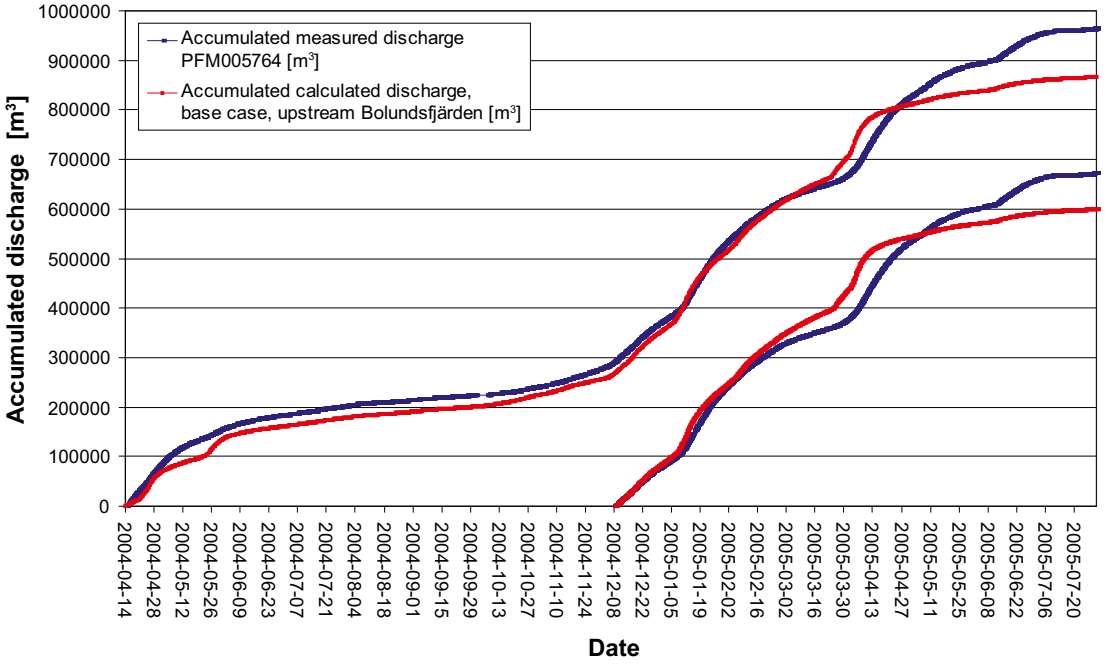

Figure 5-12. *Accumulated discharge (m³) between 2004-04-14 and 2005-07-31 and between 2004-12-08 and 2005-07-31 at PFM005764, upstream Lake Bolundsfjärden.*

5.3 Groundwater head elevations

Figure 5-13 shows the locations of the 32 monitoring points used in the base case evaluation. The chosen points have continuous data series, covering most of the simulation period. Three points have been excluded in the evaluation due to their location near the model boundary (SFM0004, SFM0005 and SFM0026) and one due to its location in a boundary grid cell with time-varying sea water level (SFM0024).

Figures 5-14 to 5-20 show a comparison between measured and calculated groundwater head elevations and depths to the phreatic surface. Some boreholes are located in local depressions or slopes in the interpolated model topography. This makes the absolute head elevation sensitive to deviations in the topography in the interpolated grid, and it may be more representative to use the calculated and measured depth to the phreatic surface as a basis for comparison. This is done in Figures 5-14 to 5-20 for SFM0001, SFM0002, SFM0003, SFM0011, SFM0020, SFM0021 and SFM0030.

At locations where the slope in the model topography is relatively steep and the geology differs from cell to cell, such as near shorelines around Lake Eckarfjärden, the comparison of head elevations between measured and calculated data is very dependent on the actual position of the borehole in relation to the interpolated 40 m-grid. In such cases, it is advisable to also evaluate the head elevations in a neighbouring grid cell, having corresponding topography and geology further down the slope. For SFM0014 and SFM0016, results are also shown in neighbouring grid cells towards the lake from the actual borehole coordinate.

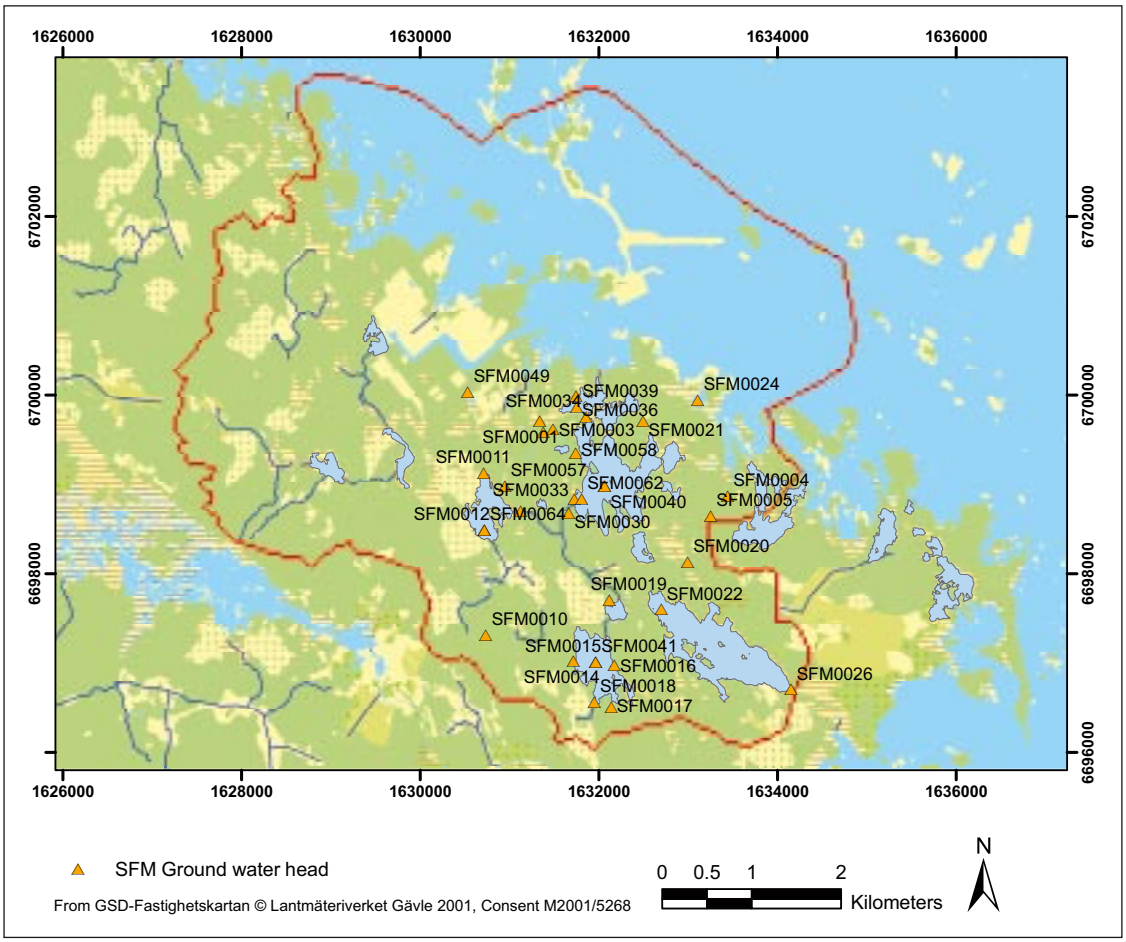

Figure 5-13. *Locations of monitoring points used for calibration and evaluation in terms of groundwater head elevations. The red line indicates the boundary of the model area.*

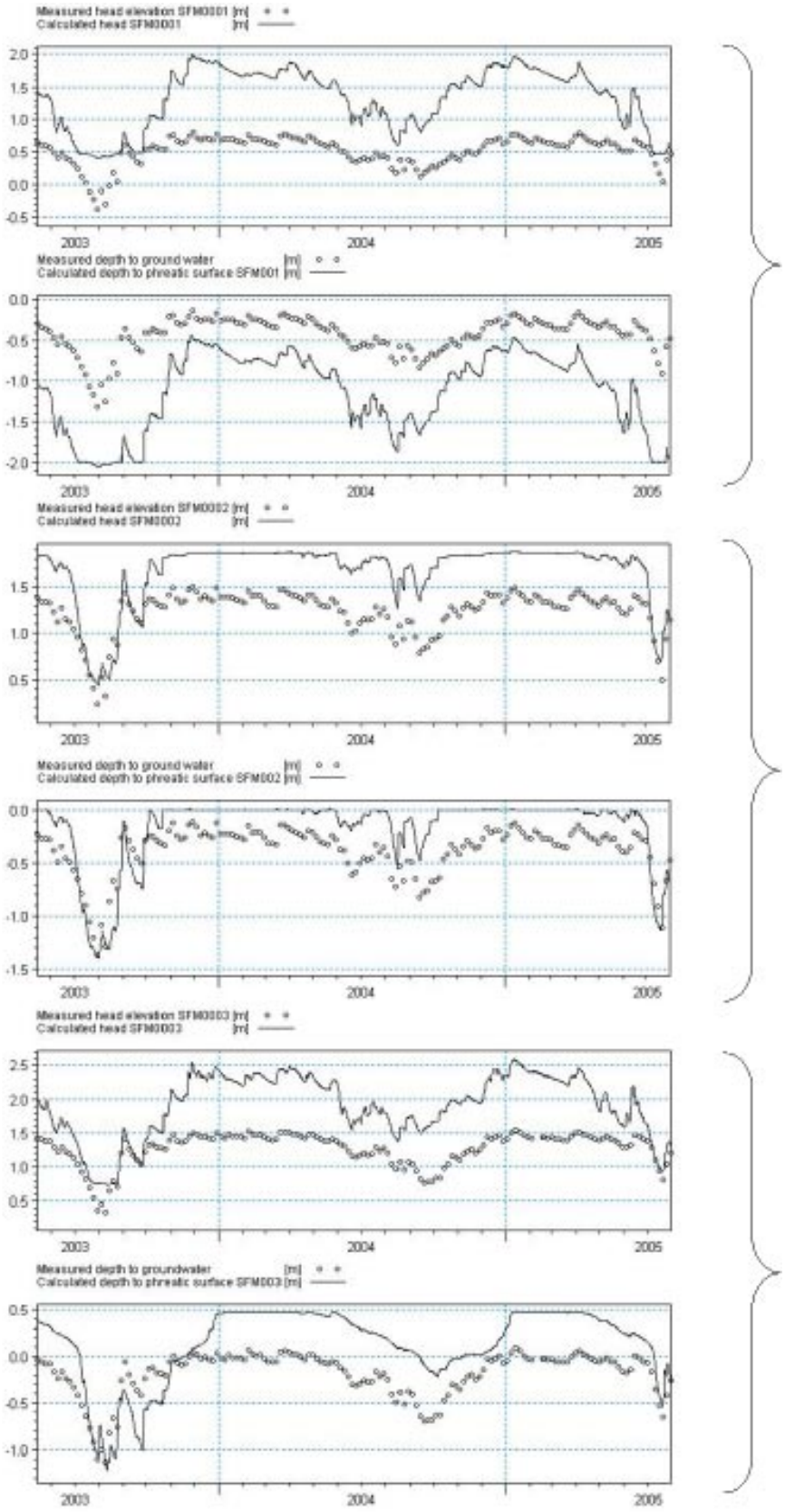

Figure 5-14. *Comparison between measured and calculated groundwater head elevation and depth to the phreatic surface in SFM0001, SFM0002 and SFM0003. The brackets mark boreholes where both the head elevation and the depth to the phreatic surface are shown.*

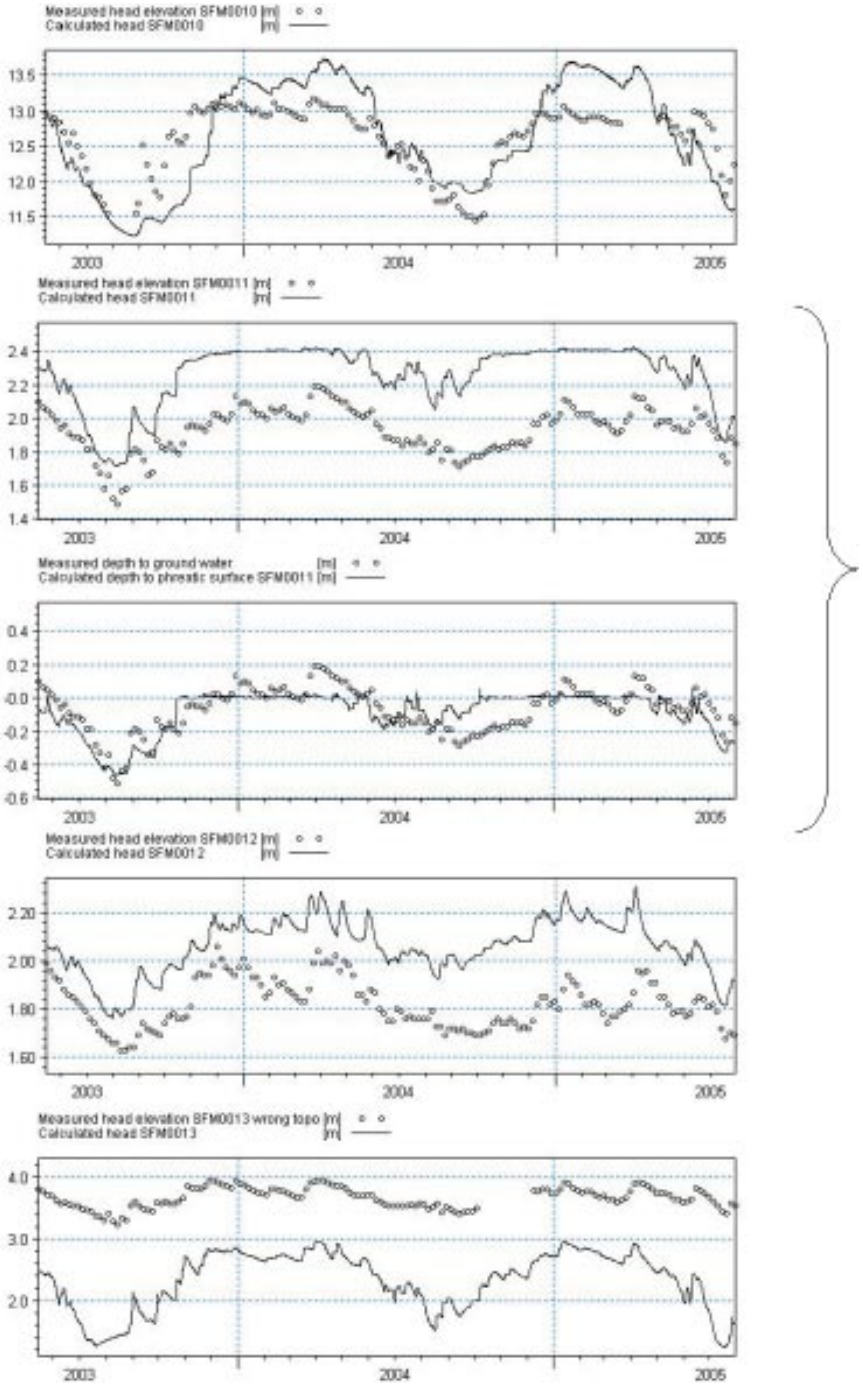

Figure 5-15. *Comparison between measured and calculated groundwater head elevation in SFM0010, between measured and calculated groundwater head elevation and depth to phreatic surface in SFM0011 and between measured and calculated groundwater head elevation in SFM0012 and SFM00013. Measured head elevations in SFM00013 should be reduced with 2.42 m, due to an erroneous absolute level of the top of the casing of the borehole. The brackets mark boreholes where both the head elevation and the depth to the phreatic surface are shown.*

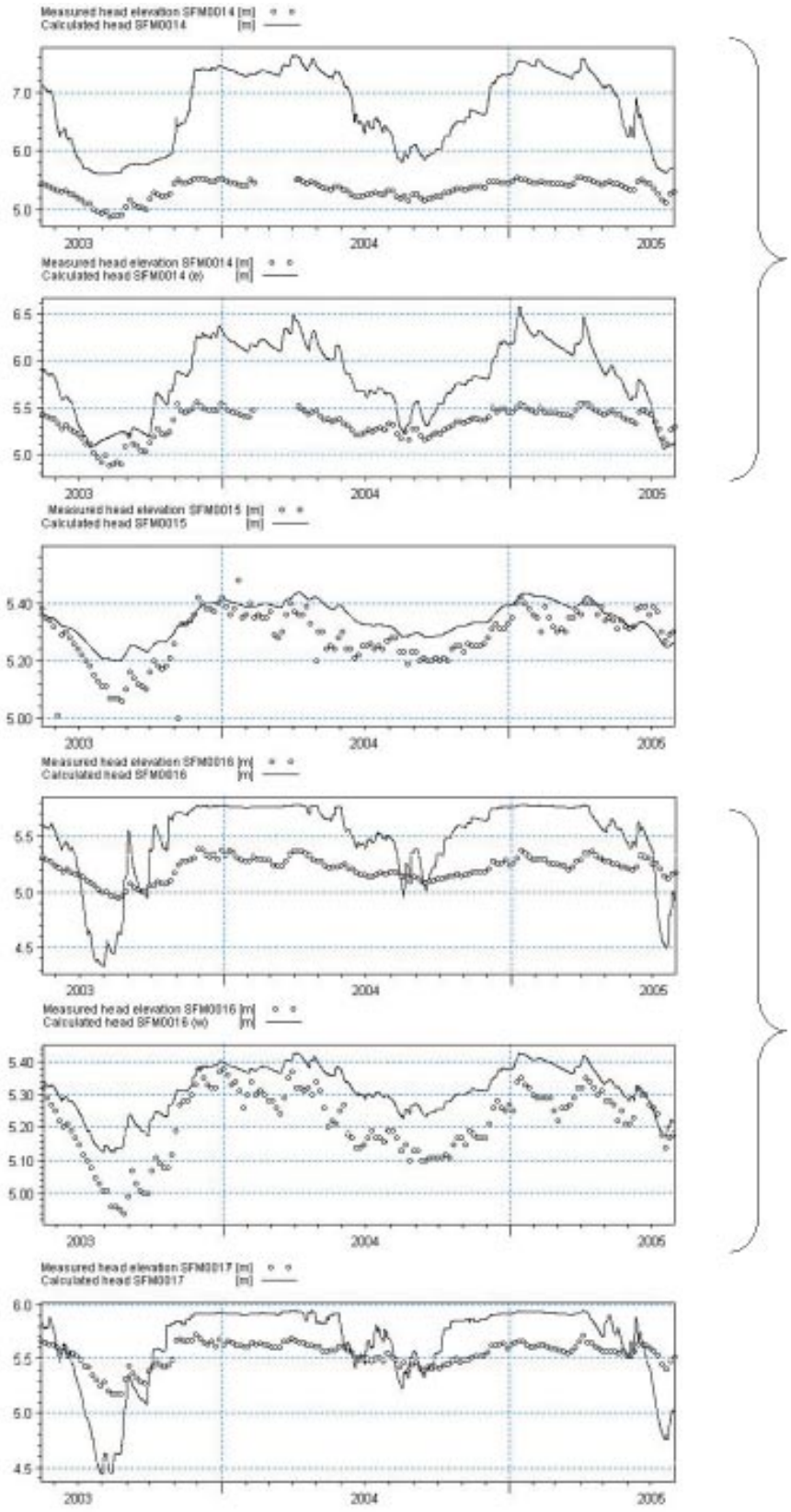

Figure 5-16. *Comparison between measured and calculated groundwater head elevation in SFM0014 (two grid cells) SFM0015, and SFM0016 (two grid cells) and SFM0017. The brackets mark boreholes where the head elevations in two neighbouring grid cells are shown.*

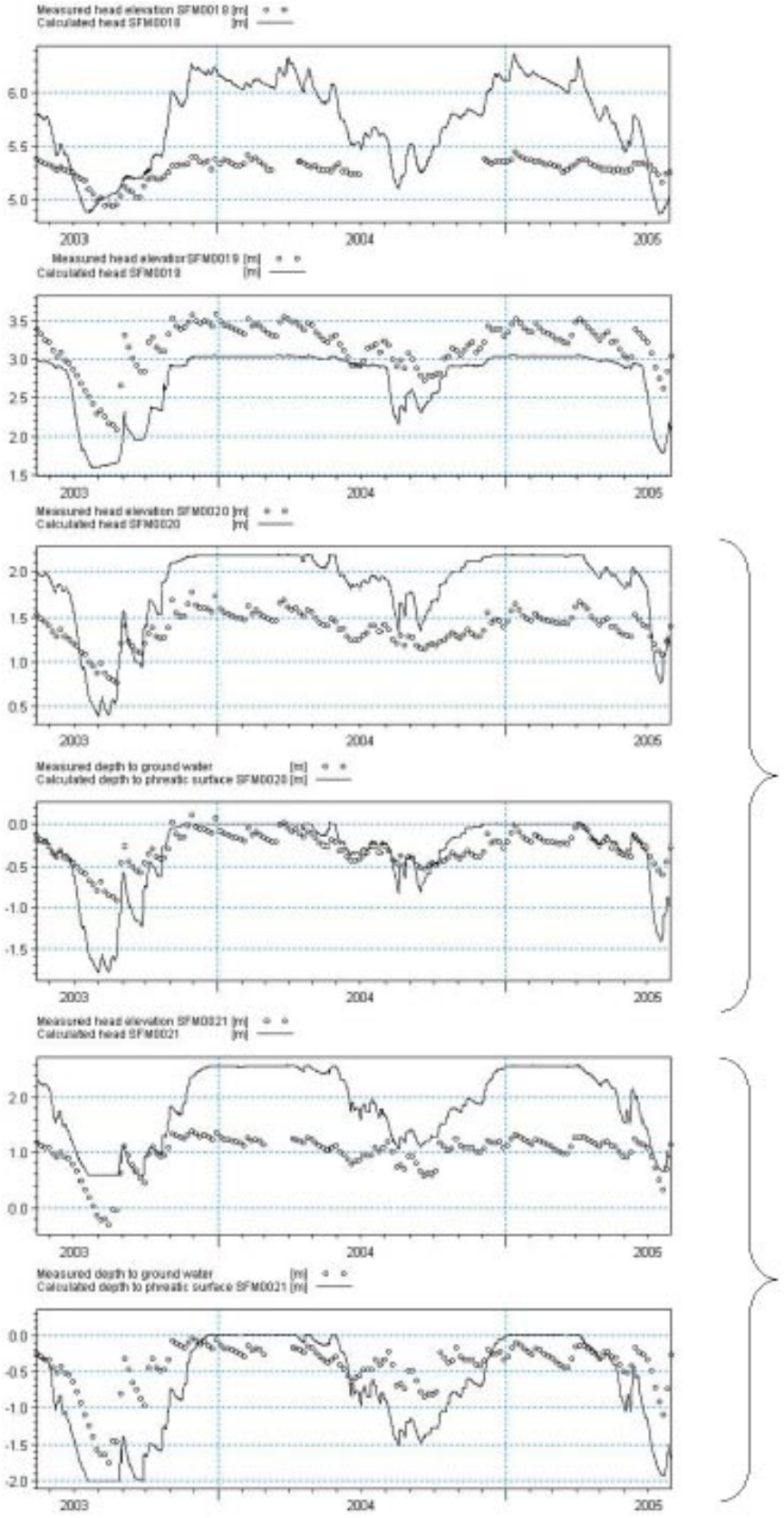

Figure 5-17. *Comparison between measured and calculated groundwater head elevation in SFM0018 and SFM0019 and between mesured and calculated head elevation and depth to phreatic surface in SFM0020 and SFM0021. The brackets mark boreholes where both the head elevation and the depth to the phreatic surface are shown.*

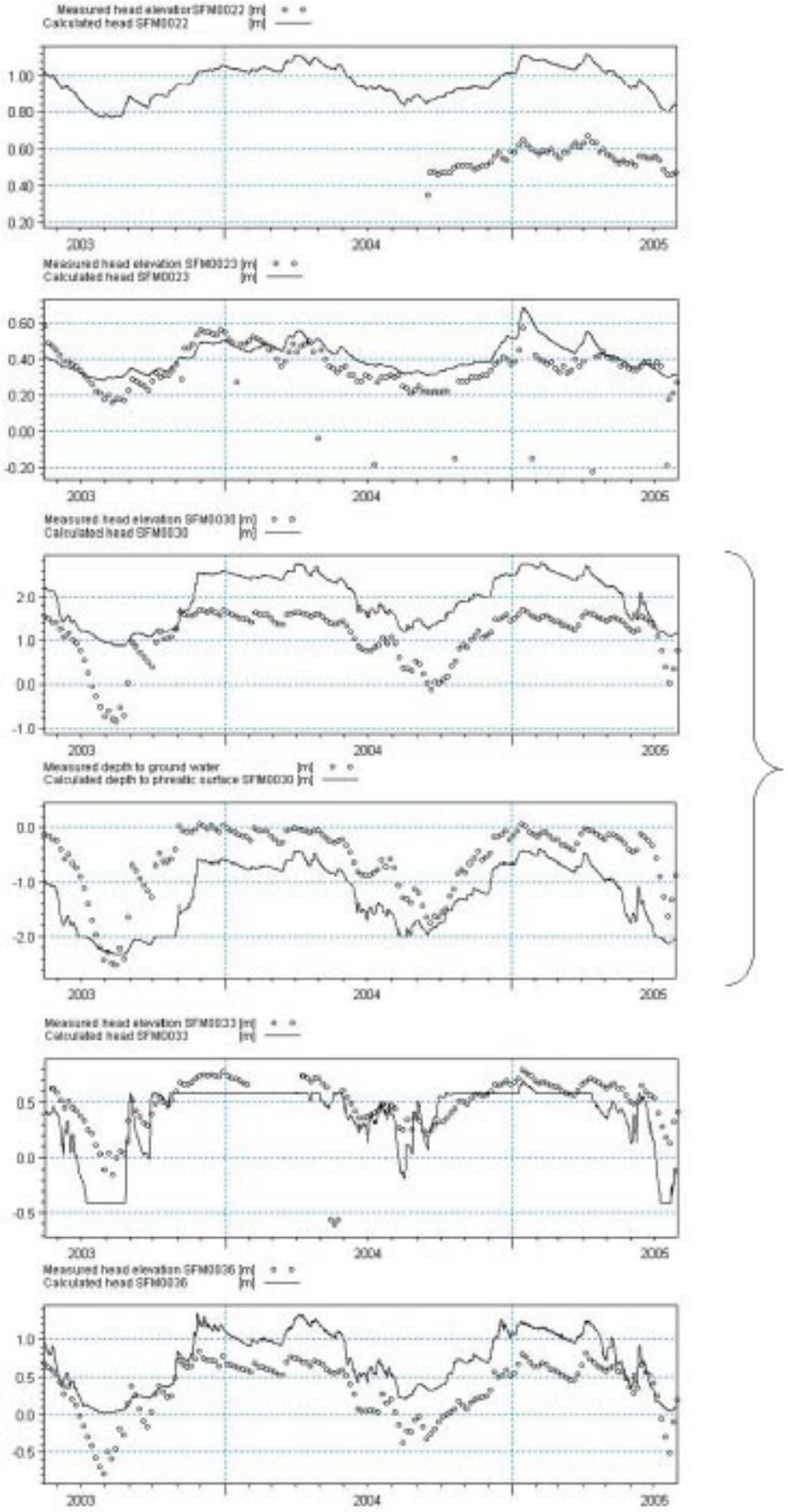

Figure 5-18. *Comparison between measured and calculated groundwater head elevation in SFM0022 and SFM0023, between measured and calculated head elevation and depth to phreatic surface in SFM0030 and between measured and calculated groundwater head in SFM0033 and SFM0036. The brackets mark boreholes where both the head elevation and the depth to the phreatic surface are shown.*

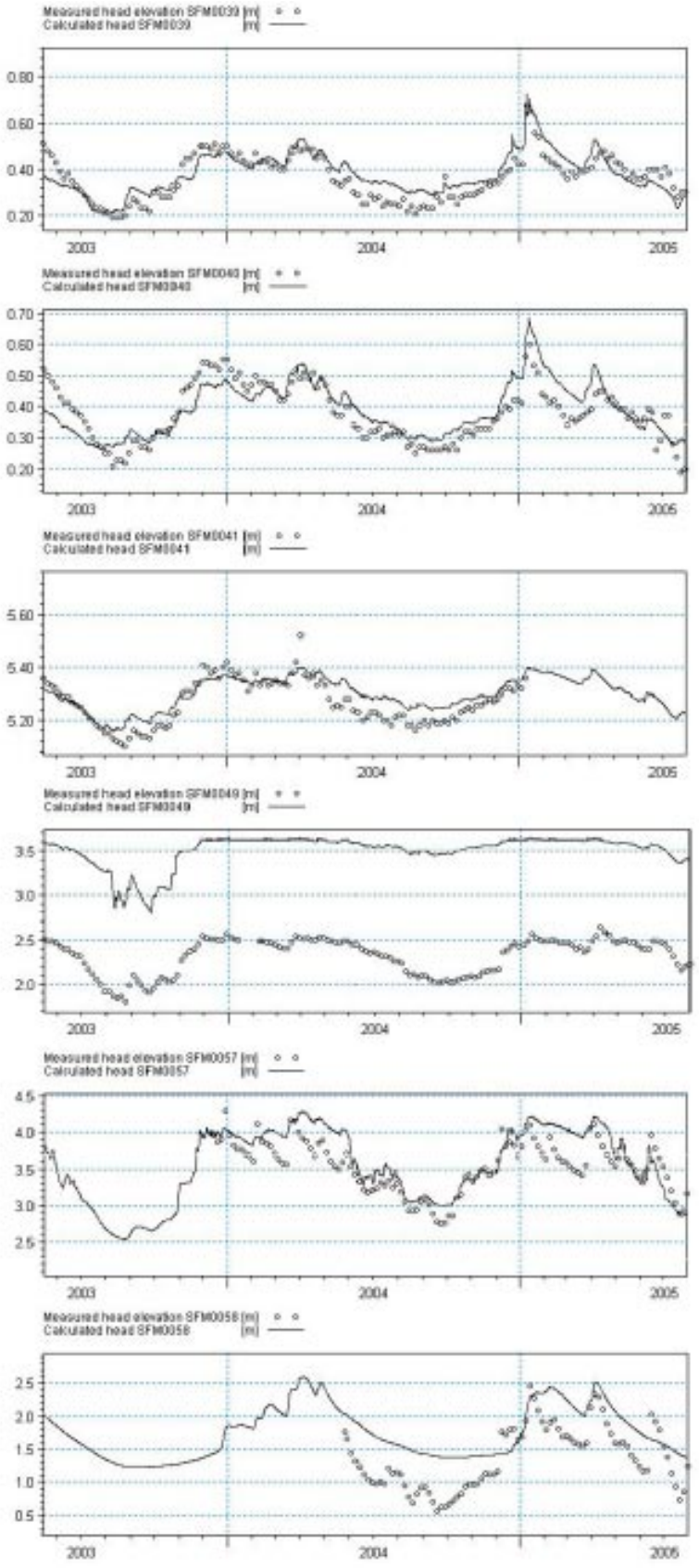

Figure 5-19. *Comparison between measured and calculated groundwater head elevation in SFM0039, SFM0040, SFM0041, SFM0049, SFM0057 and SFM0058.*

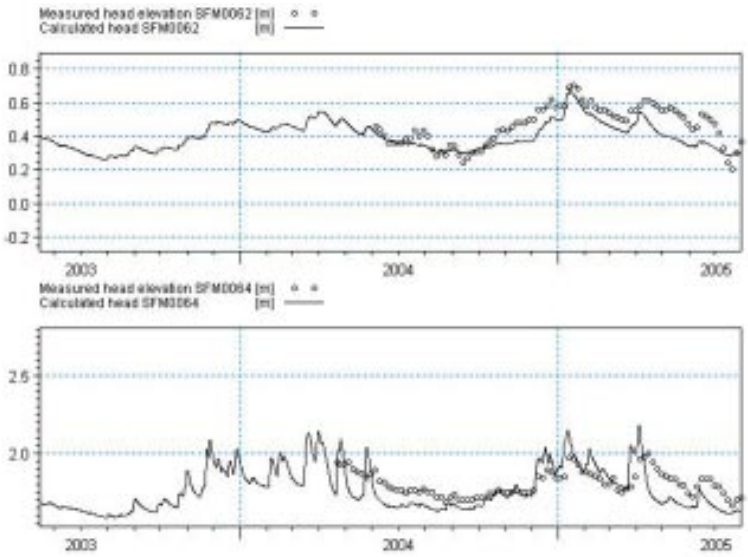

Figure 5-20. *Comparison between measured and calculated groundwater head elevation in SFM0062 and SFM0064.*

The results from the base case simulation show that boreholes located below lakes have very good agreement between calculated and observed groundwater head elevations, with two exceptions: SFM0012 and SFM0022. The model also shows a reasonably good agreement between calculated and measured data in many other points, with an absolute mean error for evaluated boreholes of 31 cm. Different types of differences between calculated and measured data can be noted, of which the major differences and their possible causes are as follows:

- Variations in amplitude due to transpiration processes.
- Variations in absolute mean head due to differences between borehole casing levels and the interpolated DEM. The topography, which influences the depth to the filter where groundwater head is measured, also affects how deep the transpiration processes can reach; there is a limitation in the model code that only allows transpiration within the uppermost calculation layer. In the model, filter levels are described using surveyed absolute elevations.
- Deviations in absolute mean head elevations due to local errors in the applied hydraulic conductivities.
- Variations in the process of refilling of the aquifer after dry periods, for example a too slow groundwater table rise after dry summers. This may be due to local deviations in the applied pF-curves in the unsaturated zone description.
- Variations in near-surface groundwater elevations. For example, the calculated groundwater level reaches the ground surface during the fall and spring at some locations, where the measured depth is just below the ground surface. This may be due to the presence of near-surface high conductive layers.

Based on the above, three type areas with similar types of calculation-measurement differences can be identified: Lake boreholes, near-shore boreholes and land/hill boreholes. Table 5-1 shows a rough classification of the various differences between calculated and measured groundwater heads and depths within the model area. Local differences in curves and sizes of deviations are evaluated for the same boreholes as seen in Figures 5-14 to 5-20.

Table 5-1. Classification of differences between calculated and measured groundwater heads. Classes C1–C8 are explained below the table.

Borehole	C1[1]	C2[2]	C3[3]	C4[4]	C5[5]	C6[6]	C7[7]	C8[8]	Deviation (m)[9]
SFM0001		X					X		+1.3
SFM0002		X						X	+0.4
SFM0003		X							+0.5
SFM0010					X				+0.5[10]
SFM0011	X							X	
SFM0012		X							+0.2
SFM0013		X					X		–1.4
SFM0014		X					X		+0.4
SFM0015	X								
SFM0016		X	X				X		+0.4
SFM0017		X	X				X		+0.2
SFM0018		X	X				X		+0.5
SFM0019		X							–0.5
SFM0020			X					X	
SFM0021			X					X	
SFM0022		X							+0.4
SFM0023	X								
SFM0030		X		X					–0.5
SFM0033			X					X	
SFM0036		X		X					+0.4
SFM0039	X								
SFM0040	X								
SFM0041	X								
SFM0049		X							+1.0
SFM0057	X								
SFM0058				X		X			
SFM0062	X								
SFM0064	X								

[1]C1: Good agreement.

[2]C2: Error in absolute head.

[3]C3: Too large evapotranspiration during summer.

[4]C4: Too small evapotranspiration during summer.

[5]C5: Too slow increase in head during fall.

[6]C6: Too small amplitude.

[7]C7: Too large amplitude.

[8]C8: Groundwater on ground surface.

[9]General comment based on an ocular view of absolute head deviations.

[10]During summer.

5.4 Water balance

Table 5-2 shows the monthly accumulated water balance during the period 2003-05-15 to 2005-05-04 for the land part of the model area. A negative value is an inflow to the area, and a positive value is an outflow from the area. Figure 5-21 shows the total accumulated water balance over the same period.

Table 5-2. Total accumulated water balance for base case in Forsmark between 2003-05-15 and 2005-05-04 [mm].

Date	Precipi-tation	Canopy storage change	Evapotran-spiration	OL storage change	OL boundary inflow	OL boundary outflow	OL to river	SubSurface storage change	SubSurface boundary inflow	SubSurface boundary outflow	Baseflow to river	Baseflow from river	Error
2003-05-15	0.0	0.0	0.0	0.0	0.0	0.0	0.0	0.0	0.0	0.0	0.0	0.0	0.0
2003-06-14	–46.8	–1.8	83.4	–8.5	–0.1	0.1	3.1	–26.3	–1.5	0.7	0.7	0.0	3.2
2003-07-14	–67.6	–1.8	174.8	–22.9	–0.1	0.1	4.6	–75.6	–4.4	1.0	1.1	–0.1	9.1
2003-08-13	–117.1	–0.5	276.3	–31.2	–0.1	0.1	4.8	–113.1	–7.7	1.2	1.3	–0.2	13.9
2003-09-12	–219.9	–1.8	335.2	–25.6	–0.8	1.1	6.5	–77.7	–9.7	1.6	1.5	–0.2	10.2
2003-10-12	–274.0	–1.6	365.1	–22.9	–0.8	1.3	8.4	–59.4	–11.0	2.2	1.9	–0.2	9.1
2003-11-11	–336.6	0.4	371.8	–12.9	–0.8	2.2	12.2	–25.7	–12.0	4.1	2.5	–0.2	4.8
2003-12-11	–409.8	0.4	373.9	1.6	–1.4	6.1	23.1	10.1	–12.7	7.5	3.6	–0.3	1.9
2004-01-10	–438.6	0.3	375.0	2.4	–2.2	10.0	36.2	16.5	–13.4	10.2	5.0	–0.3	1.1
2004-02-09	–452.8	0.0	375.9	3.0	–2.6	11.7	45.3	15.8	–14.1	12.8	6.2	–0.3	1.0
2004-03-10	–478.2	–1.0	385.8	2.4	–4.1	16.0	56.1	16.2	–14.7	15.4	7.5	–0.3	1.2
2004-04-09	–549.9	–1.8	403.3	9.2	–4.5	22.6	75.2	33.9	–15.2	19.4	9.0	–0.3	0.9
2004-05-09	–581.3	–1.8	441.8	3.4	–4.6	24.7	87.0	15.3	–15.8	22.7	10.5	–0.3	1.6
2004-06-08	–634.4	0.3	506.1	–0.9	–4.6	25.8	94.7	–4.1	–16.6	24.1	11.6	–0.3	1.7
2004-07-08	–696.6	–1.8	598.6	–8.4	–5.0	26.1	97.8	–24.6	–18.4	24.6	12.2	–0.3	4.2
2004-08-07	–753.7	–1.8	673.7	–13.5	–5.9	27.4	100.1	–39.6	–19.8	25.2	12.8	–0.3	4.6
2004-09-06	–809.9	–1.8	736.8	–16.4	–6.0	27.5	101.9	–43.7	–21.5	25.6	13.2	–0.3	5.3
2004-10-06	–839.7	–0.6	768.1	–17.9	–12.1	33.0	102.8	–44.6	–23.5	25.9	13.6	–0.4	4.6
2004-11-05	–878.4	0.1	774.9	–12.8	–12.4	34.1	105.6	–24.6	–24.4	27.4	14.3	–0.4	3.4
2004-12-05	–910.0	0.4	778.5	–6.9	–14.4	36.5	108.9	–8.6	–25.3	28.7	15.1	–0.4	2.6
2005-01-04	–965.4	0.1	781.1	2.9	–32.8	59.4	119.8	15.8	–26.0	30.9	16.3	–0.4	1.8
2005-02-03	–1,015.8	0.3	785.3	8.5	–142.7	179.2	134.1	28.3	–26.6	33.1	17.8	–0.4	1.1
2005-03-05	–1,028.0	–1.0	788.6	4.6	–143.3	183.0	147.6	21.4	–27.2	36.7	19.2	–0.4	1.3
2005-04-04	–1,093.1	0.2	810.7	13.2	–143.3	186.4	159.5	35.0	–27.8	40.0	20.6	–0.4	1.1
2005-05-04	–1,108.8	0.0	863.9	–0.1	–143.4	187.6	168.5	–0.4	–28.4	42.6	21.8	–0.4	3.0

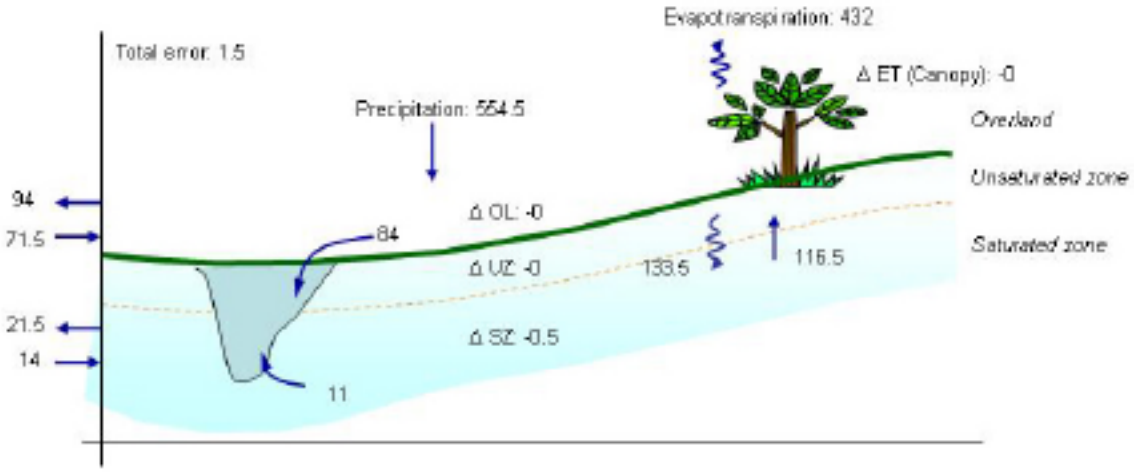

Figure 5-21. *Average annual water balance (mm/year) during the period 2003-05-15 to 2005-05-04 for the land part of the model area. The saturated boundary in- and outflows also contain the communication with bottom layer boundaries. Due to the fluctuating sea level, water can be exchanged both ways across the overland boundary.*

The annual average precipitation over the almost 2 years is 554.5 mm/year, whereas the calculated evapotranspiration is 432 mm/year. This means that the net precipitation is 124 mm/year, including the numerical error, of which 106.5 mm/year is net surface runoff and the remaining 17.5 mm/year is net groundwater recharge. From the net groundwater recharge, 11 mm/year discharges to the stream network (MIKE 11) and the rest discharges to the sea. Due to the fluctuation of the internal head boundary in the sea, water can be transferred both directions across the overland boundary. Note that the exchange with the boundaries for the saturated zone includes the communication with the bottom layer boundary.

The potential evapotranspiration is on average 453 mm/year, which means that the calculated evapotranspiration on average is 95% of the potential evapotranspiration. Moreover, 78% of the precipitation is emitted through evapotranspiration. Since the model area can be characterized as wet, having many mires, lakes and a groundwater table close to the ground surface, it is likely that the actual evapotranspiration is quite high in the area. The large amount of water evaporating in the area implies relatively small runoff. Table 5-3 shows a detailed average annual water balance (mm/year) for the different components included in the total water balance.

Table 5-3. Detailed average annual water balance of the land part of the model area (mm/year).

Water balance item	Average annual amount (mm/year), negative for inflow and positive for outflow
Precipitation	–554.4
Evaporation from Canopy	145.4
Canopy through fall to OL	–409.0
Evaporation from ponded water	17.5
Upward flow from SZ to OL	–70.2
Downward flow from OL to SZ	52.4
Inflow to OL from boundary of sub-catchment	–71.7
Outflow from OL to boundary of sub-catchment	93.8
Overland outflow to MIKE 11 river	974.5
Overland outflow from MIKE 11 river	–890.2
Infiltration from OL to UZ	–303.0
Direct evaporation from soil	54.5
Transpiration from the root zone	168.3
Recharge from UZ to SZ	–81.2
Upward flow from SZ to overland	70.2
Downward flow from OL to SZ	–52.4
Evapotranspiration directly from SZ	46.3
Inflow to SZ from sub-catchment	–4.5
SZ flow out of the sub-catchment	19.2
MIKE 11 baseflow to SZ	–0.2
SZ baseflow to MIKE 11	10.9
SZ flow to internal head boundaries	2.1
Flow from internal head boundaries	–9.7

6 Sensitivity analysis

This chapter presents a sensitivity study, based on the initial calibration described in chapter 4. For parameters such as hydraulic conductivities in the saturated zone, with “global” effects (i.e. parameters affecting model results in the whole model area), the analysis has been performed with the “full” Forsmark model, described in previous chapters. On the contrary, there are many parameters with “local” effects, such as parameters affecting the evapotranspiration. For such parameters, the model has been scaled down to a column model, representing two different type areas. One such area is at SFM0010, which is located on land in the upstream part of the model area and has an average depth to the groundwater table of 1.3 m. The other area is at SFM0017, which is located close to the shore of Lake Eckarfjärden and with a shallow groundwater table (on average 0.2 m). Note that specific parameters in the column model have been evaluated in the full model.

The column model was established to reduce the computation times and allow for a larger amount of parameters to be tested. The input data for each column model are taken directly from the equivalent grid cell in the full model. However, the number of computational layers was reduced to include 5 bedrock layers, compared to 7 in the full model. Moreover, the bottom boundary condition was set to a time-varying head elevation from the base case simulation, using the full model. No-flow was set at the horizontal boundaries of each column model. This implies that the column models are restricted to local conditions, completely neglecting interactions with surrounding areas.

Table 6-1 summarizes the different simulations included in the sensitivity analysis. Note that parameter values from previous simulations are included in each subsequent simulation case, provided that the parameter values improved model performance.

In supplement to Table 6-1, three additional simulations were made. The purposes of these simulations were to test (1) the effect of describing the bottom layer boundary with a no flow condition, (2) the effect of using a constant meteorological input to the model, (3) a simulation combining the most important vegetation and unsaturated zone parameters simulated according to Table 6-1. These three simulations were carried out using the full model.

The results were evaluated using the following five boreholes:

- SFM0010, which is located in the upper part of the model area. SFM0010 demonstrates a slow rise of the groundwater table rises during fall. The borehole is included in the column study.
- SFM0012, which is located below Lake Gällsboträsket.
- SFM0015, which is located below Lake Eckarfjärden.
- SFM0017, which is located near the shoreline of Lake Eckarfjärden. In the base case simulations, there is too high evapotranspiration during the summer at this borehole. The borehole is included in the column study.
- SFM0030, which is located close to the inlet to Lake Bolundsfjärden. In the base case simulations, there is a too high absolute head elevation and a somewhat too large depth to the groundwater table at this borehole.

Table 6-1. Simulations included in the sensitivity analysis.

Simulation case	Investigated parameter	Model type
Sens 1	Horizontal hydraulic conductivity in geological soil layers increased with a factor of 5	Full
Sens 2	Horizontal hydraulic conductivity in geological soil layers reduced with a factor of 5	Full
Sens 3	Vertical hydraulic conductivity in lake sediments increased in Fiskarfjärden and Gällsboträsket	Full
Sens 4	Vertical hydraulic conductivity in geological soil layers reduced by a factor of 10	Full
Sens 5	Local topography errors corrected for SFM0019, SFM0021, SFM0030 and SFM0058	Full
Sens 6	Horizontal discretization reduced from 40 to 20 m	Full
Sens 7	Root mass distribution, A_{root}, for coniferous forest increased from 1 to 2	Full
Sens 8	Unsaturated field capacity of coarse till reduced with a factor of 0.5	Column
Sens 9	Unsaturated hydraulic conductivity increased by a factor of 5	Column
Sens 10	Empirical coefficient *n*, describing the hydraulic conductivity of the unsaturated zone, increased by 5 (leads to lower conductivities at low soil water contents)	Column
Sens 11	Air entry in pF-curve of coarse till: 0–0.5 m from reference 0.5–2 m, air entry 0	Column
Sens 12	Air entry in pF-curve of coarse till: 0–0.5 m, no air entry (specific concave shape) 0.5–2 m from reference	Column
Sens 13	Air entry in pF-curve of coarse till: 0–0.5 m from reference 0.5–2 m, air entry at pF = 1.7	Column
Sens 14	Air entry in pF-curve of coarse till: 0–0.5 m, air entry at pF 1 0.5–2 m, air entry at pF 1.7	Column
Sens 15	Unsaturated specific yield in pF-curve of coarse till increased by a factor of 1.5 for the uppermost 50 cm and by a factor of 2 on the depths 0.5–2 m (affects the fluctuation of groundwater heads)	Column
Sens 16	Leaf area index decreased from 7 to 5 for coniferous forest	Column
Sens 17	Root depth of coniferous forest decreased from 0.8 m to 0.5 m	Column
Sens 18	K_c in ET reduced from 1 to 0.9	Column
Sens 19	A_{root} for coniferous forest increased from 1 to 2 (changed root mass distribution)	Column
Sens 20	A_{root} for coniferous forest decreased from 1 to 0.5 (changed root mass distribution)	Column

The mean absolute errors for the simulation cases are presented in Tables 6-2 to 6-7. These calculations are based on the differences between measured and calculated data at the same locations and times. The error (or residual) for an observation-calculation data pair is then

$$E_{i,t} = Obs_{i,t} - Calc_{i,t}$$

where $E_{i,t}$ is the difference between the observed and calculated values at location i and time t. The mean absolute error, MAE, at location i where n observations exist is

$$MAE_i = \left|\overline{E}_i\right| = \frac{\sum_t \left|E_{i,t}\right|}{n}.$$

For the column model, the results are presented in terms of total recharge for SFM0010 and SFM0017. As mentioned previously, the simulation period is 2003-05-15 to 2005-07-31. The simulations are run in a semi-stationary condition, using a hot start from the base case simulation to generate the initial conditions for each sensitivity simulation.

6.1 Saturated zone parameters

6.1.1 Horizontal hydraulic conductivity in geological soil layers

In simulation case Sens 1, the horizontal hydraulic conductivity in all of the geological soil layers was increased by a factor of 5 compared to the base case. In simulation case Sens 2, the horizontal hydraulic conductivity in all of the geological soil layers was decreased by a factor of 5 compared to the base case.

Figures 6-1 to 6-5 show a comparison between measured head elevations, calculated head elevations from base case and the results from Sens 1 and Sens 2. In most cases, an increased conductivity produces a lower groundwater table, and the opposite for a decreased horizontal conductivity.

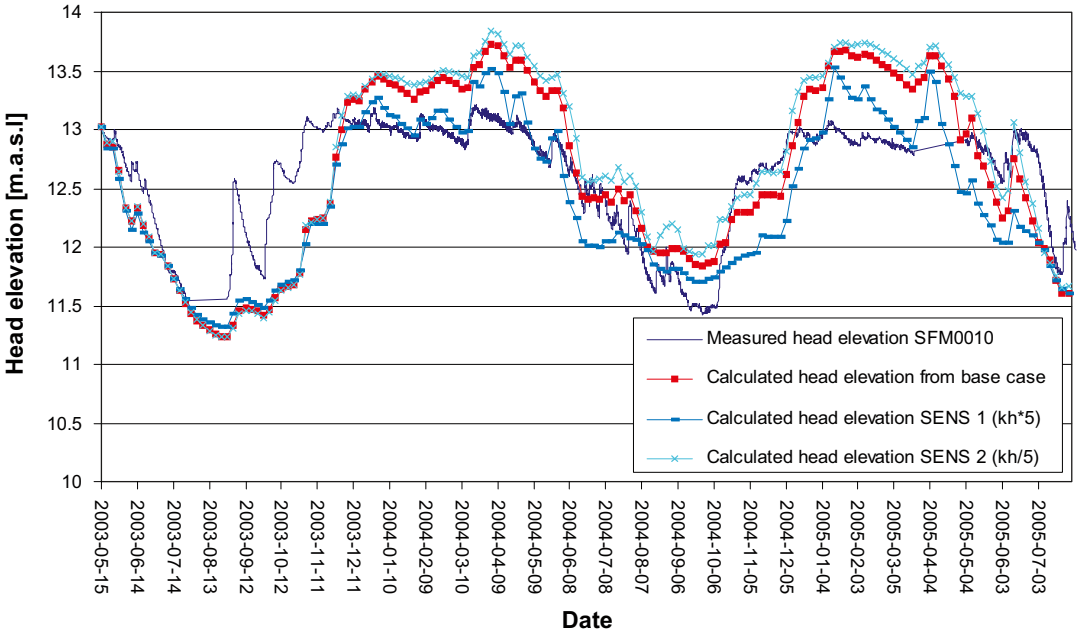

Figure 6-1. *Results in SFM0010 from the sensitivity analysis of the horizontal conductivity in the soil layers.*

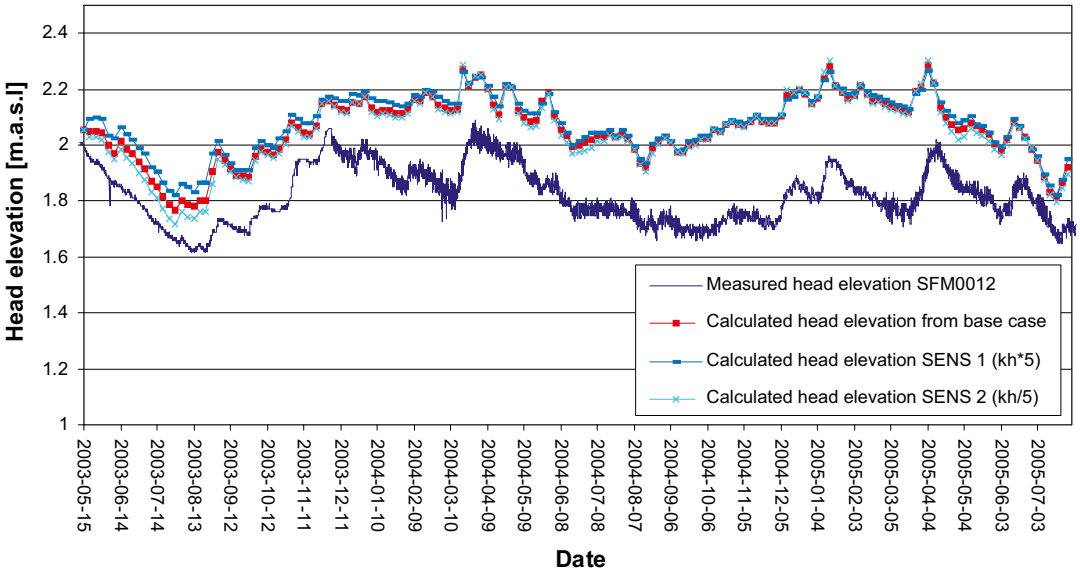

Figure 6-2. *Results in SFM0012 from the sensitivity analysis of the horizontal conductivity in the soil layers.*

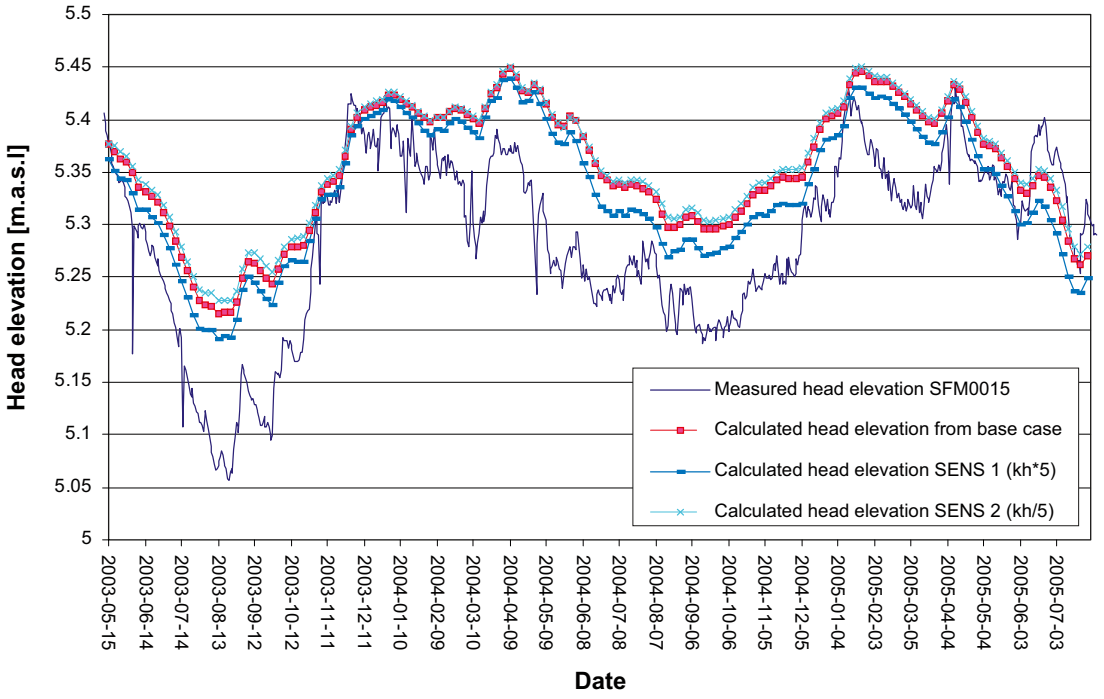

Figure 6-3. *Results in SFM0015 from the sensitivity analysis of the horizontal conductivity in the soil layers.*

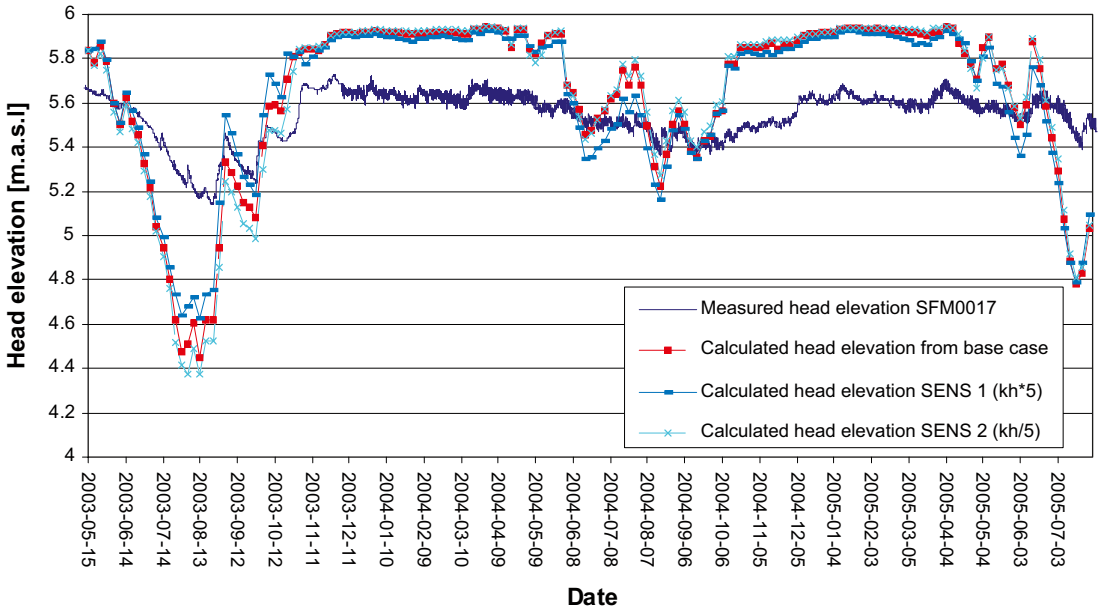

Figure 6-4. *Results in SFM0017 from the sensitivity analysis of the horizontal conductivity in the soil layers.*

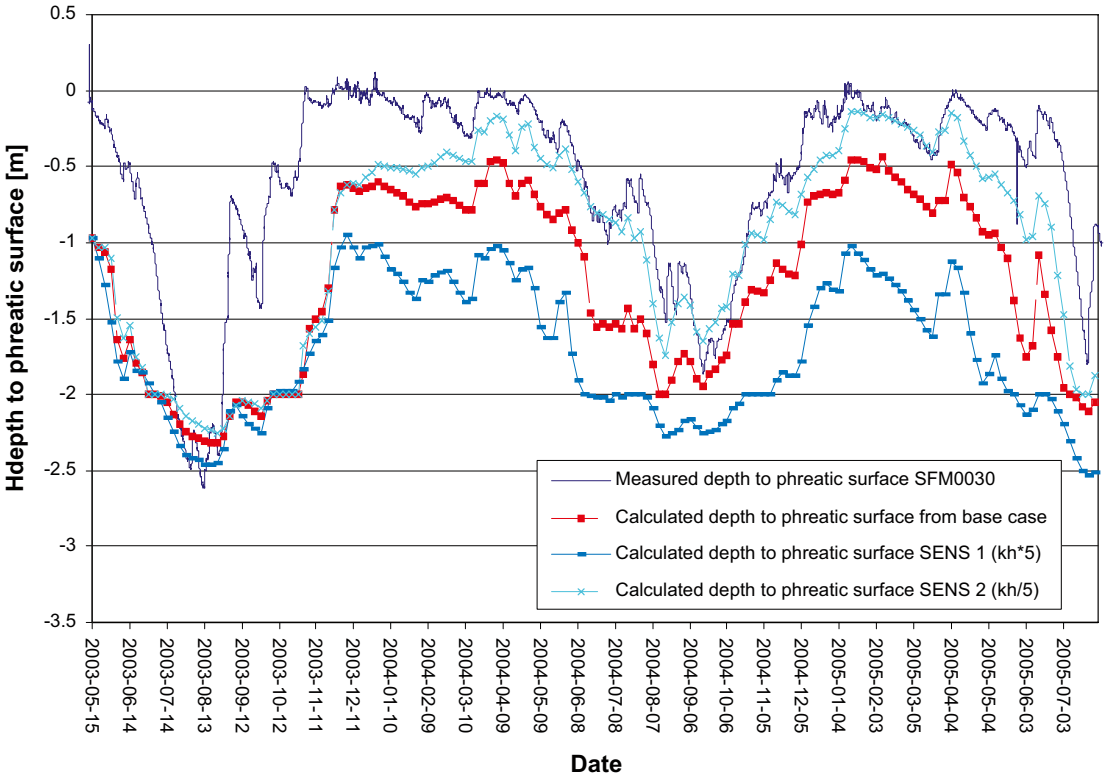

Figure 6-5. *Results in SFM0030 from the sensitivity analysis of the horizontal conductivity in the soil layers.*

Table 6-2 shows a comparison of statistical mean absolute errors. Sens 1, with increased horizontal hydraulic conductivities in the soil layers, generally yields an improved agreement between observed and calculated data.

6.1.2 Vertical hydraulic conductivitiy in lake sediments

Based on results presented in section 6.1.1, the subsequent sensitivity analysis includes the increased horizontal hydraulic conductivities in the soil layers from Sens 1. The base case showed a generally good agreement between measured and observed water levels in most of the lakes. Below the lakes Fiskarfjärden and Gällsboträsket, the contact between the lake and the groundwater was too small, resulting in to little groundwater flow into the lakes and too high groundwater head elevations. To increase the contact in these areas, the vertical hydraulic conductivities of the lake sediments clay and gyttja were increased from $1 \cdot 10^{-8}$ m/s to $1 \cdot 10^{-6}$ m/s below Lake Gällsboträsket and to $2 \cdot 10^{-7}$ m/s below Lake Fiskarfjärden.

Figures 6-6 to 6-10 show a comparison between measured head elevations, calculated head elevations from Sens 1 and the results from Sens 3. The effect of the parameter change is only noted for SFM0012, located below Lake Gällsboträsket, where the head elevation is lowered by around 20 cm (see Figure 6-7). There is also a considerable improvement for SFM0022 (not shown in the figures), located below Lake Fiskarfjärden.

Table 6-2. Comparison of statistical mean absolute errors (MAE) between base case, Sens 1 and Sens 2. "+" represents an improvement, "o" no change and "–" reduced agreement compared to base case.

Borehole	MAE, base case	MAE, Sens 1 (K_h soil·5)	MAE, Sens 2 (K_h soil/5)	Improved agreement with Sens 1 (K_h soil·5)	Improved agreement with Sens 2 (K_h soil/5)
SFM0001	0.7	0.78	0.62	–	+
SFM0002	0.25	0.22	0.26	+	–
SFM0003	0.36	0.27	0.4	+	–
SFM0010	0.41	0.29	0.46	+	–
SFM0011	0.07	0.07	0.08	o	–
SFM0012	0.23	0.26	0.22	–	+
SFM0014	0.43	0.27	0.55	+	–
SFM0015	0.05	0.05	0.05	o	o
SFM0016	0.09	0.1	0.09	–	o
SFM0017	0.26	0.24	0.28	+	–
SFM0018	0.58	0.37	0.72	+	–
SFM0019	0.44	0.44	0.44	o	o
SFM0020	0.2	0.21	0.2	–	o
SFM0021	0.43	0.55	0.37	–	+
SFM0022	0.43	0.31	0.48	+	–
SFM0023	0.06	0.06	0.06	o	o
SFM0030	0.69	1.11	0.46	–	+
SFM0033	0.2	0.15	0.23	+	–
SFM0036	0.39	0.2	0.53	+	–
SFM0039	0.04	0.04	0.04	o	o
SFM0040	0.04	0.04	0.04	o	o
SFM0041	0.03	0.03	0.03	o	o
SFM0049	1.17	1.11	1.22	+	–
SFM0057	0.2	0.17	0.27	+	–
SFM0058	0.45	0.25	0.58	+	–
SFM0062	0.07	0.07	0.08	o	–
SFM0064	0.1	0.08	0.11	+	–

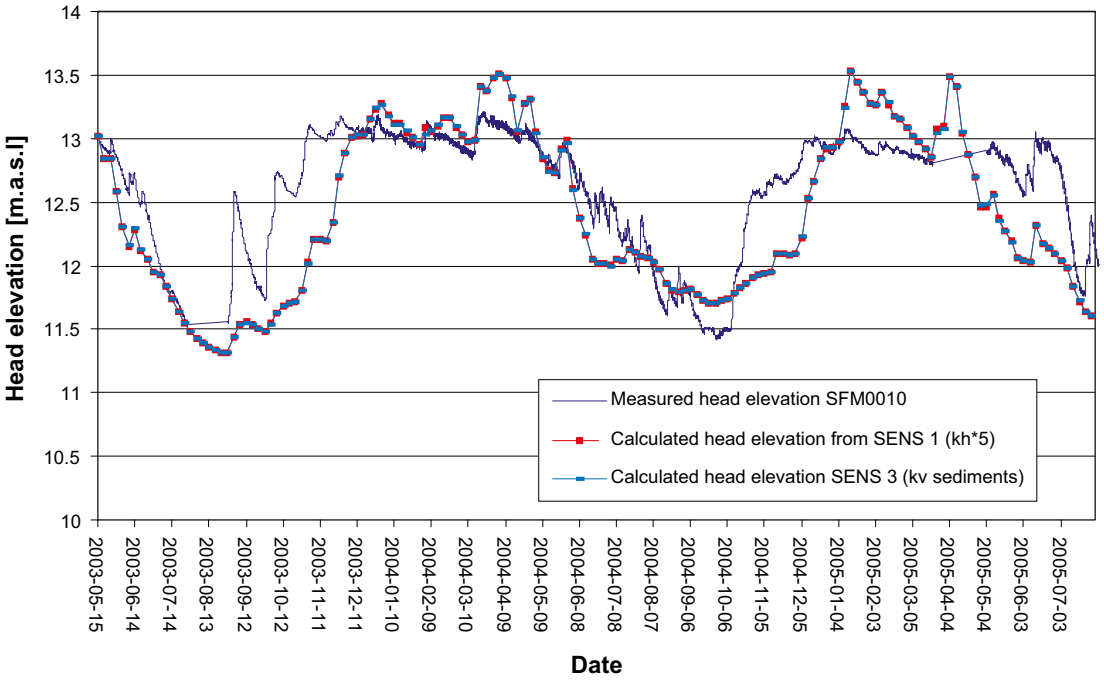

Figure 6-6. *Results in SFM0010 from sensitivity analysis of the vertical conductivity in lake sediments. The simulation was based on Sens 1 (with increased horizontal conductivity in the soil layers).*

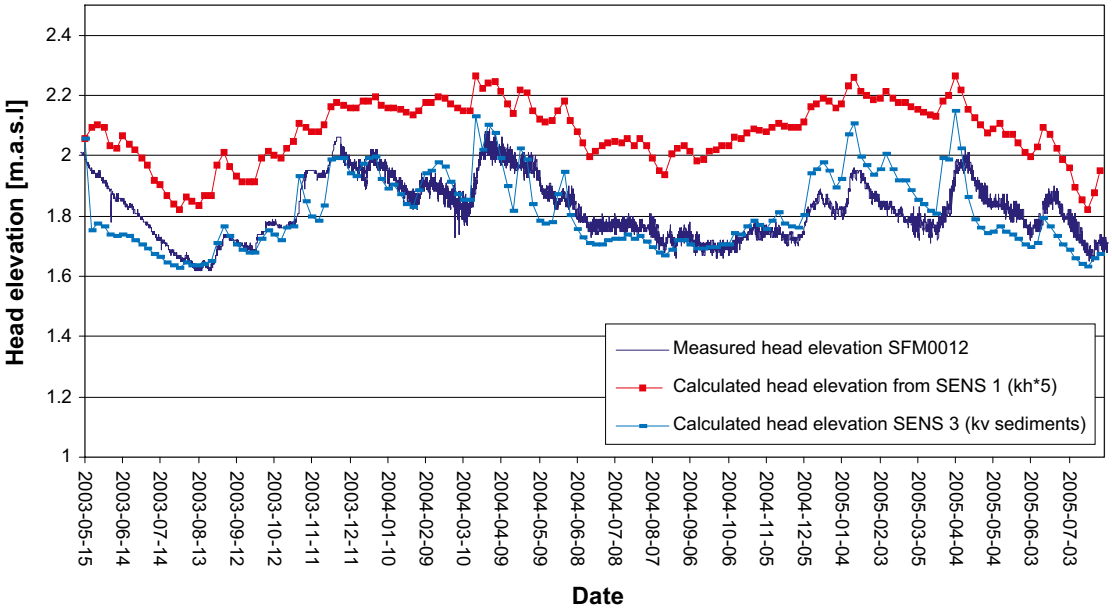

Figure 6-7. *Results in SFM0012 from the sensitivity analysis of the vertical conductivity in lake sediments. The simulation was based on Sens 1 (with increased horizontal conductivity in the soil layers).*

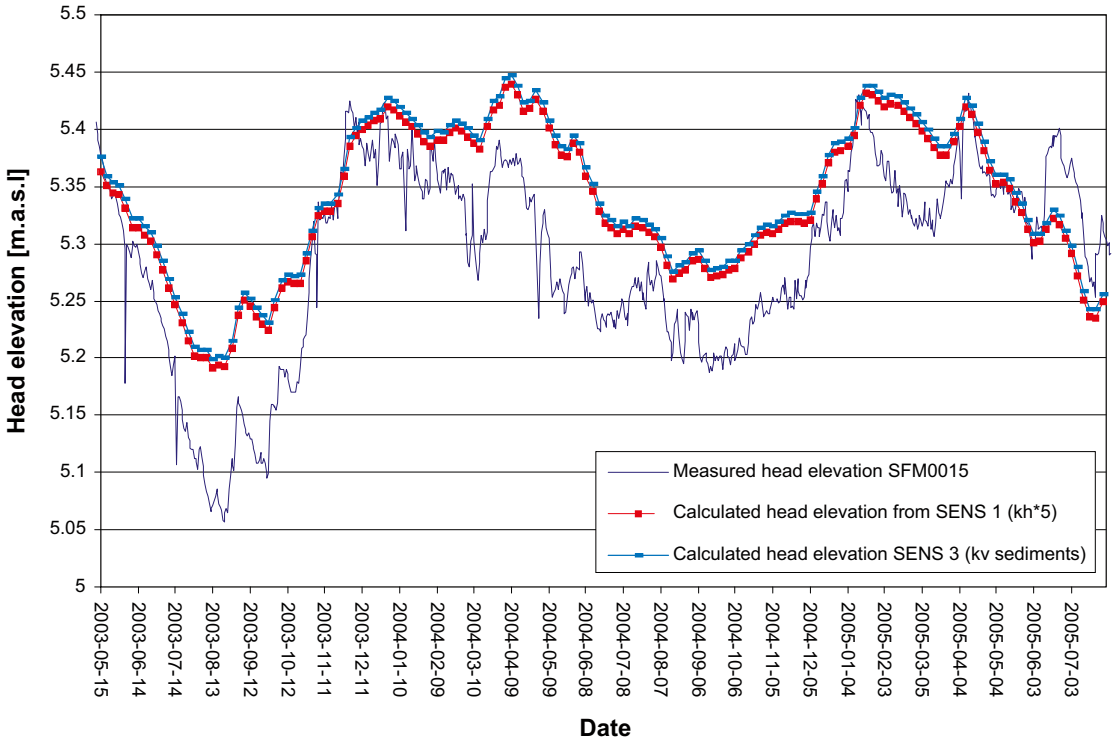

Figure 6-8. *Results in SFM0015 from the sensitivity analysis of the vertical conductivity in lake sediments. The simulation was based on Sens 1 (with increased horizontal conductivity in the soil layers).*

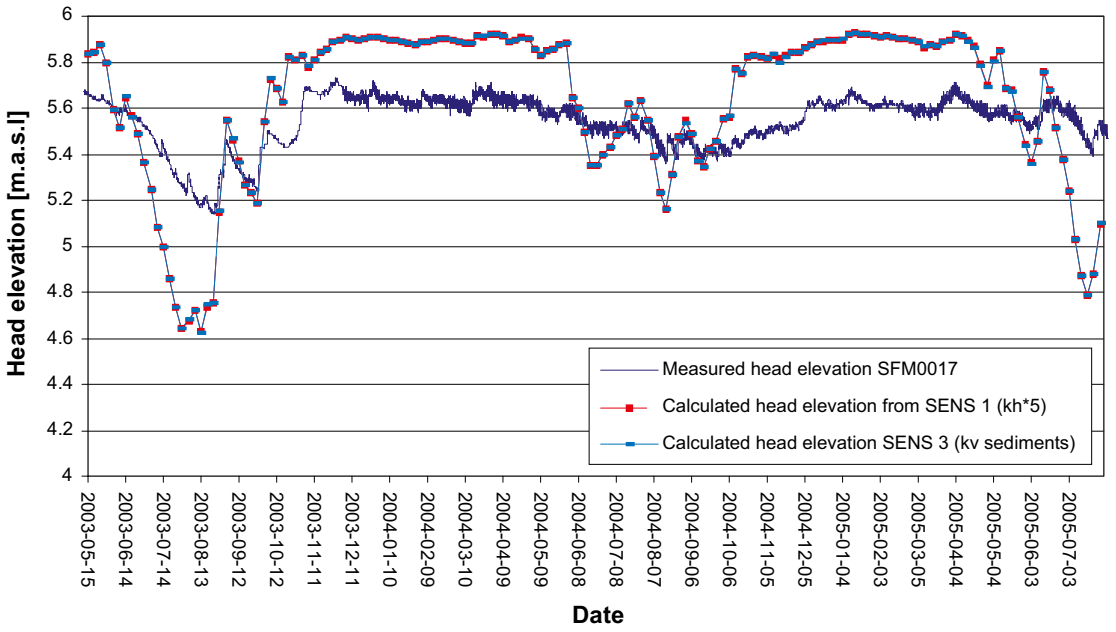

Figure 6-9. *Results in SFM0017 from the sensitivity analysis of the vertical conductivity in lake sediments. The simulation was based on Sens 1 (with increased horizontal conductivity in the soil layers).*

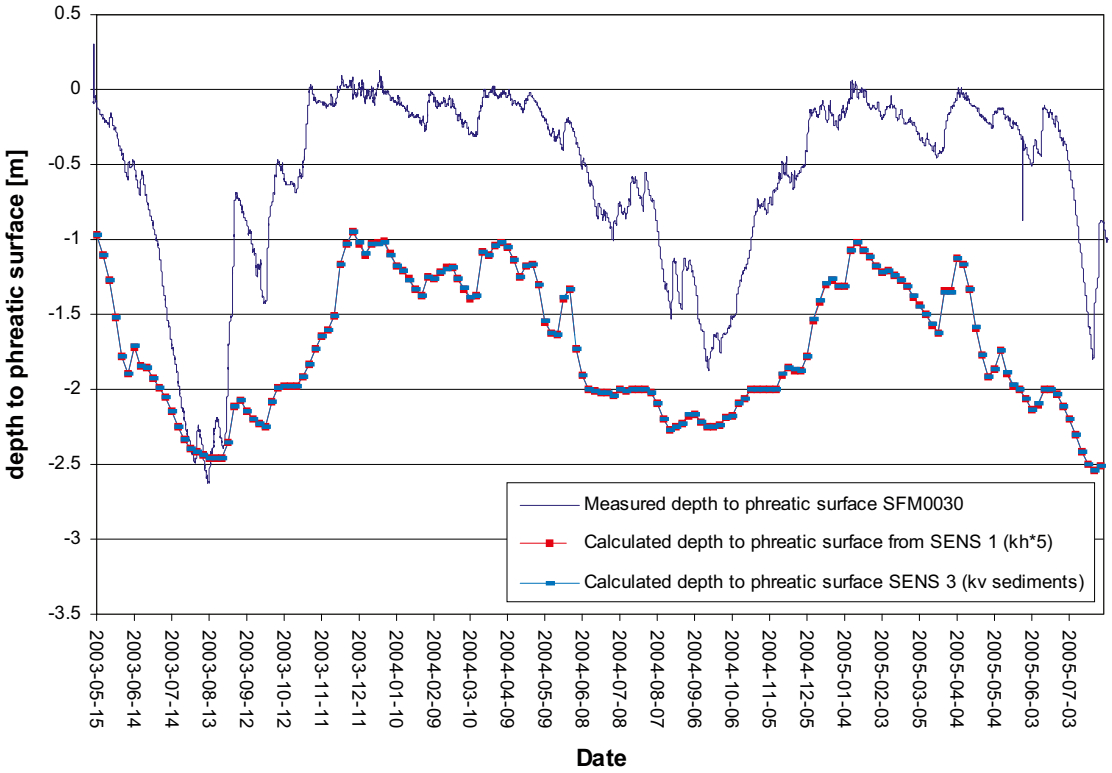

Figure 6-10. *Results in SFM0030 from the sensitivity analysis of the vertical conductivity in lake sediments. The simulation was based on Sens 1 (with increased horizontal conductivity in the soil layers).*

Table 6-3 shows a comparison of statistical mean absolute errors between Sens 1 and Sens 3. Sens 3, with increased vertical hydraulic conductivities in the lake sediments below Fiskarfjärden and Gällsboträsket, shows an improved agreement between observed and calculated data mainly for boreholes close to these lakes, and no or little effect on other boreholes.

6.1.3 Vertical hydraulic conductivity in geological soil layers

Based on the results presented in section 6.1.2, the subsequent sensitivity analysis includes the parameters from Sens 3, i.e. increased horizontal hydraulic conductivities in the soil layers, and increased vertical hydraulic conductivities in the lake sediments below Fiskarfjärden and Gällsboträsket.

In Sens 4, the vertical hydraulic conductivity in the geological soil layers was reduced by a factor of 10, which generally yields a higher calculated groundwater level. Figures 6-11 to 6-15 show a comparison between measured head elevations, calculated head elevations from Sens 3 and the results from Sens 4.

Table 6-3. Comparison of statistical mean absolute errors (MAE) between Sens 1 and Sens 3. "+" represents an improvement, "o" no change and "–" reduced agreement compared to Sens 1.

Borehole	MAE, Sens 1 (K_h soil·5)	MAE, Sens 3 (K_h soil·5, K_v lake sediments)	Improved agreement with Sens 3
SFM0001	0.78	0.78	o
SFM0002	0.22	0.22	o
SFM0003	0.27	0.27	o
SFM0010	0.29	0.28	+
SFM0011	0.07	0.07	o
SFM0012	0.26	0.06	+
SFM0014	0.27	0.27	o
SFM0015	0.05	0.05	o
SFM0016	0.10	0.10	o
SFM0017	0.24	0.24	o
SFM0018	0.37	0.37	o
SFM0019	0.44	0.44	o
SFM0020	0.21	0.21	o
SFM0021	0.55	0.55	o
SFM0022	0.31	0.11	+
SFM0023	0.06	0.06	o
SFM0030	1.11	1.11	o
SFM0033	0.15	0.15	o
SFM0036	0.2	0.2	o
SFM0039	0.04	0.04	o
SFM0040	0.04	0.04	o
SFM0041	0.03	0.03	o
SFM0049	1.11	1.11	o
SFM0057	0.17	0.17	o
SFM0058	0.25	0.25	o
SFM0062	0.07	0.07	o
SFM0064	0.08	0.08	o

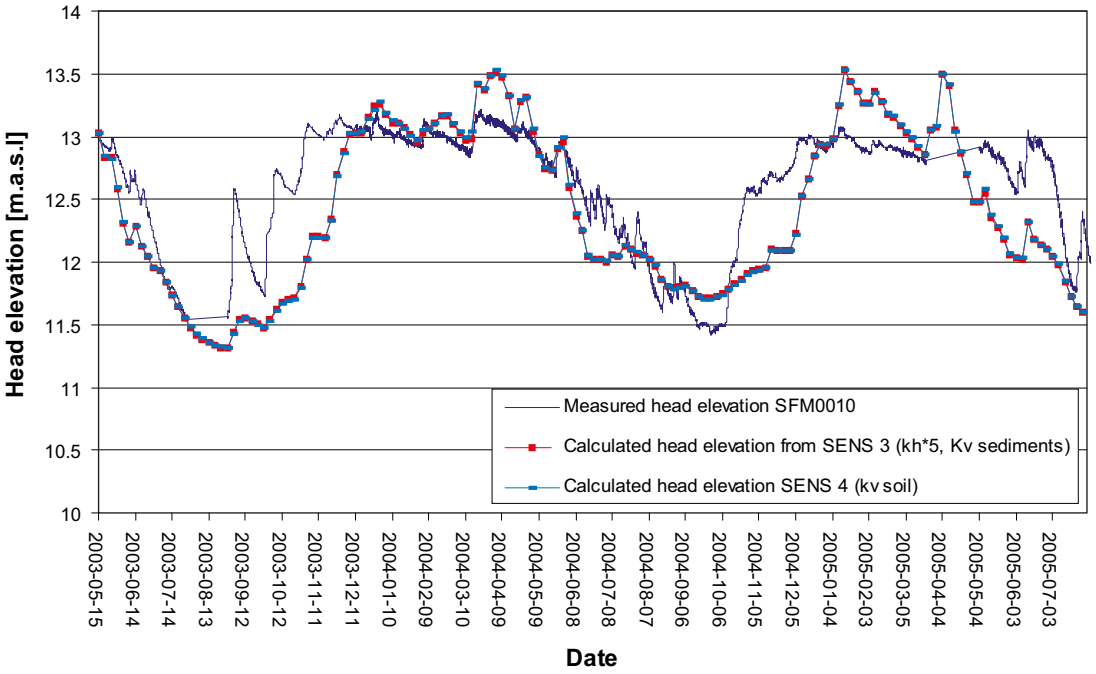

Figure 6-11. *Results in SFM0010 from the sensitivity analysis of the vertical conductivity in geological soil layers. The simulation was based on Sens 3 (with increased horizontal conductivity in the soil layers and increased vertical conductivity in sediments below the lakes Fiskarfjärden and Gällsboträsket).*

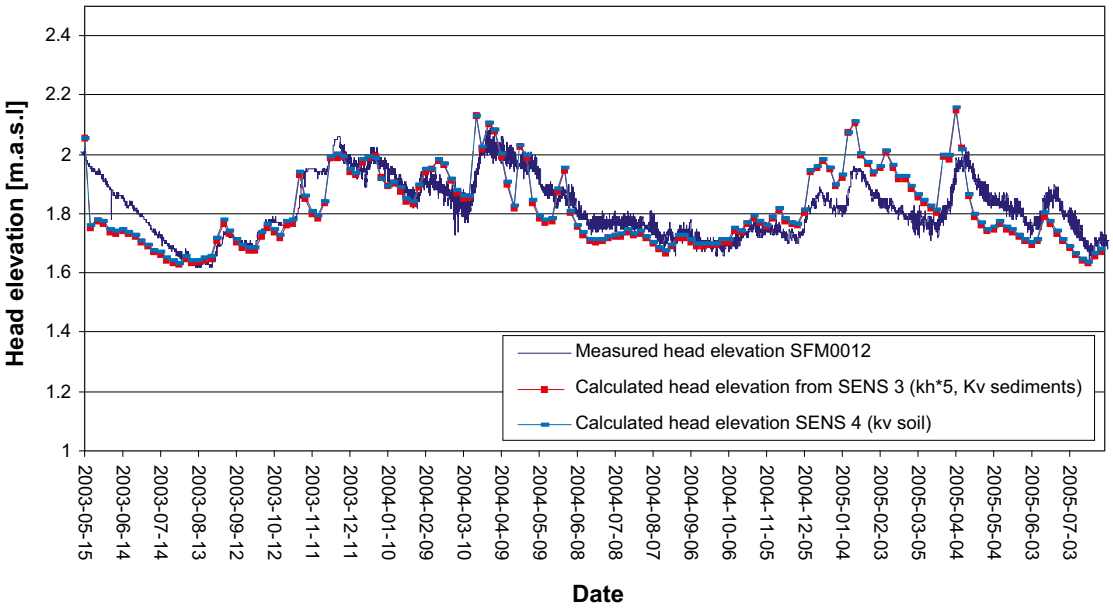

Figure 6-12. *Results in SFM0012 from the sensitivity analysis of the vertical conductivity in geological soil layers. The simulation was based on Sens 3 (with increased horizontal conductivity in the soil layers and increased vertical conductivity in sediments below the lakes Fiskarfjärden and Gällsboträsket).*

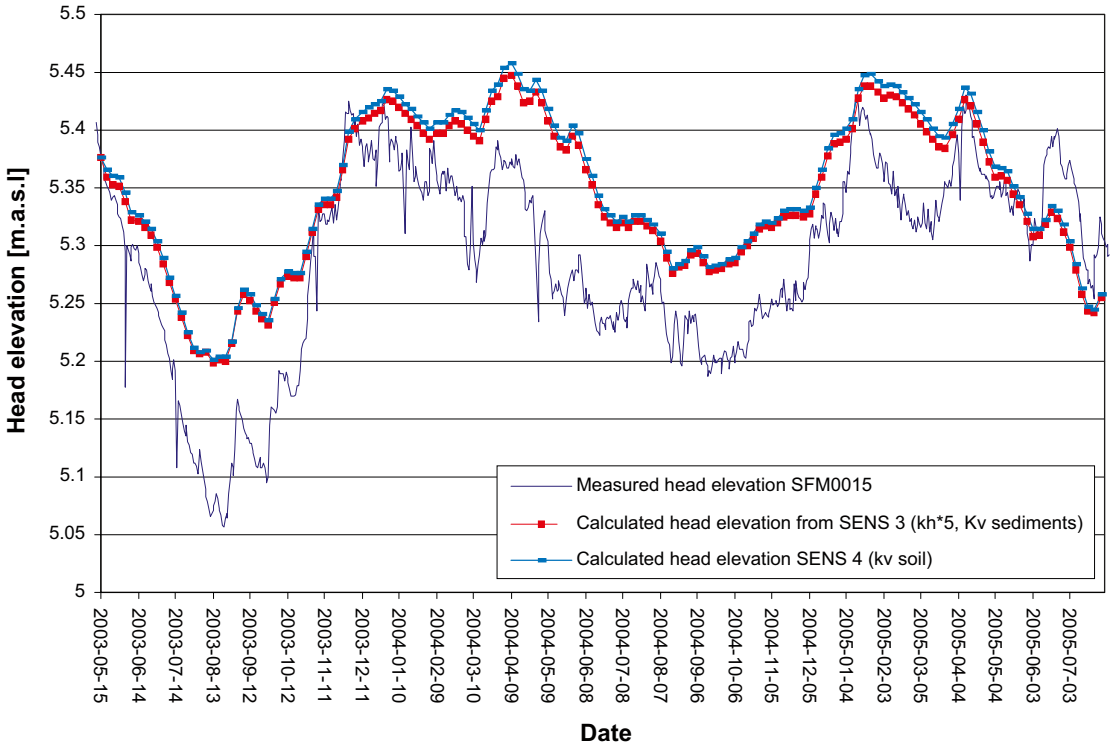

Figure 6-13. *Results in SFM0015 from the sensitivity analysis of the vertical conductivity in geological soil layers. The simulation was based on Sens 3 (with increased horizontal conductivity in the soil layers and increased vertical conductivity in sediments below the lakes Fiskarfjärden and Gällsboträsket).*

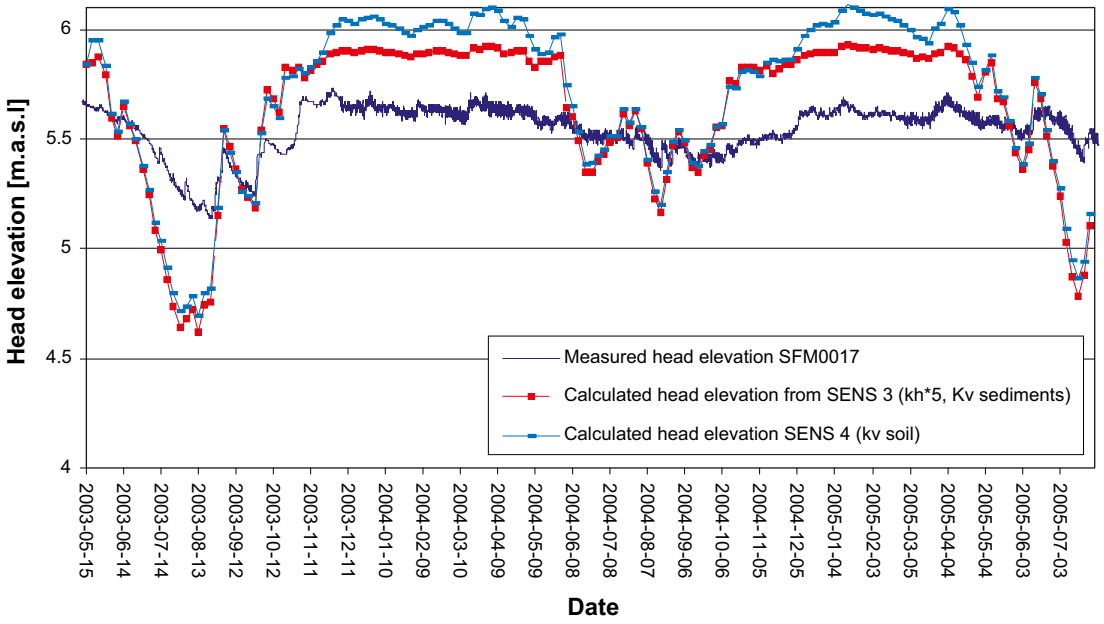

Figure 6-14. *Results in SFM0017 from the sensitivity analysis of the vertical conductivity in geological soil layers. The simulation was based on Sens 3 (with increased horizontal conductivity in the soil layers and increased vertical conductivity in sediments below the lakes Fiskarfjärden and Gällsboträsket).*

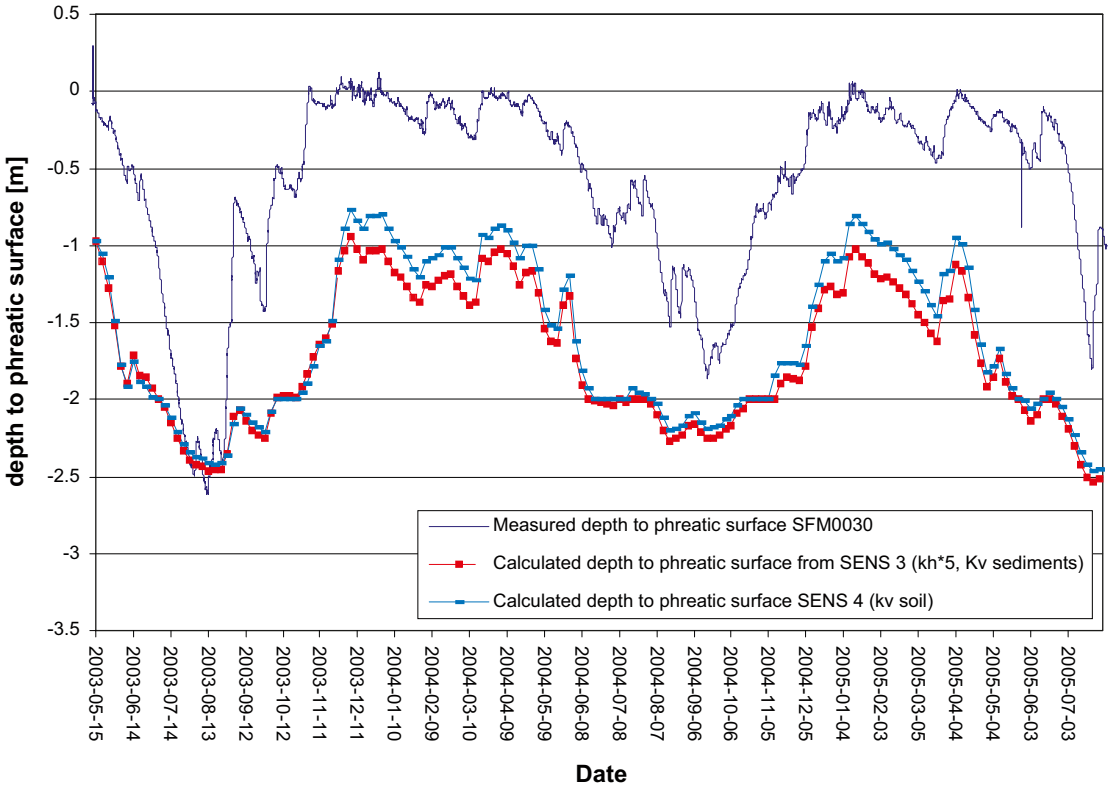

Figure 6-15. *Results in SFM0030 from the sensitivity analysis of the vertical conductivity in geological soil layers. The simulation was based on Sens 3 (with increased horizontal conductivity in the soil layers and increased vertical conductivity in sediments below the lakes Fiskarfjärden and Gällsboträsket).*

Table 6-4 shows a comparison of statistical mean errors between Sens 3 and Sens 4. Sens 4, with reduced vertical hydraulic conductivities in the geological soil layers, shows an improvement in some boreholes, no change in a number of boreholes and a reduced agreement in some boreholes. For the boreholes with a reduced agreement, the changes are very small, whereas for others the result is a time series with better agreement with observations. Therefore, the reduction of the vertical hydraulic conductivity in the soil layers was kept in subsequent simulations.

6.1.4 Summary of hydraulic conductivity results

Overall, the results from the sensitivity analysis of the hydraulic conductivities in the saturated zone indicate a correlation between the location of the borehole in the interpolated model topography and the effect of the different sensitivity cases. Most boreholes with an improved agreement for a higher horizontal conductivity are located on a local high or hillside. Reducing the horizontal conductivity provides a significant improvement in three boreholes, all located in a local depressions. For boreholes where a decrease of the horizontal conductivity yields a better agreement, a reduction of the vertical conductivity also improves the agreement. Theoretically combining the different tested conductivities, around 80% of the analyzed boreholes have an error of less than 0.3 m. However, six boreholes still have large deviations from the observed data. In four of these, it is likely that the interpolated topography is causing the deviations.

Table 6-5 shows how a combination of the different hydraulic conductivity cases, from Sens 1 to Sens 4, results in an “optimum” solution for each borehole. Note that such an “optimum” simulation has not actually been performed.

Table 6-4. Comparison of statistical mean absolute errors (MAE) between Sens 3 and Sens 4. "+" represents an improvement, "o" no change and "–" reduced agreement compared to Sens 3.

Borehole	MAE, Sens 3 (K_h soil·5, K_v lake sediments)	MAE, Sens 4 (K_h soil·5, K_v lake sediments, K_v soil/10)	Improved agreement with Sens 4
SFM0001	0.78	0.76	+
SFM0002	0.22	0.22	o
SFM0003	0.27	0.28	–
SFM0010	0.28	0.28	o
SFM0011	0.07	0.07	o
SFM0012	0.06	0.06	o
SFM0014	0.27	0.31	–
SFM0015	0.05	0.06	–
SFM0016	0.1	0.13	–
SFM0017	0.24	0.32	–
SFM0018	0.37	0.4	–
SFM0019	0.44	0.37	+
SFM0020	0.21	0.21	o
SFM0021	0.55	0.66	–
SFM0022	0.11	0.19	–
SFM0023	0.06	0.06	o
SFM0030	1.11	1.03	+
SFM0033	0.15	0.14	+
SFM0036	0.2	0.21	–
SFM0039	0.04	0.04	o
SFM0040	0.04	0.04	o
SFM0041	0.03	0.03	o
SFM0049	1.11	1.11	o
SFM0057	0.17	0.17	o
SFM0058	0.25	0.26	–
SFM0062	0.07	0.07	o
SFM0064	0.08	0.08	o

Table 6-5. Comparison of statistical mean absolute errors (m) between tested variations on hydraulic conductivities in the saturated zone to find an optimum solution.

Borehole	Location in interpolated DEM	Base case	K_h·5	K_h/5	K_v sed·100 (K_h·5)	K_v/10 (K_h·5, K_v sed·100)	Choice of best K
SFM0001	Local depression	0.70	0.78	0.62	0.78	0.76	**0.62**
SFM0002	Slope or local height	0.25	0.22	0.26	0.22	0.22	**0.22**
SFM0003	Slope or local height	0.36	0.27	0.40	0.27	0.28	**0.27**
SFM0010	Slope or local height	0.41	0.28	0.46	0.28	0.28	**0.28**
SFM0011	Local depression	0.07	0.07	0.08	0.07	0.07	**0.07**
SFM0012	Lake bottom	0.23	0.26	0.22	0.06	0.06	**0.06**
SFM0014	Slope or local height	0.43	0.27	0.55	0.27	0.31	**0.27**
SFM0015	Lake bottom	0.05	0.05	0.05	0.05	0.06	**0.05**
SFM0016	Slope or local height	0.09	0.10	0.09	0.10	0.13	**0.09**
SFM0017	Slope or local height	0.26	0.24	0.28	0.24	0.32	**0.24**
SFM0018	Slope or local height	0.58	0.37	0.72	0.37	0.40	**0.37**
SFM0019	Local depression	0.44	0.44	0.44	0.44	0.37	**0.37**
SFM0020	Local depression	0.20	0.21	0.20	0.21	0.21	**0.20**
SFM0021	Local depression	0.43	0.55	0.37	0.55	0.66	**0.37**
SFM0022	Lake bottom	0.43	0.31	0.48	0.11	0.19	**0.11**
SFM0023	Lake bottom	0.06	0.06	0.06	0.06	0.06	**0.06**
SFM0030	Local depression	0.69	1.11	0.46	1.11	1.03	**0.46**
SFM0033	Lake bottom	0.20	0.15	0.23	0.15	0.14	**0.15**
SFM0036	Slope or local height	0.39	0.20	0.53	0.20	0.21	**0.20**
SFM0039	Lake bottom	0.04	0.04	0.04	0.04	0.04	**0.04**
SFM0040	Lake bottom	0.04	0.04	0.04	0.04	0.04	**0.04**
SFM0041	Lake bottom	0.03	0.03	0.03	0.03	0.03	**0.03**
SFM0049	Local depression	1.17	1.11	1.22	1.11	1.11	**1.11**
SFM0057	Slope or local height	0.20	0.17	0.27	0.17	0.17	**0.17**
SFM0058	Slope or local height	0.45	0.25	0.58	0.25	0.26	**0.25**
SFM0062	Lake bottom	0.07	0.07	0.08	0.07	0.07	**0.07**
SFM0064	Lake bottom	0.10	0.08	0.11	0.08	0.08	**0.08**
Mean error		0.31					**0.23**

6.2 Topography

Four grid cells demonstrate a deviation of 1 m or more between the interpolated DEM and the actual measured ground surface elevation. The model topography was changed manually at these grid cells, and used in a simulation based on Sens 4; this sensitivity case involves an increased horizontal conductivity in the soil layers, a reduced vertical conductivity in the lake sediments underneath Gällsboträsket and Fiskarfjärden, and a reduced vertical conductivity in the soil layers. Table 6-6 summarizes the corrections that were made in the model topography. The changes were made on a pre-processed DEM, with a grid resolution of 40 m.

Figures 6-16 to 6-19 show a comparison between measured head elevations, calculated head elevations from Sens 4, and the results from Sens 5. During the wet season, groundwater levels in SFM0019 are raised by around 10 cm, whereas the change is very small during summers. In SFM0058, during summer the effect on the head elevation is around 10 cm. In SFM0021, the change in the local topography results in a groundwater table above the ground surface. Moreover, in SFM0030 there is no effect, which indicates that the groundwater level follows the topography.

Table 6-7 shows a comparison of statistical mean absolute errors between Sens 4 and Sens 5. Sens 5, with a correction made of the local topography, shows an improved agreement with observations in three points, and no or small effects in other areas. The topographic corrections to the pre-processed DEM were kept in subsequent simulations.

Table 6-6. Manual corrections to the interpolated DEM.

Borehole ID	Correction (m)
SFM0019	+0.92
SFM0021	–1.15
SFM0030	–1.40
SFM0058	–1.72

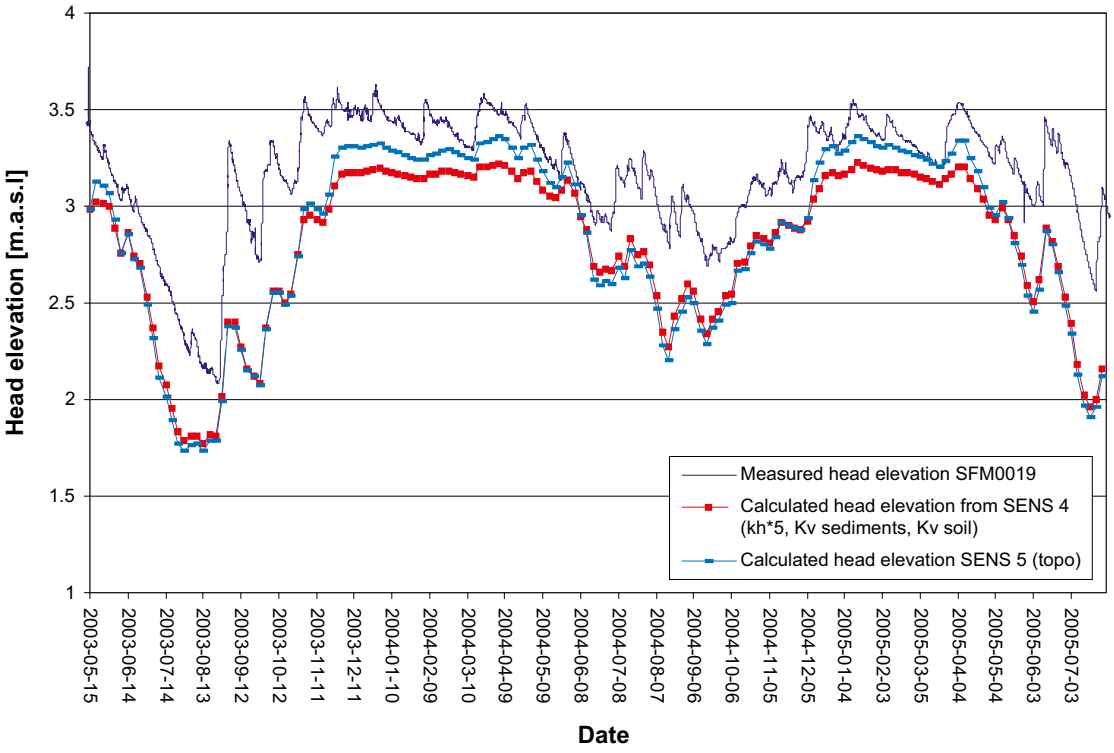

Figure 6-16. *Results in SFM0019 from the sensitivity analysis of local topographical deviations. The simulation was based on Sens 4 (with increased horizontal conductivity in the soil layers, increased vertical conductivity in sediments below the lakes Fiskarfjärden and Gällsboträsket and decreased vertical conductivity in geological soil layers).*

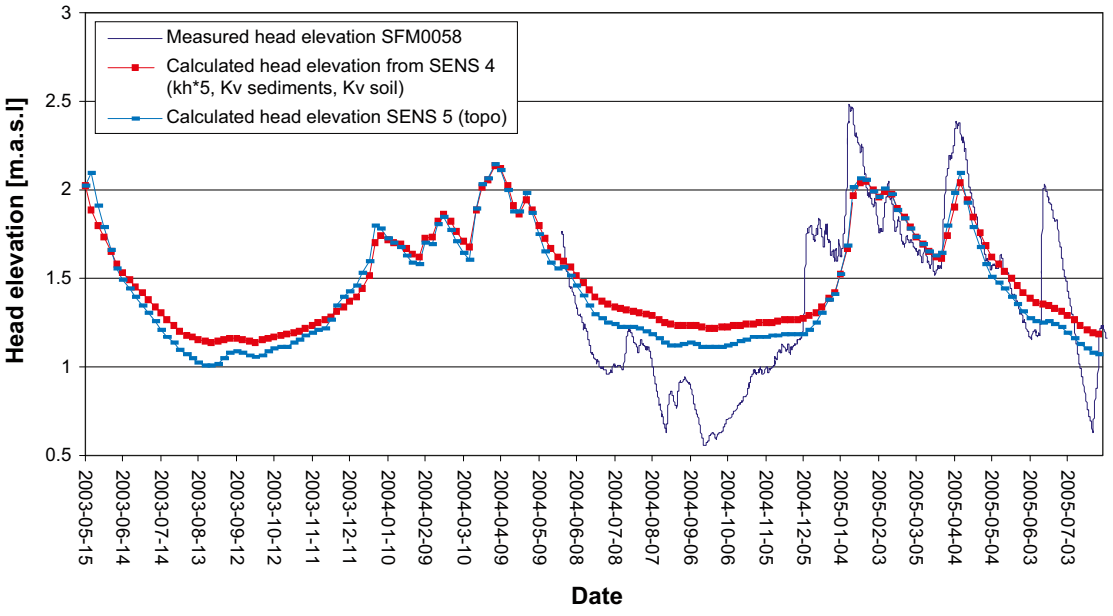

Figure 6-17. *Results in SFM0058 from the sensitivity analysis of local topography deviations. The simulation was based on Sens 4 (with increased horizontal conductivity in the soil layers, increased vertical conductivity in sediments below the lakes Fiskarfjärden and Gällsboträsket, and decreased vertical conductivity in geological soil layers).*

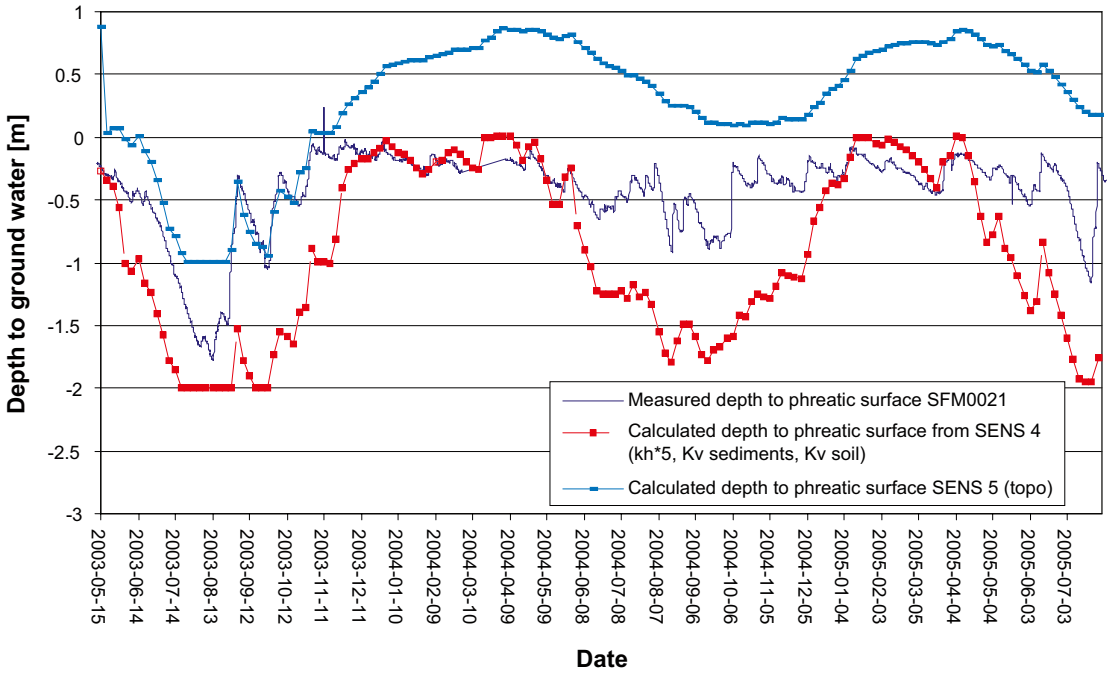

Figure 6-18. *Results in SFM0021 from the sensitivity analysis of local topography deviations. The simulation was based on Sens 4 (with increased horizontal conductivity in the soil layers, increased vertical conductivity in sediments below the lakes Fiskarfjärden and Gällsboträsket, and decreased vertical conductivity in geological soil layers).*

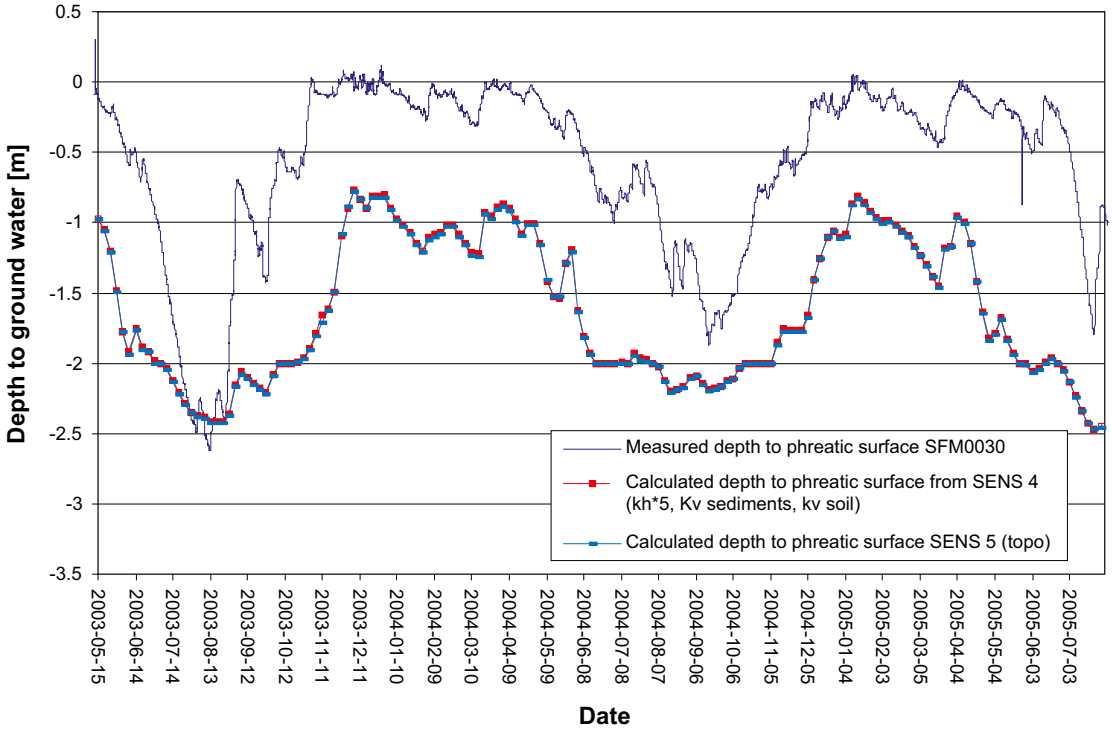

Figure 6-19. *Results in SFM0030 from the sensitivity analysis of local topography deviations. The simulation was based on Sens 4 (with increased horizontal conductivity in the soil layers, increased vertical conductivity in sediments below the lakes Fiskarfjärden and Gällsboträsket, and decreased vertical conductivity in geological soil layers).*

Table 6-7. Comparison of statistical mean absolute errors (MAE) between Sens 4 and Sens 5. "+" represents an improvement, "o" no change and "–" reduced agreement compared to Sens 4.

Borehole	MAE, Sens 4 (K_h soil·5, K_v lake sediments, K_v soil/10)	MAE, Sens 5 (K_h soil·5, K_v lake sediments, K_v soil/10, local topography)	Improved agreement with Sens 5
SFM0001	0.76	0.76	o
SFM0002	0.22	0.22	o
SFM0003	0.28	0.24	+
SFM0010	0.28	0.28	o
SFM0011	0.07	0.07	o
SFM0012	0.06	0.06	o
SFM0014	0.31	0.31	o
SFM0015	0.06	0.06	o
SFM0016	0.13	0.13	o
SFM0017	0.32	0.32	o
SFM0018	0.4	0.4	o
SFM0019	0.37	0.33	+
SFM0020	0.21	0.21	o
SFM0021	0.66	0.66	o
SFM0022	0.19	0.19	o
SFM0023	0.06	0.06	o
SFM0030	1.03	1.03	o
SFM0033	0.14	0.14	o
SFM0036	0.21	0.21	o
SFM0039	0.04	0.04	o
SFM0040	0.04	0.04	o
SFM0041	0.03	0.03	o
SFM0049	1.11	1.11	o
SFM0057	0.17	0.17	o
SFM0058	0.26	0.22	+
SFM0062	0.07	0.07	o
SFM0064	0.08	0.08	o

6.3 Model resolution

One simulation was made to evaluate the effect of the spatial resolution of the model, increasing the horizontal resolution of the numerical grid from 40 to 20 m; the vertical discretization was not changed. A higher grid resolution results in a higher level of detail in the pre-processed DEM, the soil profile definitions and the vegetation parameter distribution. However, the manually corrected topography from Sens 5 was not included in the simulation, as these topography changes were made in the 40 m grid. Therefore, the results are compared to Sens 4. Moreover, due to long simulation times, the model was not run using a hot start as initial condition (the base case hot start was run with a 40 m grid). Thus, the initial conditions differ somewhat from the other sensitivity simulations. Figures 6-20 to 6-24 compare measured head elevations, calculated head elevations from Sens 4, and the results from Sens 6. As can be seen in these figures, the effect of the increased grid resolution is relatively small.

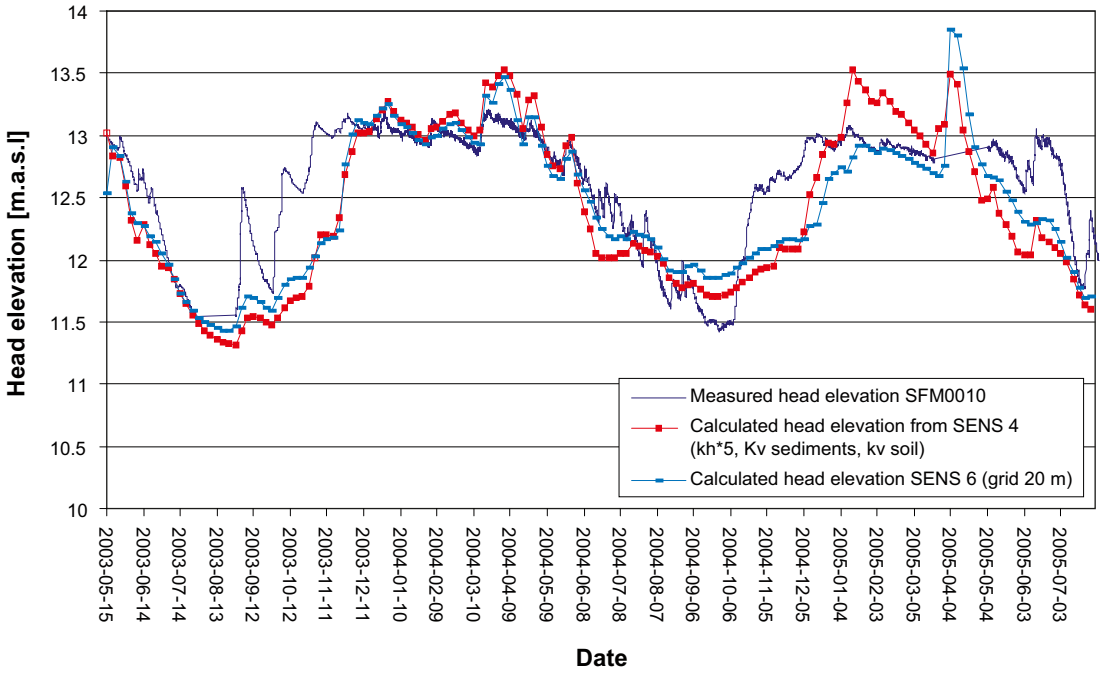

Figure 6-20. *Results in SFM0010 from the sensitivity analysis of the grid resolution. The simulation was based on Sens 4 (with increased horizontal conductivity in the soil layers, increased vertical conductivity in sediments below the lakes Fiskarfjärden and Gällsboträsket, and decreased vertical conductivity in geological soil layers).*

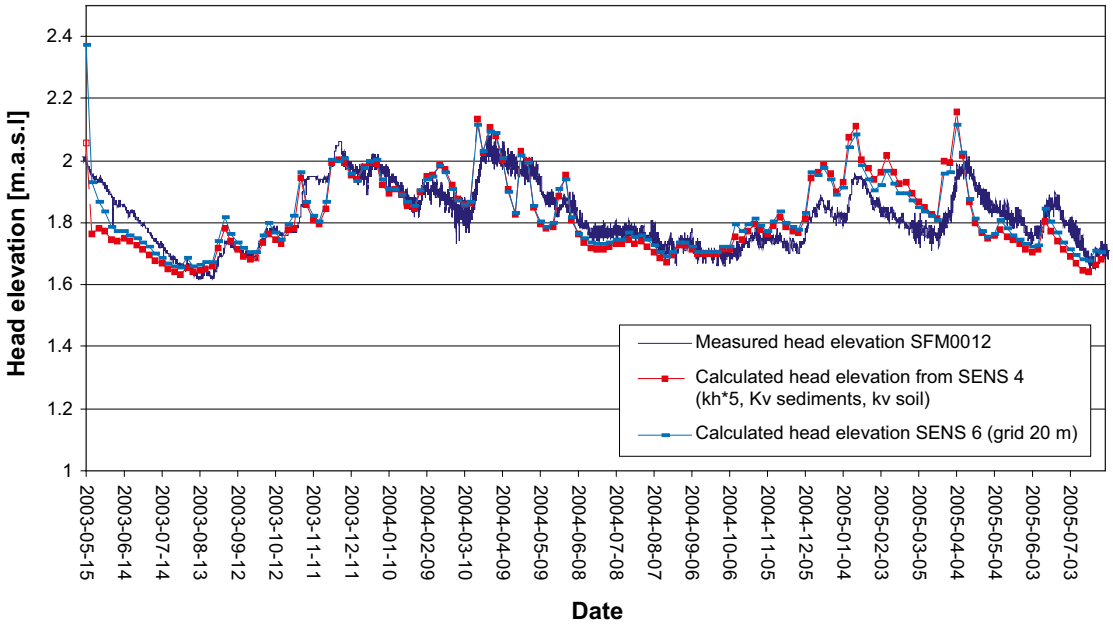

Figure 6-21. *Results in SFM0012 from the sensitivity analysis of the grid resolution. The simulation was based on Sens 4 (with increased horizontal conductivity in the soil layers, increased vertical conductivity in sediments below the lakes Fiskarfjärden and Gällsboträsket, and decreased vertical conductivity in geological soil layers).*

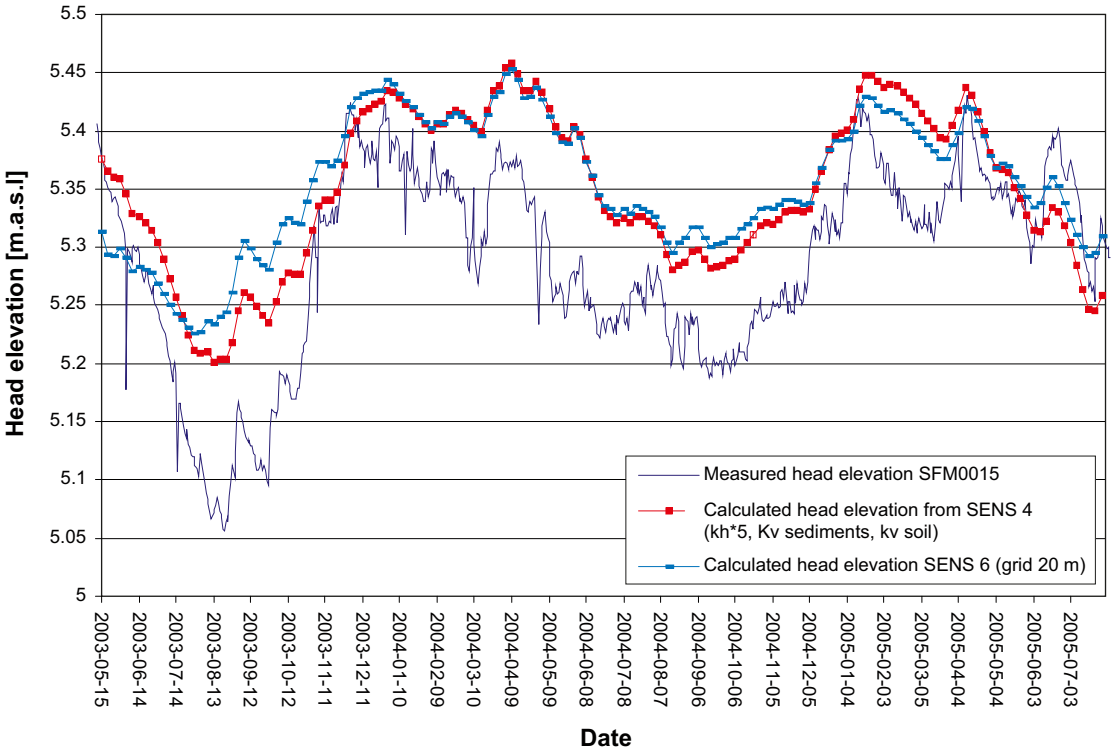

Figure 6-22. *Results in SFM0015 from the sensitivity analysis of the grid resolution. The simulation was based on Sens 4 (with increased horizontal conductivity in the soil layers, increased vertical conductivity in sediments below the lakes Fiskarfjärden and Gällsboträsket, and decreased vertical conductivity in geological soil layers).*

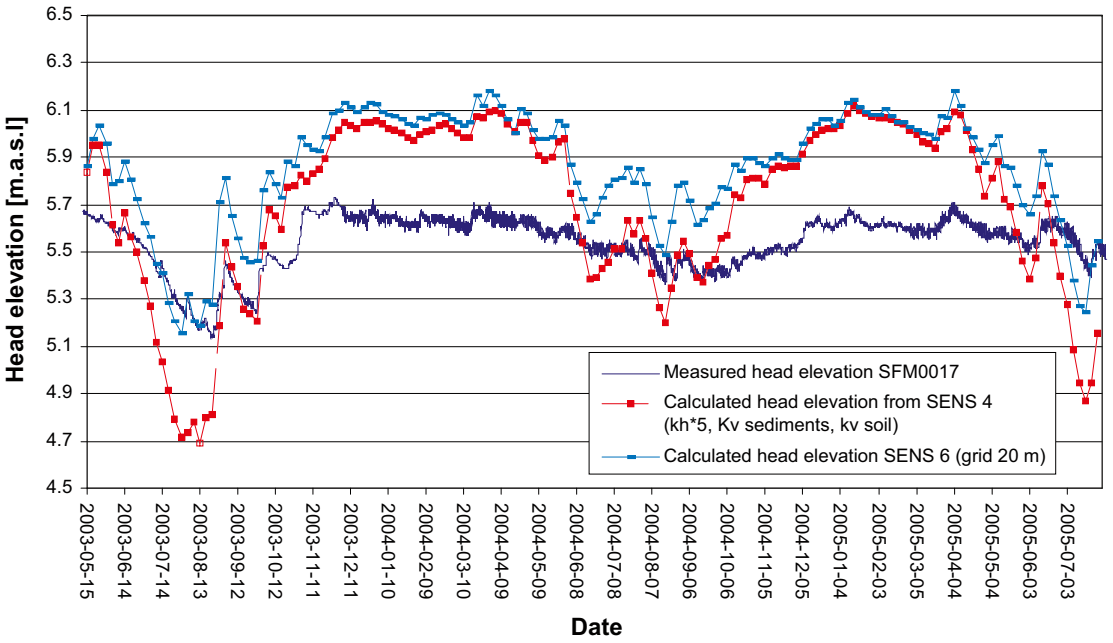

Figure 6-23. *Results in SFM0017 from the sensitivity analysis of the grid resolution. The simulation was based on Sens 4 (with increased horizontal conductivity in the soil layers, increased vertical conductivity in sediments below the lakes Fiskarfjärden and Gällsboträsket, and decreased vertical conductivity in geological soil layers).*

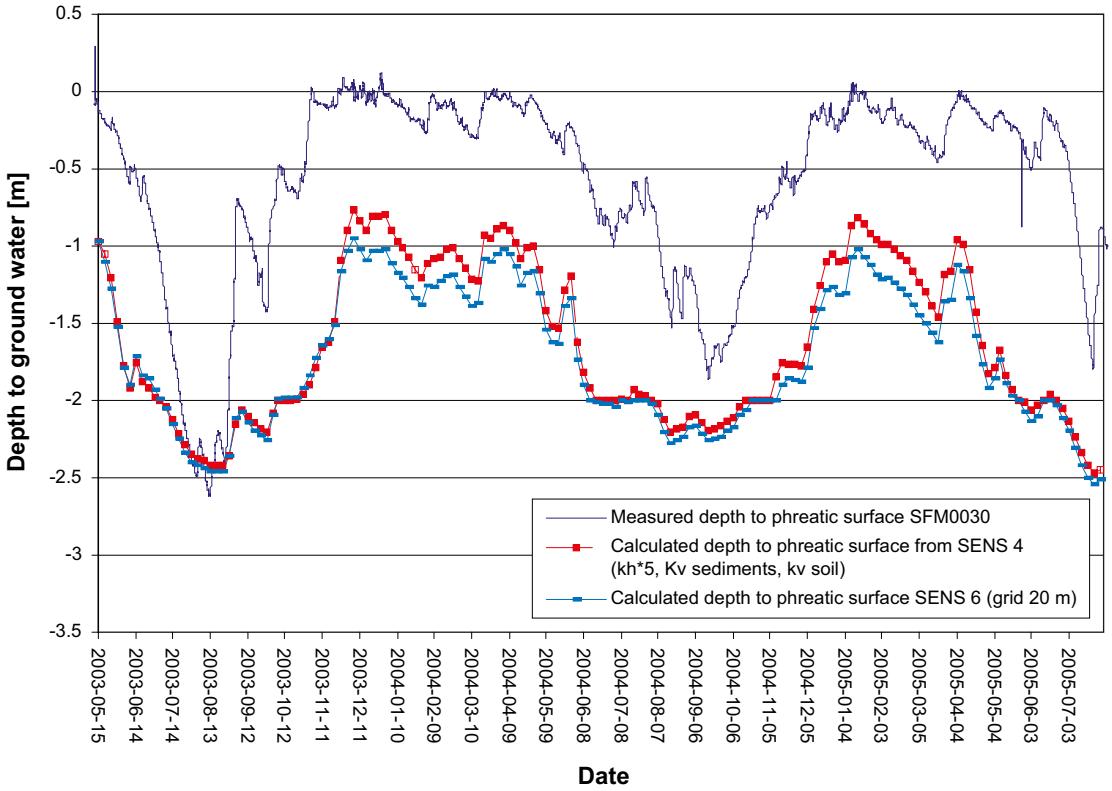

Figure 6-24. *Results in SFM0030 from the sensitivity analysis of the grid resolution. The simulation was based on Sens 4 (with increased horizontal conductivity in the soil layers, increased vertical conductivity in sediments below the lakes Fiskarfjärden and Gällsboträsket, and decreased vertical conductivity in geological soil layers).*

Table 6-8 shows a comparison of statistical mean absolute errors between Sens 4 and Sens 6. The results show that Sens 6 (grid resolution 20 m) has a better agreement between observed and calculated data in 10 of 27 evaluated points. The total absolute mean error changes from 0.28 m to 0.26 m, which indicates that it is not generally beneficial to have a high grid resolution in the input data, especially if the longer simulation times are taken into account.

Table 6-8. Comparison of statistical mean absolute errors (MAE) between Sens 4 and Sens 6. "+" represents an improvement, "o" no change and "–" reduced agreement compared to Sens 4.

Borehole	MAE, Sens 4 (K_h soil·5, K_v lake sediments, K_v soil/10)	MAE, Sens 6 (K_h soil·5, K_v lake sediments, K_v soil/10, 20 m grid)	Improved agreement with Sens 6
SFM0001	0.76	0.7	+
SFM0002	0.22	0.26	–
SFM0003	0.28	0.15	+
SFM0010	0.28	0.22	+
SFM0011	0.07	0.08	–
SFM0012	0.06	0.06	o
SFM0014	0.31	0.2	+
SFM0015	0.06	0.06	o
SFM0016	0.13	0.13	o
SFM0017	0.32	0.37	–
SFM0018	0.4	0.23	+
SFM0019	0.37	0.22	+
SFM0020	0.21	0.14	+
SFM0021	0.66	0.72	–
SFM0022	0.19	0.19	o
SFM0023	0.06	0.07	–
SFM0030	1.03	1.03	o
SFM0033	0.14	0.14	o
SFM0036	0.21	0.18	+
SFM0039	0.04	0.04	o
SFM0040	0.04	0.04	o
SFM0041	0.03	0.04	o
SFM0049	1.11	1.24	–
SFM0057	0.17	0.16	+
SFM0058	0.26	0.32	–
SFM0062	0.07	0.07	o
SFM0064	0.08	0.07	+

6.4 Vegetation parameters

The column model was used to evaluate the effects of the vegetation parameters. The simulation cases are described in sections 6.4.1–4, and the results are presented in section 6.4.5.

6.4.1 Root mass distribution

The root mass distribution, A_{root}, was evaluated using the column model of SFM0010 and SFM0017. The analysis included $A_{root} = 0.5$ (corresponding to a more evenly distributed root mass) and $A_{root} = 2$ (corresponding to more root mass in the uppermost part of the soil profile). The latter A_{root} case means that more water can transpire closer to the ground surface, whereas the former case ($A_{root} = 0.5$) implies that the transpiration has a more even depth distribution.

6.4.2 Leaf area index

The leaf area index, *LAI*, is defined as the area of leaves per unit ground area. This index can typically vary between 0 and 10, depending of vegetation type and season. The leaf area index of coniferous forest, covering large parts of the model area, is set to 7 in the base case simulation. A simulation using a $LAI = 5$ was evaluated using the column model. A smaller *LAI* reduces the leaf density, hence reducing canopy evaporation.

6.4.3 Root depth

The root depth of the crop or vegetation type affects the total evapotranspiration. The root depth for the coniferous forest that covers large parts of the model area is set to 800 mm in the base case simulation. A simulation using a root depth of 500 mm was evaluated in the column model. This increases the transpiration near the ground surface.

6.4.4 Crop coefficient

The crop coefficient, K_c, is used to adjust the "reference" potential evapotranspiration relative to the "actual" potential evapotranspiration of the specific crops in the model area, which directly affects the evapotranspiration. A K_c value of 1, which is used in the base case, means that the maximum potential evapotranspiration will always be equal to the reference potential evapotranspiration. A simulation using a K_c value of 0.9 was evaluated using the column model.

6.4.5 Summary of vegetation parameter results

Figure 6-25 compares the calculated groundwater recharge in SFM0010 for the different sensitivity simulations. Figure 6-26 shows the corresponding result in SFM0017. A positive recharge value equals groundwater recharge, whereas a negative recharge value equals groundwater discharge. Hence, the net recharge value for the whole simulation period reflects both groundwater recharge and the total evapotranspiration; higher recharge values are due to less evapotranspiration, and the contrary for smaller recharge values.

For SFM0010, the total recharge during the simulation period is positive, which means that water infiltrates from the unsaturated zone to the saturated zone. Figure 6-25 shows that a decreased leaf area index (*LAI*) results in less evapotranspiration, and thus more groundwater recharge. Reducing the root depth yields a slight reduction of the net recharge. The crop coefficient (K_c) decreases the evapotranspiration, which also results in more groundwater recharge. Decreasing the root mass distribution A_{root} (i.e. to a more even root mass distribution) reduces the evapotranspiration and therefore also the groundwater recharge. Moreover, a higher A_{root} allows more evapotranspiration close to the ground surface, which slightly reduces groundwater recharge.

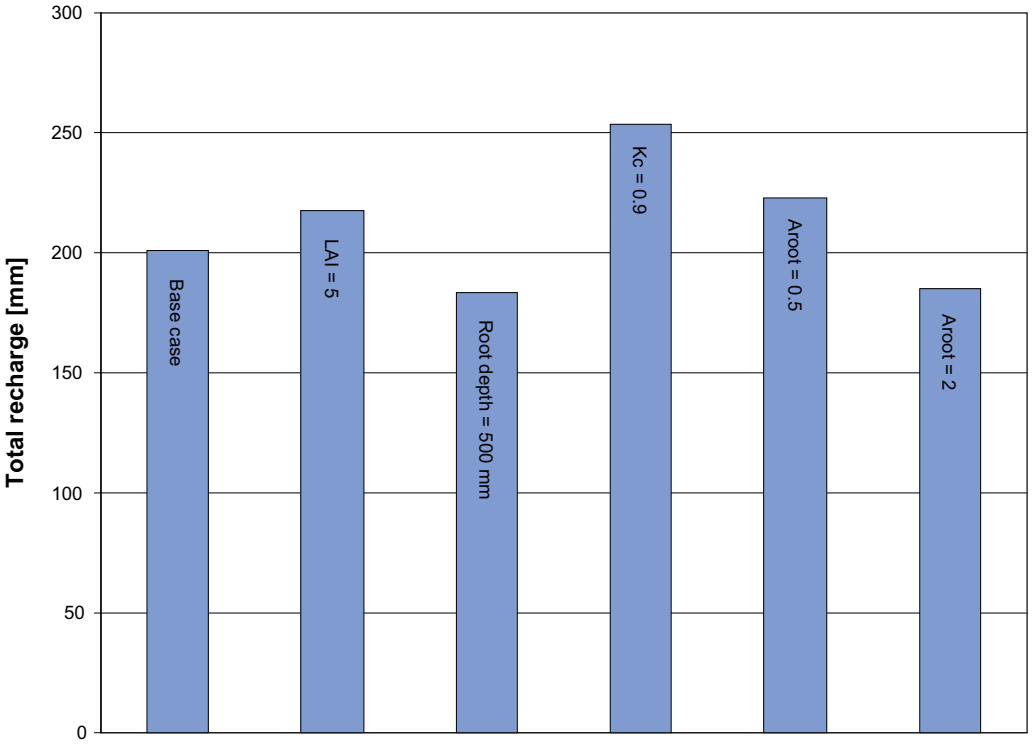

Figure 6-25. *Comparison between the total groundwater recharge for SFM0010, based on the different sensitivity simulations of vegetation parameters (May 2003 to May 2005).*

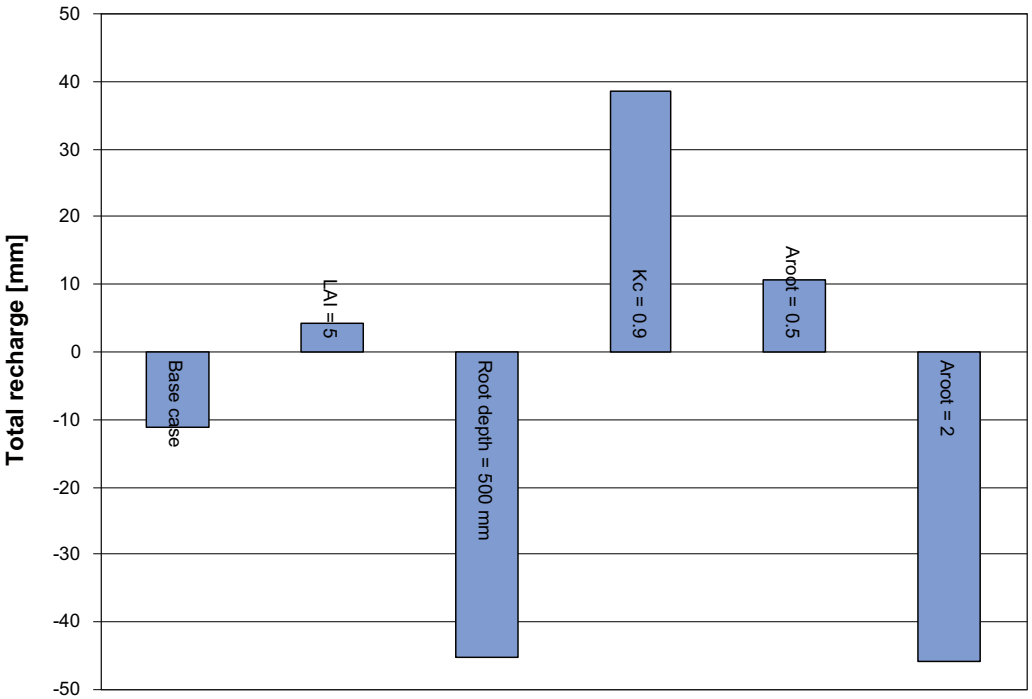

Figure 6-26. *Comparison between the total recharge for SFM0017 for the different sensitivity simulations of vegetation parameters (May 2003 to May 2005).*

For SFM0017, the total groundwater recharge over the simulated period is negative in the base case, which means that groundwater discharges from the saturated zone to the unsaturated zone. According to Figure 6-26, decreasing the leaf area index (*LAI*) results in a smaller evapotranspiration, and thus increases the recharge to a positive value. Reducing the root depth, the net discharge from the saturated zone increases. Decreasing the crop coefficient (K_c) decreases the evapotranspiration, which results in more recharge. Moreover, decreasing the root mass distribution (A_{root}) to a more even distribution reduces the evapotranspiration with a higher recharge as result; increasing A_{root} allows a higher evapotranspiration close to the ground surface, which in turn increases the evapotranspiration and thus the total groundwater discharge.

SFM0017 is located in a typical groundwater discharge area. Increasing the evapotranspiration in such an area increases upward water flow. This is especially significant in cases considering small root depths and high A_{root} values. Decreasing the evapotranspiration, e.g. by lowering the crop coefficient K_c, less water can flow from the saturated zone to the unsaturated zone, which decreases the discharge so that recharge in the considered case becomes positive. A similar behaviour, but to a less extent, can be seen when the A_{root} value is decreased. The results from Figures 6-25 and 6-26 are summarized in Table 6-10. The table shows the changes in the annual total recharge, expressed as percentages.

6.5 Unsaturated zone parameters

A number of variations were made in the coarse till properties in the unsaturated zone using the three-column model. Sections 6.5.1–4 describe the simulation cases, and the results are presented in section 6.5.5.

6.5.1 Field capacity in the unsaturated zone

Simulations were made considering a 50% reduction of the unsaturated field capacity of coarse till, which in effect allows water to percolate down to the saturated zone at lower soil moisture content. However, no changes were made of the difference between the field capacity and the effective porosity, corresponding to the unsaturated specific yield. Figures 6-27 and 6-28 show the pF-curves used in the analysis for the uppermost 50 cm and the depth interval 50–200 cm.

6.5.2 Hydraulic conductivity in the unsaturated zone

Since MIKE SHE uses a 1D approach to simulate water flow in the unsaturated zone, the hydraulic conductivity in the unsaturated zone is active only in the vertical direction. The hydraulic conductivity directly affects the infiltration capacity of the soil. The here evaluated

Table 6-10. Changes in total recharge (mm/year) for the different vegetation parameters evaluated in the column model.

	Total recharge (mm/year), SFM0010	Change in %	Total recharge (mm/year), SFM0017	Change in %
Base case	100.6		–5.6	
LAI = 5	108.6	7.9	2.0	–136.2
Root depth = 0.5 m	91.5	–9.1	–22.6	303.8
K_c = 0.9	126.8	26.0	19.2	–442.9
A_{root} = 0.5	111.5	10.8	5.3	–194.4
A_{root} = 2	92.5	–8.1	–22.9	308.7

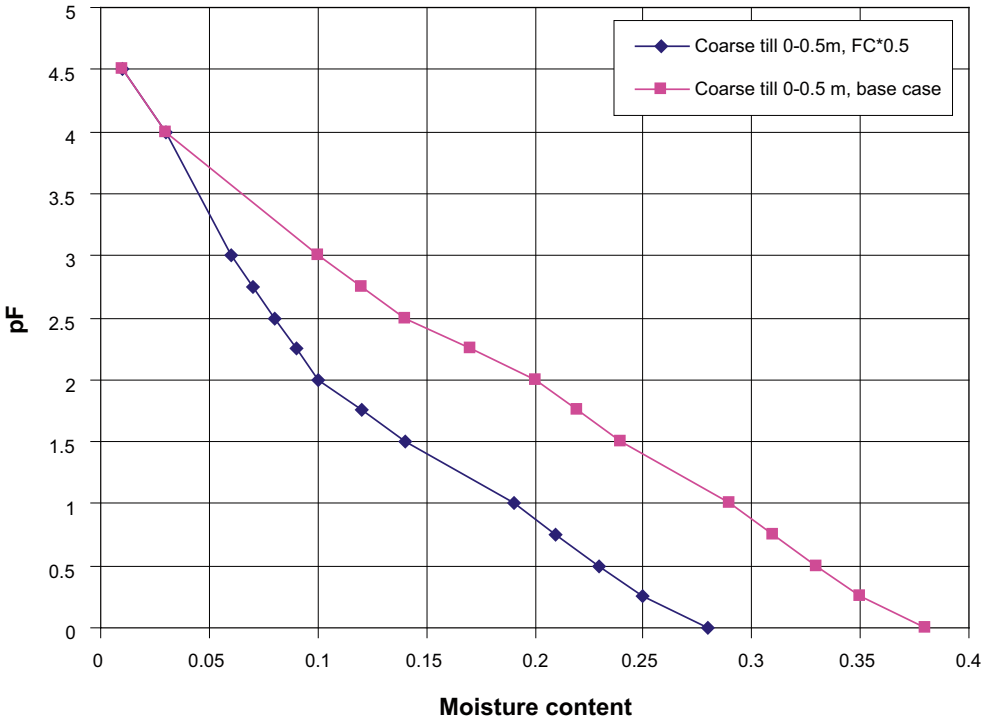

Figure 6-27. *Relation between moisture potential, pF, and moisture content for the uppermost 50 cm of the coarse till soil profile. The field capacity is reduced by 50% relative the base case.*

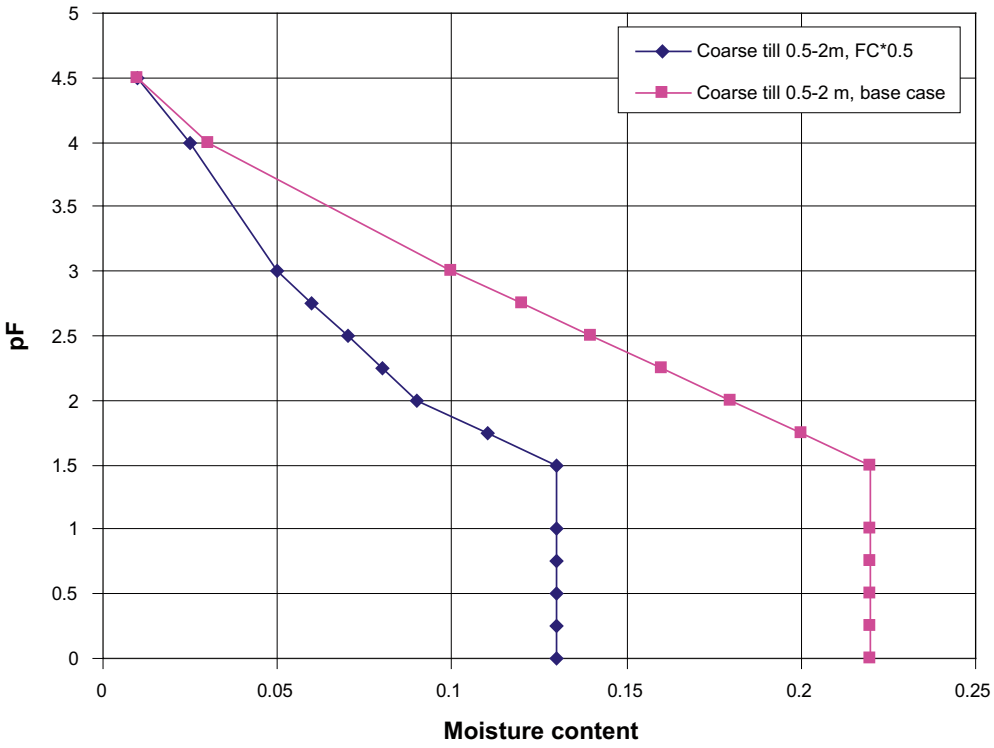

Figure 6-28. *Relation between moisture potential, pF, and moisture content for the coarse till soil profile 50–200 cm below ground surface. The field capacity is reduced by 50% relative the base case.*

cases include a K_s value of coarse till equal to $1.5 \cdot 10^{-4}$ m/s for the uppermost 50 cm, and K_s = $7.5 \cdot 10^{-6}$ m/s for the underlying 150 cm. These sensitivity cases correspond to an increase by a factor of 5, which in effect allows higher infiltration to the saturated zone.

The empirical constant n is used in the Averjanov equation to calculate the hydraulic conductivity curve /DHI 2007/. This constant influences the hydraulic conductivity-soil water content relationship. The Averjanov equation for the hydraulic conductivity curve is as follows:

$$K(\theta) = K_s \left(\frac{\theta - \vartheta_r}{\theta_s - \theta_r} \right)^n$$

where K_s is the saturated hydraulic conductivity, θ_s is the saturated moisture content, and θ_r is the residual moisture content. The evaluation included a simulation where the n value of coarse till was increased from 5 to 10, which leads to lower conductivity values at small soil water contents.

6.5.3 Air entry level

The air entry (tension) level can be seen in the pF-curves; it equals the point of inflection, below which no air is present in the soil. Up to the air entry level, the water content changes very little with increasing tension, resulting in percolation to the saturated zone. Above the air entry level, the water content can change rapidly. A number of variations of the air entry level were evaluated using the three-column model. In all of these simulations, the field capacity and the total porosity were the same as in the base case. Figures 6-29 to 6-32 show the different pF-curves used in the analysis. Table 6-11 shows the parameters used in each simulation case.

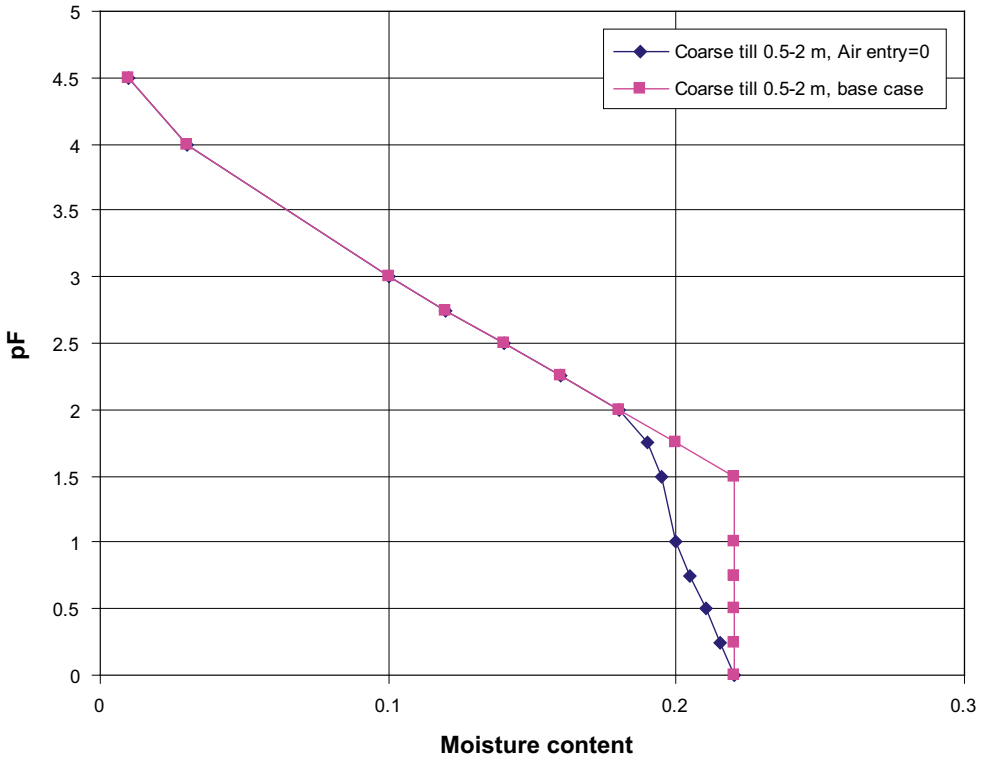

Figure 6-29. *Relation between moisture potential, pF, and moisture content for coarse till 50 to 200 cm below ground surface. The air entry level is set at pF = 0. The field capacity and the total porosity are equal to those in the base case.*

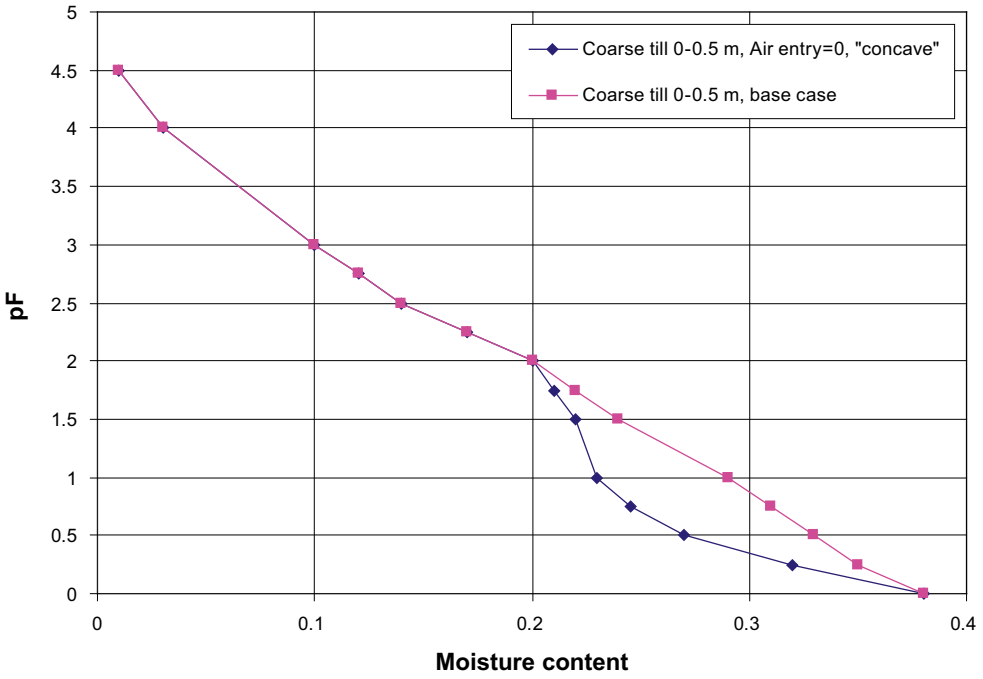

Figure 6-30. *Relation between moisture potential, pF, and moisture content for the uppermost 50 cm of the coarse till profile. The air entry level, the field capacity and the total porosity are equal to those in the base case, but the shape of the pF-curve is concave for tensions below field capacity.*

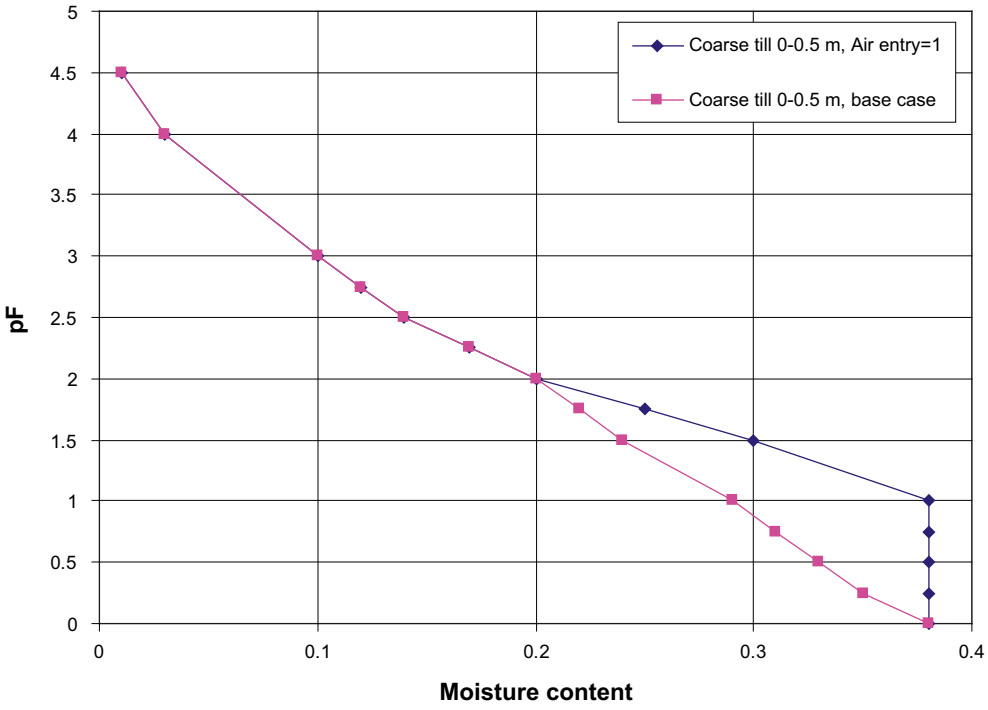

Figure 6-31. *Relation between moisture potential, pF, and moisture content for the uppermost 50 cm of the coarse till profile. The air entry level is set at pF = 1. The field capacity and the total porosity are equal to those in the base case.*

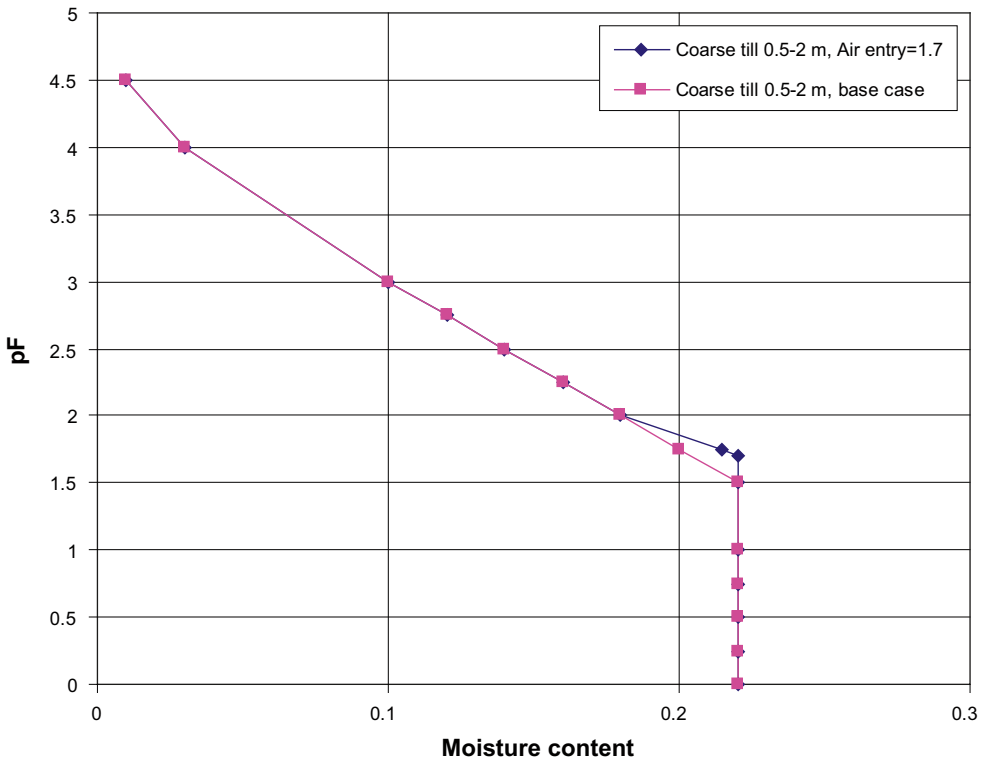

Figure 6-32. *Relation between moisture potential, pF, and moisture content for coarse till 50 to 200 cm below ground surface. The air entry level is set at pF = 1.7. The field capacity and the total porosity are equal to those in the base case.*

Table 6-11. Simulation cases concerning air entry levels for coarse till.

Simulation case	Air entry level for coarse till
Air entry 1 (Sens 11)	0–0.5 m: pF = 0 (as in base case)
	0.5–2 m: pF = 0 (changed from base case, pF = 1.5)
Air entry 2 (Sens 12)	0–0.5 m: pF = 0 (changed to a concave shape)
	0.5–2 m: pF = 1.5 (as in base case)
Air entry 3 (Sens 13)	0–0.5 m: pF = 0 (as in base case)
	0.5–2 m: pF = 1.7 (changed from base case, pF = 1.5)
Air entry 4 (Sens 14)	0–0.5 m: pF = 1 (changed from pF = 0)
	0.5–2 m: pF = 1.7 (changed from base case, pF = 1.5)

6.5.4 Specific yield in the unsaturated zone

The unsaturated specific yield (S_y), which influences groundwater fluctuations, is defined as the volume that an unconfined aquifer releases from storage per unit surface area of aquifer per unit decline of the groundwater table, corresponding to the difference between the field capacity and the effective porosity. Higher S_y-values implies smaller groundwater table fluctuations, and the opposite for smaller S_y-values. A simulation was performed considering an increase of S_y by a factor 1.5 in the uppermost 50 cm of the coarse till profile, and by a factor 2 below 50 cm. The field capacity was kept equal to that in the base case. Figures 6-33 and 6-34 show the pF-curves for the sensitivity cases.

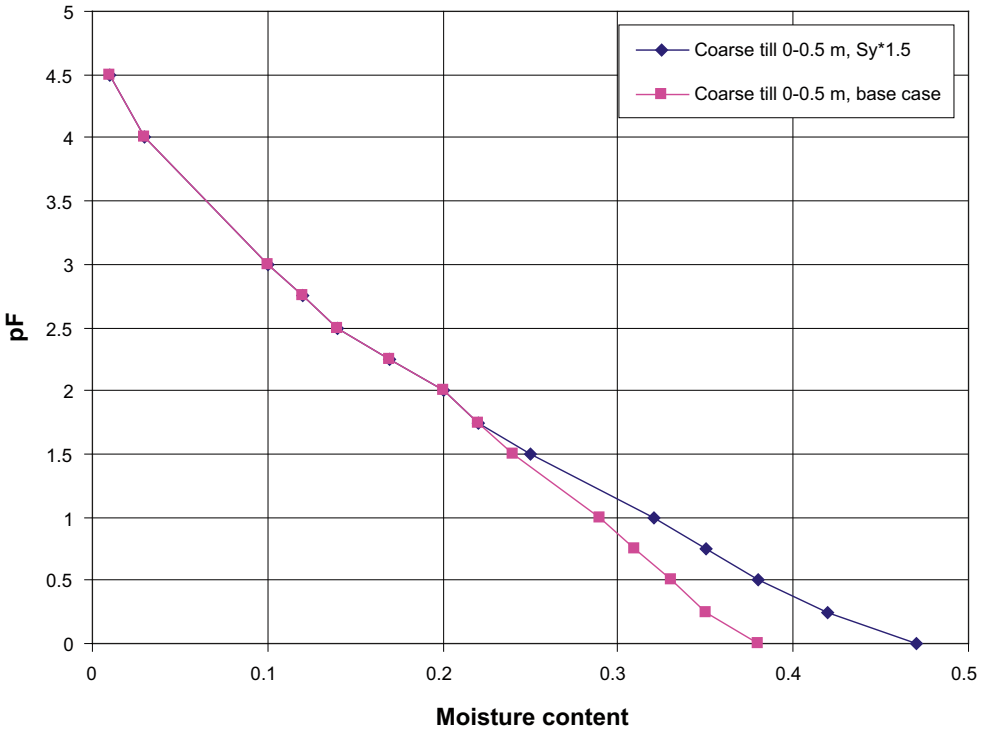

Figure 6-33. *Relation between moisture potential, pF, and moisture content for the uppermost 50 cm of the coarse till soil profile. The air entry level and the field capacity equal those in the base case, whereas the total porosity and the specific yield are increased by a factor of 1.5.*

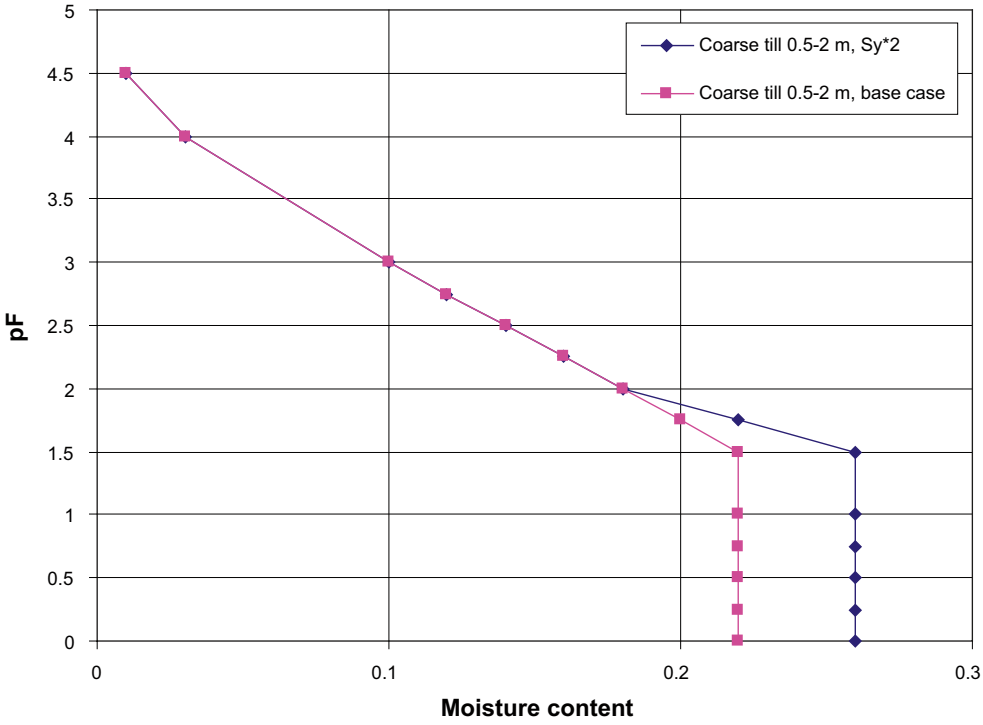

Figure 6-34. *Relation between moisture potential, pF, and moisture content for coarse till 50 to 200 cm below ground surface. The air entry level and the field capacity equal those in the base case, whereas the total porosity and the specific yield are increased by a factor of 2.*

6.5.5 Summary of unsaturated zone parameter results

Figures 6-35 and 6-36 compare the sensitivity cases considering unsaturated zone parameters, in terms of the calculated total recharge at SFM0010 and SFM0017, respectively. A positive recharge represents groundwater recharge, whereas a negative recharge represents groundwater discharge to the unsaturated zone. The recharge value includes both groundwater recharge and evapotranspiration; a higher recharge is the result of less evapotranspiration.

The total recharge over the simulation period is positive at SFM0010, which hence implies that groundwater recharge occurs at this monitoring well. Increasing the saturated hydraulic conductivity increases the infiltration and capillary flux capacities of the soil; at SFM0010, the latter seems to be of higher importance. This is the underlying reason for the observation that

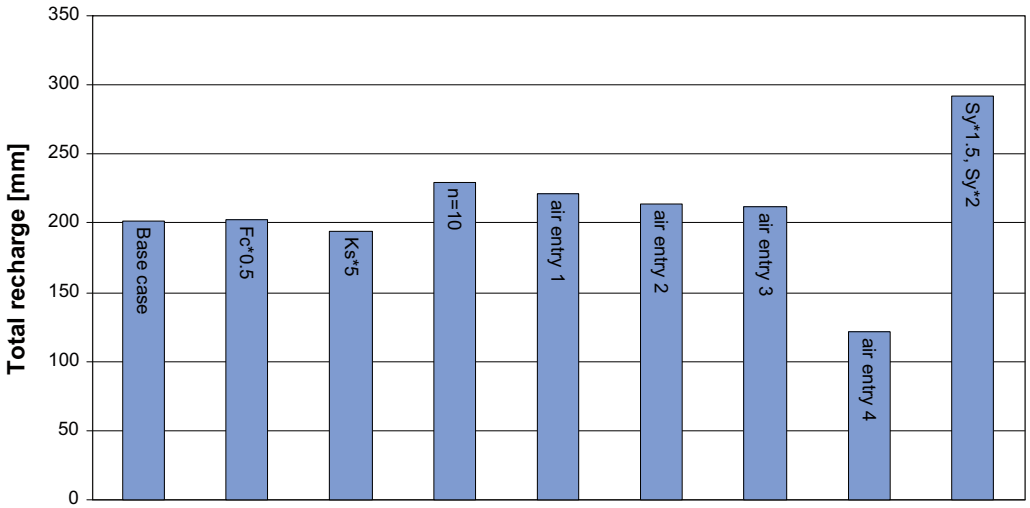

Figure 6-35. *Comparison between sensitivity cases considering unsaturated zone parameters, in terms of the total recharge at SFM0010 (simulation period May 2003 to May 2005).*

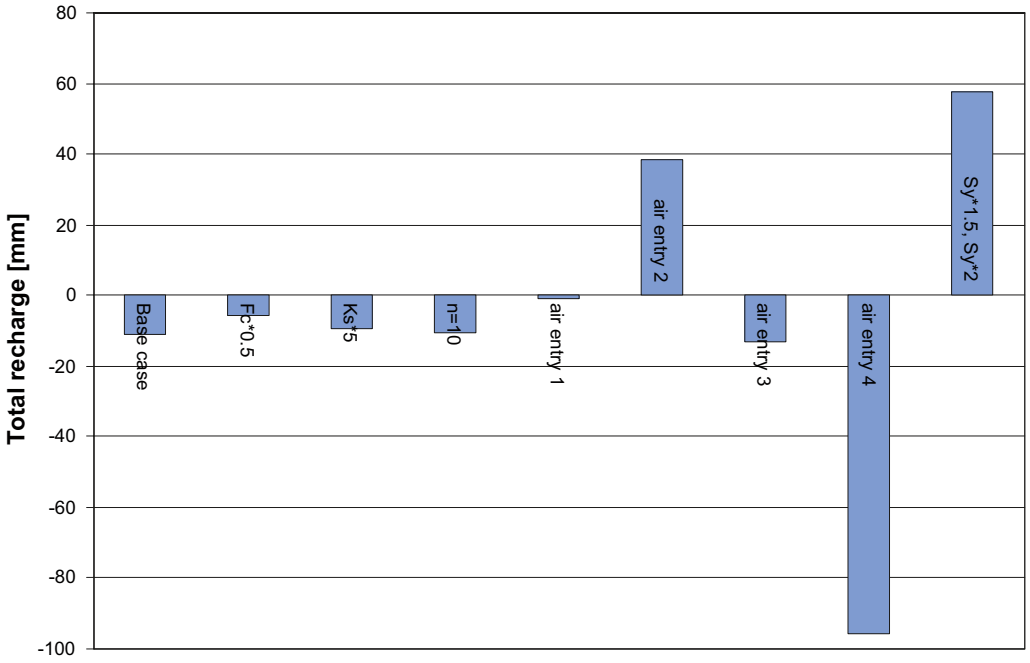

Figure 6-36. *Comparison between sensitivity cases considering unsaturated zone parameters, in terms of the total recharge at SFM0017 (simulation period May 2003 to May 2005).*

an increased hydraulic conductivity to some extent increases the evapotranspiration. The same principle holds when changing the hydraulic conductivity curve through the *n* constant in the Averjanov equation. In the investigated case, the hydraulic conductivity decreases by increasing *n*, which consequently gives the opposite result compared to an increase of the conductivity, i.e. a decrease of the evapotranspiration.

In the figures, one can also note that the water content at field capacity has a small effect on the recharge, and consequently also a small effect on the evapotranspiration. Even a relatively large reduction of the field capacity gives a slightly reduced evapotranspiration. Due to less retaining forces, changing the pF-curve without changing the effective porosity gives higher recharge and less evapotranspiration. The present analysis has only involved changes of the part of the pF-curve above the water content at field capacity. The same principle can be seen when decreasing pF, i.e. less evapotranspiration and higher recharge.

The largest effect on the recharge is obtained by the case "air entry 4", in which the pF value at saturation is increased from 0 to 1 (corresponding to air entry at a tension of 10 cm) in the upper 50 cm of the soil profile. The other air entry cases have a relatively small effect at SFM0010. The largest increase of the recharge, due to a reduced evapotranspiration, is obtained by increasing the effective porosity in the pF-curve (i.e. the specific yield).

In the base case, the total recharge over the simulation period is negative at SFM0017, which corresponds to groundwater discharge. A very small or no effect is observed when the hydraulic conductivity curve is changed, both by changing the saturated hydraulic conductivity and the *n* constant in the Averjanov equation. Similar to SFM0010 (see above), keeping the effective porosity unchanged, the water content at field capacity has a small effect on the recharge. Even a relatively large reduction of the field capacity only leads to slightly reduced evapotranspiration, and in this case also reduced groundwater discharge.

Changing the pF-curve at water contents above the field capacity, the SFM0017 results are similar to those obtained at SFM0010. However, the shallow groundwater table at SFM0017 implies that the calculated recharge is more sensitive to parameter changes in the upper soil profile (cases "air entry 2" and "air entry 4") compared to SFM0010. However, the largest effect is observed for the same sensitivity case ("air entry 4") as for SFM0010; increasing the specific yield has the largest effect on the recharge. The results in Figures 6-35 and 6-36 are summarized in Table 6-12, which shows the change in annual total recharge, expressed as a percentage.

Table 6-12. Changes in total recharge (mm/year) for different unsaturated zone parameters evaluated by the column model. *FC* = field capacity, K_s = hydraulic conductivity at full saturation, *n* = Averjanov constant, and S_y = specific yield.

	Total recharge (mm/year) at SFM0010	Change in %	Total recharge (mm/year) at SFM0017	Change in %
Base case	100.6		–5.6	
FC·0.5	101.1	0.5	–3.0	–47.2
K_s·5	97.3	–3.3	–4.9	–13.4
n = 10	114.9	14.2	–5.3	–5.2
Air entry 1	110.6	9.9	–0.4	–93.3
Air entry 2	106.8	6.1	19.4	–445.2
Air entry 3	106.2	5.5	–6.6	18.5
Air entry 4	60.6	–39.8	–48.0	755.9
S_y·1.5, S_y·2	146.0	45.0	28.8	–613.0

6.6 Vegetation and unsaturated zone parameters: Full model evaluation

The importance of vegetation parameters was observed both in the base case and the sensitivity analysis concerning vegetation parameters using the column model; the latter model was sensitive to the root mass distribution, A_{root}. Using the full model, a simulation was performed using in the full scale model with $A_{root} = 2$ for all coniferous forest (cf. section 6.6.1). Those parameters that showed significant effect on the results in that sensitivity analysis were tested in a separate simulation; tested parameters include a combination of unsaturated zone parameters, values of the hydraulic conductivity in the saturated zone and vegetation parameters; see section 6.6.2.

6.6.1 Root mass distribution

Simulation case Sens 7 uses root mass distribution $A_{root} = 2$ for all coniferous forest, allowing more transpiration in the uppermost part of the soil profile. Figures 6-37 to 6-41 compare measured head elevations, calculated head elevations from Sens 5 and the results from Sens 7. As shown in these figures, the effect of A_{root} on the groundwater head elevation is insignificant; there is no effect on head elevations due to increased evapotranspiration. This is most likely due to that the actual evaporation is close to the potential value, and cannot be increased further.

Table 6-13 compares statistical mean errors between sensitivity cases Sens 5 and Sens 7. Sens 7, involving an increase of A_{root} from 1 to 2, has insignificant effects.

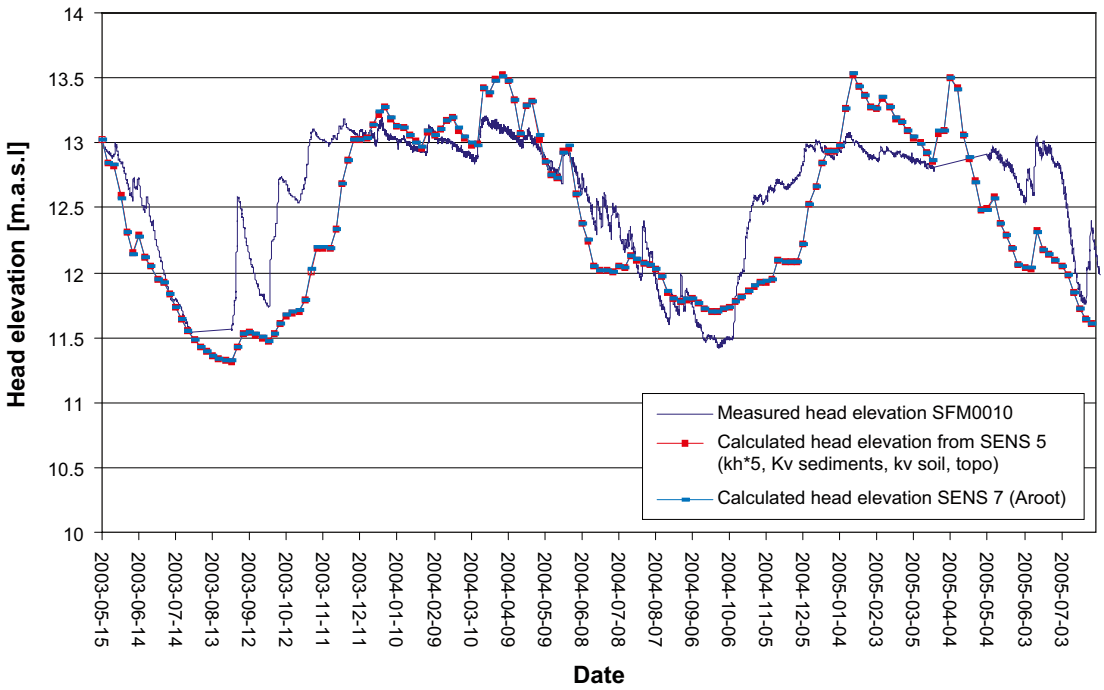

Figure 6-37. *Sensitivity results at SFM0010 concerning A_{root}. The simulation is based on Sens 5 (with an increased horizontal hydraulic conductivity in the soil layers, an increased vertical hydraulic conductivity in sediments underneath Fiskarfjärden and Gällsboträsket, a decreased vertical hydraulic conductivity in geological soil layers, and a corrected local topography).*

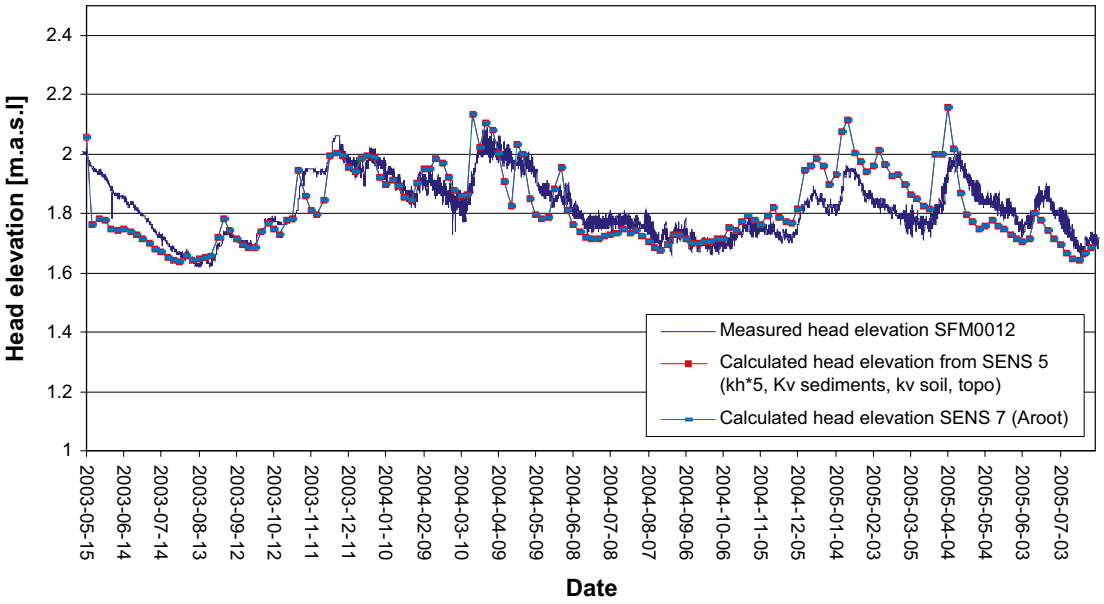

Figure 6-38. *Sensitivity results at SFM0012 concerning A_{root}. The simulation is based on Sens 5 (with an increased horizontal hydraulic conductivity in the soil layers, an increased vertical hydraulic conductivity in sediments underneath Fiskarfjärden and Gällsboträsket, a decreased vertical hydraulic conductivity in geological soil layers, and a corrected local topography).*

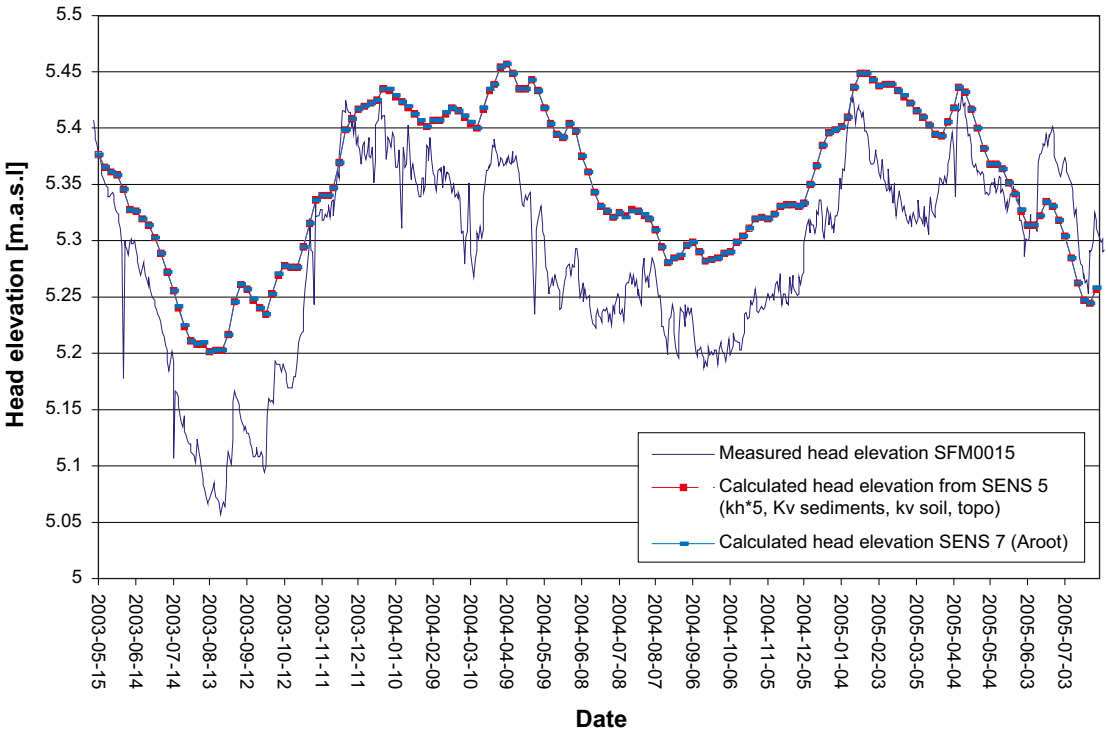

Figure 6-39. *Sensitivity results at SFM0015 concerning A_{root}. The simulation is based on Sens 5 (with an increased horizontal hydraulic conductivity in the soil layers, an increased vertical hydraulic conductivity in sediments underneath Fiskarfjärden and Gällsboträsket, a decreased vertical hydraulic conductivity in geological soil layers, and a corrected local topography).*

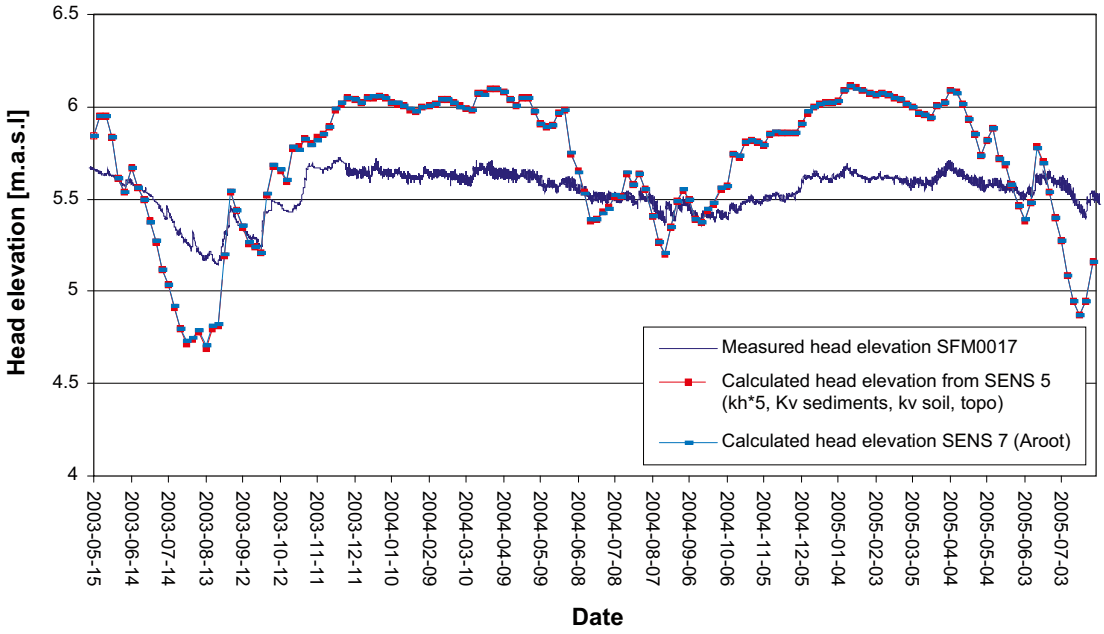

Figure 6-40. *Sensitivity results at SFM0017 concerning A_{root}. The simulation is based on Sens 5 (with an increased horizontal hydraulic conductivity in the soil layers, an increased vertical hydraulic conductivity in sediments underneath Fiskarfjärden and Gällsboträsket, a decreased vertical hydraulic conductivity in geological soil layers, and a corrected local topography).*

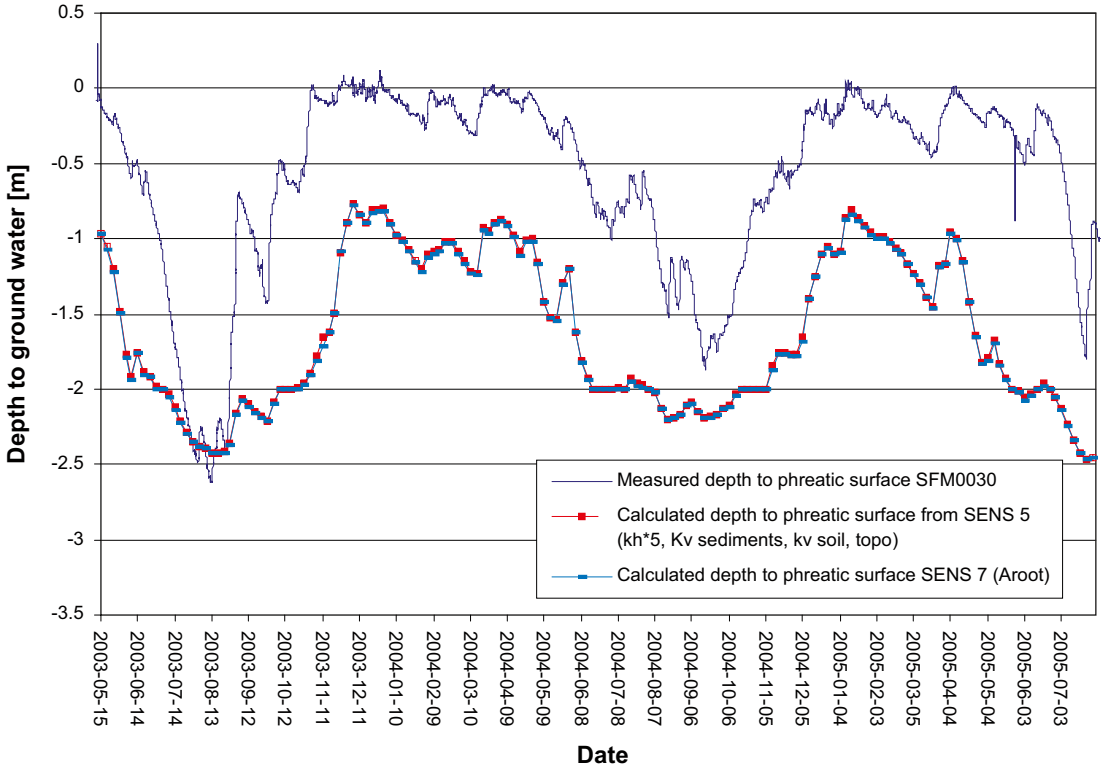

Figure 6-41. *Sensitivity results at SFM0030 concerning A_{root}. The simulation is based on Sens 5 (with an increased horizontal hydraulic conductivity in the soil layers, an increased vertical hydraulic conductivity in sediments underneath Fiskarfjärden and Gällsboträsket, a decreased vertical hydraulic conductivity in geological soil layers, and a corrected local topography).*

Table 6-13. Comparison of statistical mean absolute errors (MAE) between Sens 5 and Sens 7.

Borehole	MAE, Sens 5 (K_h soil·5, K_v lake sediments, K_v soil/10, local topography)	MAE, Sens 7 (K_h soil·5, K_v lake sediments, K_v soil/10, local topography, A_{root} = 2)
SFM0001	0.76	0.76
SFM0002	0.22	0.22
SFM0003	0.24	0.24
SFM0010	0.28	0.28
SFM0011	0.07	0.07
SFM0012	0.06	0.06
SFM0014	0.31	0.31
SFM0015	0.06	0.06
SFM0016	0.13	0.13
SFM0017	0.32	0.32
SFM0018	0.4	0.4
SFM0019	0.33	0.33
SFM0020	0.21	0.21
SFM0021	0.66	0.66
SFM0022	0.19	0.19
SFM0023	0.06	0.06
SFM0030	1.03	1.03
SFM0033	0.14	0.14
SFM0036	0.21	0.21
SFM0039	0.04	0.04
SFM0040	0.04	0.04
SFM0041	0.03	0.03
SFM0049	1.11	1.11
SFM0057	0.17	0.17
SFM0058	0.22	0.22
SFM0062	0.07	0.07
SFM0064	0.08	0.08

6.6.2 Combination of sensitive parameters

Based on the results from the sensitivity analysis, a combination of unsaturated zone parameters, values of the hydraulic conductivity in the saturated zone and vegetation parameters was tested in a separate simulation. The chosen parameters showed significant effects in the sensitivity analysis. The simulation was based on Sens 5, involving an increased horizontal hydraulic conductivity in the soil layers, an increased vertical hydraulic conductivity in lake sediments underneath Fiskarfjärden and Gällsboträsket, a reduced vertical conductivity in the soil layers, and a corrected local topography at four borehole locations.

The simulation was run using A_{root} = 0.5 (A_{root} = 1 in the base case). Due to a smaller evapotranspiration, the result is an increased recharge in recharge areas in the column model, and a smaller discharge in discharge areas. In the considered sensitivity case, the unsaturated zone is parameterized using an increased specific yield (S_y) for coarse till; S_y was increased a factor of 1.5 in the upper soil layer and a factor 2 in the deeper soils. The pF-curves of the coarse till are shown in Figures 6-33 and 6-34. The specific yield for the saturated zone was changed by the same amount.

In addition to the increased specific yield, the storage coefficient S (used for confined aquifers) was also increased in the upper saturated zone layer. The reason for doing this is that when groundwater heads raise above the ground surface, the storage capacity is given by S. Hence, changing S may affect peaks during wet periods. Finally, the crop coefficient K_c was changed from 1 to 0.9, which gives less evaporation. All in all, the increased storage capacity was expected to reduce the evaporation and reduce the peaks in the hydraulic head.

Figures 6-42 to 6-46 compare measured groundwater head elevations, calculated head elevations from Sens 5, and the results from the combined sensitivity simulation. Table 6-14 compares the two simulations in terms of statistical mean errors for all observation boreholes. The total mean absolute error remains 0.28 m. However, an improvement can be seen in SFM0019 and SFM0030, both located in local topographical depressions. The results show that the tested parameter combination has an effect on calculated groundwater levels, typically increased levels during summer and a faster groundwater level rise during autumn. This is due to the decreased evapotranspiration as shown in Table 6-15, presenting the total water balance over the land part of the model area.

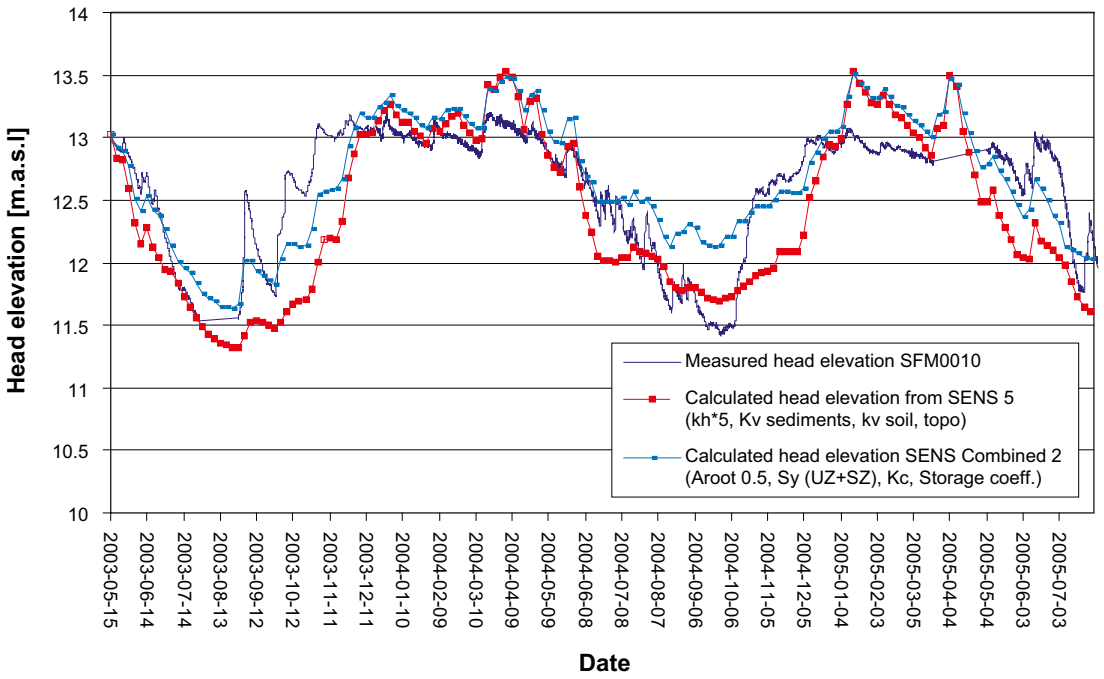

Figure 6-42. *Results at SFM0010 from the sensitivity analysis, considering combined parameters. The simulation was based on Sens 5, with an increased horizontal hydraulic conductivity in the soil layers, an increased vertical hydraulic conductivity in lake sediments underneath Fiskarfjärden and Gällsboträsket, a decreased vertical hydraulic conductivity in geological soil layers, and a corrected local topography.*

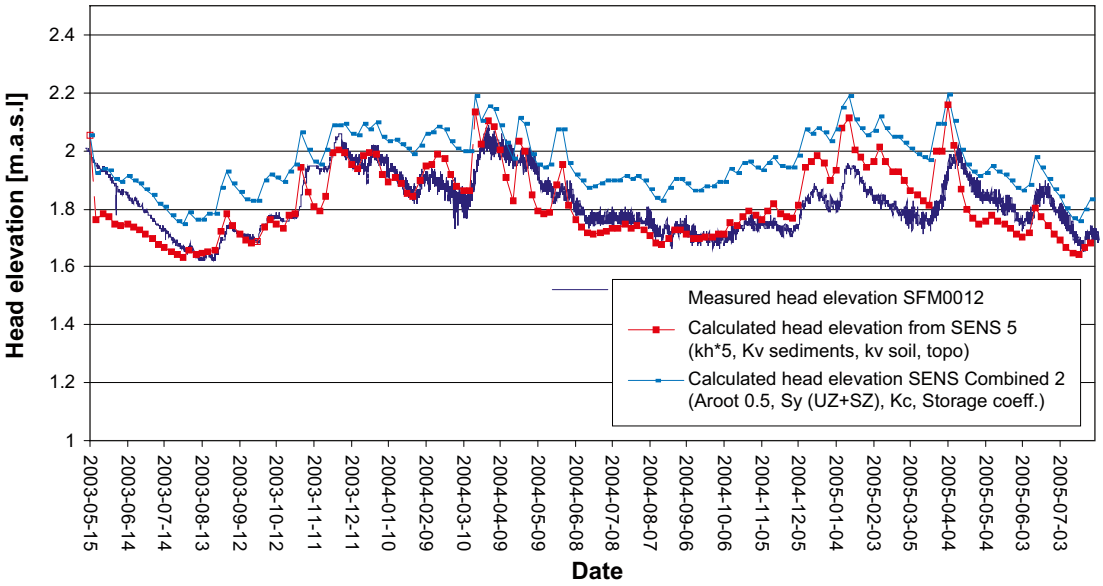

Figure 6-43. *Results at SFM0012 from the sensitivity analysis, considering combined parameters. The simulation was based on Sens 5, with an increased horizontal hydraulic conductivity in the soil layers, an increased vertical hydraulic conductivity in lake sediments underneath Fiskarfjärden and Gällsboträsket, a decreased vertical hydraulic conductivity in geological soil layers, and a corrected local topography.*

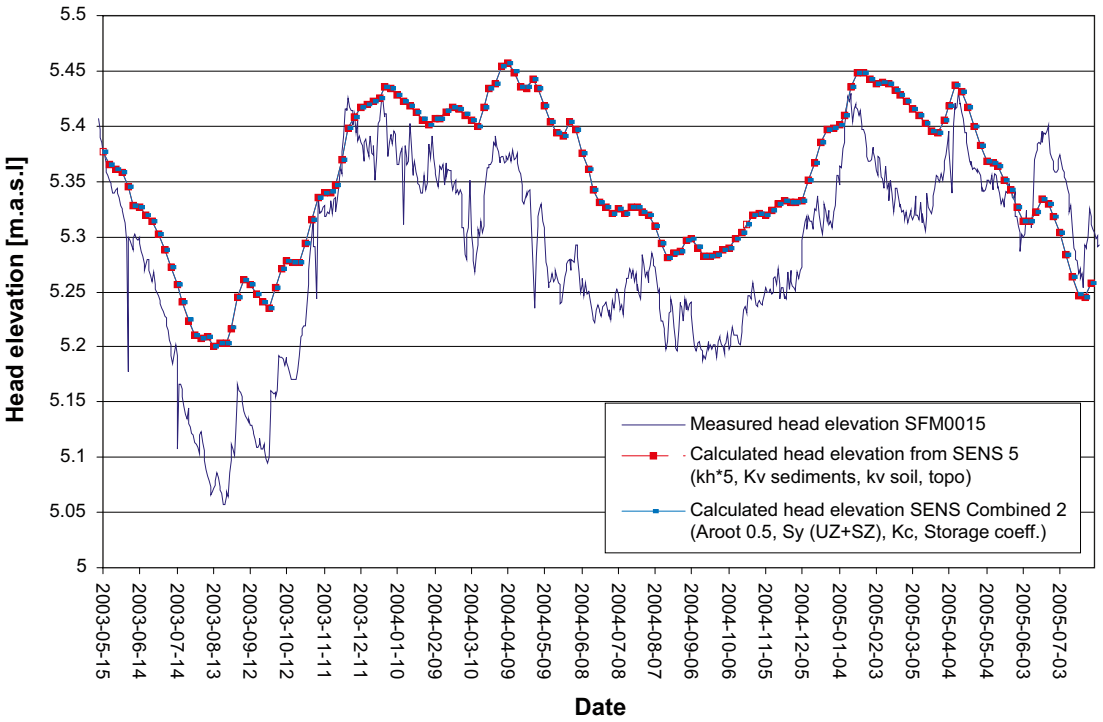

Figure 6-44. *Results at SFM0015 from the sensitivity analysis, considering combined parameters. The simulation was based on Sens 5, with an increased horizontal hydraulic conductivity in the soil layers, an increased vertical hydraulic conductivity in lake sediments underneath Fiskarfjärden and Gällsboträsket, a decreased vertical hydraulic conductivity in geological soil layers, and a corrected local topography.*

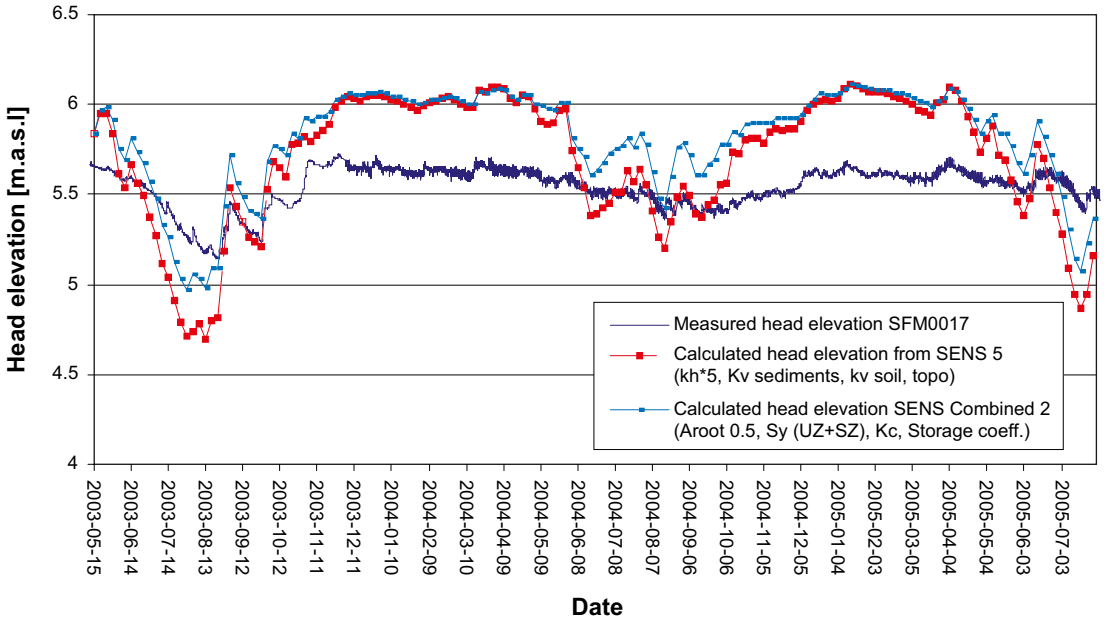

Figure 6-45. *Results at SFM0017 from the sensitivity analysis, considering combined parameters. The simulation was based on Sens 5, with an increased horizontal hydraulic conductivity in the soil layers, an increased vertical hydraulic conductivity in lake sediments underneath Fiskarfjärden and Gällsboträsket, a decreased vertical hydraulic conductivity in geological soil layers, and a corrected local topography.*

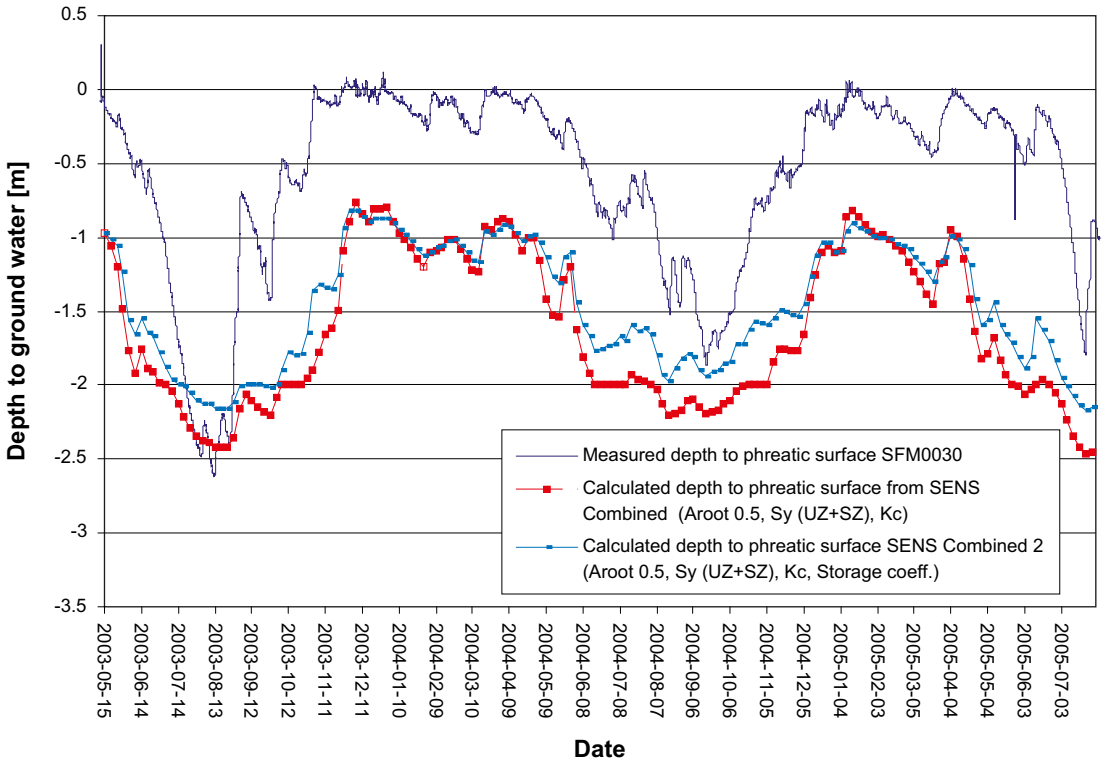

Figure 6-46. *Results at SFM0030 from the sensitivity analysis, considering combined parameters. The simulation was based on Sens 5, with an increased horizontal hydraulic conductivity in the soil layers, an increased vertical hydraulic conductivity in lake sediments underneath Fiskarfjärden and Gällsboträsket, a decreased vertical hydraulic conductivity in geological soil layers, and a corrected local topography.*

Table 6-14. Comparison of statistical mean absolute errors (MAE) between the sensitivity analysis of combined parameters and Sens 5. "+" represents an improvement, "o" no change and "–" reduced agreement compared to Sens 5.

Borehole	Location in inter-polated DEM	MAE, Sens 5 (K_h soil·5, K_v lake sediments, K_v soil/10, local topography)	MAE, combined sensitivity analysis case (K_h soil·5, K_v lake sediments, K_v soil/10, local topography, A_{root} = 0.5, S_y increased in unsaturated and saturated zones, S in saturated zone)	Effects of the combined sensitivity analysis case
SFM0001	Local depression	0.76	0.67	+
SFM0002	Slope or local height	0.22	0.3	–
SFM0003	Slope or local height	0.24	0.23	+
SFM0010	Slope or local height	0.28	0.23	+
SFM0011	Local depression	0.07	0.07	o
SFM0012	Lake bottom	0.06	0.13	–
SFM0014	Slope or local height	0.31	0.38	–
SFM0015	Lake bottom	0.06	0.06	o
SFM0016	Slope or local height	0.13	0.15	–
SFM0017	Slope or local height	0.32	0.34	–
SFM0018	Slope or local height	0.4	0.45	–
SFM0019	Local depression	0.33	0.17	+
SFM0020	Local depression	0.21	0.15	+
SFM0021	Local depression	0.66	0.83	–
SFM0022	Lake bottom	0.19	0.26	–
SFM0023	Lake bottom	0.06	0.06	o
SFM0030	Local depression	1.03	0.88	+
SFM0033	Lake bottom	0.14	0.12	+
SFM0036	Slope or local height	0.21	0.24	–
SFM0039	Lake bottom	0.04	0.04	o
SFM0040	Lake bottom	0.04	0.04	o
SFM0041	Lake bottom	0.03	0.03	o
SFM0049	Local depression	1.11	1.18	–
SFM0057	Slope or local height	0.17	0.15	+
SFM0058	Slope or local height	0.22	0.29	–
SFM0062	Lake bottom	0.07	0.06	+
SFM0064	Lake bottom	0.08	0.08	o

The total accumulated water balance over the area is shown in Table 6-15. For comparison, totals are also included in the bottom lines for the base case and the case “Sens 5”. The water balance for the base case and the case “Sens 5” (only involving the hydraulic conductivity at full saturation) are similar, except for an increased baseflow to river in “Sens 5”. However, the combined simulation case has a slightly different water balance: The evapotranspiration is reduced by c. 6%, and the total runoff to river is c. 18% higher. This can be compared with the estimated total runoff error upstream Bolundsfjärden, –11%, which is illustrated in Figure 6-47; this figure shows the measured accumulated flow, the base case, Sens 5, and the combined simulation case. Further upstream in the stream network, the estimation error increases. However, the period with measured flow data is too short to make any conclusions regarding the effects of the parameter changes. Other errors, such as the correction of snow precipitation, may more relevant; this is further commented on in chapter 7.

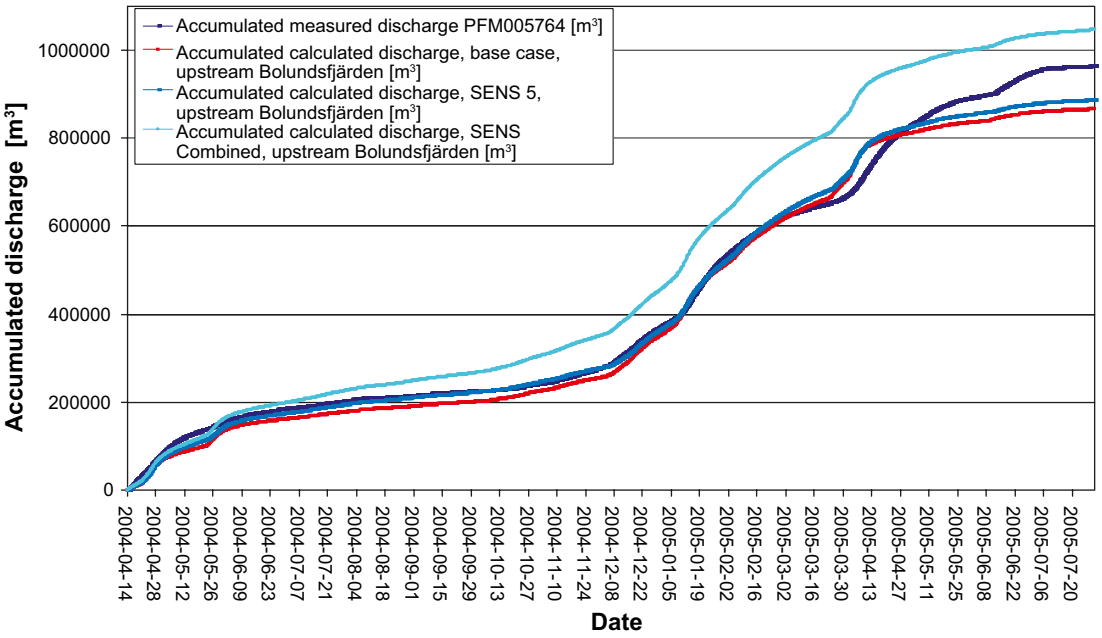

Figure 6-47. *Accumulated calculated discharge (m³) during the period 2004-04-14 to 2005-07-31 and the accumulated measured discharge at PFM005764, located upstream from Lake Bolundsfjärden. The black curve is the measured discharge, the red curve is the calculated discharge for the base case, the dark blue curve is the calculated discharge for Sens 5, and the light blue curve is the accumulated discharge from the combined simulation case.*

Table 6-15. Total accumulated water balance for sensitivity analysis of combined parameters in Forsmark between 2003-05-15 and 2005-05-04 [mm].

Date	Precipi-tation	Canopy storage change	Evapotran-spiration	OL storage change	OL boundary inflow	OL boundary outflow	OL to river	SubSurface storage change	SubSurface boundary inflow	SubSurface boundary outflow	Baseflow to river	Baseflow from river	Error
2003-05-15	0	0	0	0	0	0	0	0	0	0	0	0	0
2003-06-14	–46.8	–1.8	78.4	–7.2	–0.1	0.2	3.2	–24.6	1.7	1.2	2.1	0.0	2.8
2003-07-14	–67.6	–1.8	164.7	–21.2	–0.1	0.2	4.8	–70.9	5.2	1.6	3.0	–0.1	7.4
2003-08-13	–117.1	–0.4	261.2	–30.8	–0.1	0.2	5.4	–102.3	9.1	1.9	3.4	–0.3	11.8
2003-09-12	–219.9	–1.8	316.8	–23.6	–0.8	1.4	7.4	–66.8	10.9	2.4	4.0	–0.4	7.8
2003-10-12	–274.0	–1.3	345.1	–20.0	–0.8	1.5	9.7	–50.0	12.0	3.8	4.9	–0.4	6.3
2003-11-11	–336.6	0.4	351.4	–9.0	–0.8	2.5	14.8	–18.9	12.9	6.7	6.5	–0.4	3.6
2003-12-11	–409.8	0.4	353.4	3.4	–1.1	6.4	29.1	13.6	13.7	11.6	8.9	–0.4	1.8
2004-01-10	–438.6	0.3	354.4	3.6	–1.8	10.8	45.0	16.2	14.3	15.1	11.7	–0.5	2.0
2004-02-09	–452.8	0.0	355.3	3.1	–2.2	12.6	55.6	13.4	15.0	18.4	14.1	–0.5	2.0
2004-03-10	–478.2	–0.6	364.6	2.4	–3.2	16.2	67.4	11.8	15.7	21.8	16.6	–0.5	2.6
2004-04-09	–549.9	–1.6	381.0	9.1	–3.7	22.2	86.6	28.7	16.3	27.2	19.7	–0.5	2.5
2004-05-09	–581.3	–1.8	418.0	3.7	–3.7	24.5	99.3	8.5	17.0	31.6	22.4	–0.5	3.7
2004-06-08	–634.4	0.3	479.3	–1.6	–3.8	25.6	107.9	–8.1	18.1	33.3	24.5	–0.6	4.3
2004-07-08	–696.6	–1.8	566.6	–9.1	–4.2	25.9	111.5	–24.1	20.6	33.9	25.6	–0.6	6.6
2004-08-07	–753.7	–1.8	637.2	–13.6	–5.1	27.3	114.5	–36.0	22.0	34.6	26.7	–0.6	7.5
2004-09-06	–809.9	–1.8	696.7	–16.1	–5.1	27.3	116.7	–38.2	23.5	35.2	27.5	–0.7	8.2
2004-10-06	–839.7	–0.4	726.1	–17.2	–11.1	32.8	118.2	–38.5	25.8	35.6	28.3	–0.7	7.6
2004-11-05	–878.4	0.1	732.6	–11.7	–11.5	34.1	121.6	–21.3	26.7	38.0	29.6	–0.8	5.8
2004-12-05	–910.0	0.4	736.0	–7.0	–13.5	36.8	126.6	–7.2	27.6	39.5	31.1	–0.8	4.4
2005-01-04	–965.4	0.1	738.4	2.2	–31.6	59.2	138.4	15.5	28.3	42.2	33.4	–0.8	3.4
2005-02-03	–1,015.8	0.3	742.4	7.5	–140.3	177.9	153.2	26.4	29.0	44.8	36.4	–0.8	2.9
2005-03-05	–1,028.0	–0.9	745.4	3.8	–140.9	181.9	167.8	15.6	29.7	50.2	39.1	–0.8	3.6
2005-04-04	–1,093.1	0.2	766.2	11.2	–140.9	184.9	179.6	30.2	30.4	54.8	41.6	–0.8	3.5
2005-05-04	–1,108.8	0.1	816.8	–1.3	–141.0	186.3	188.9	–4.9	31.1	58.2	43.9	–0.9	6.2
Sens 5 2005-05-04	–1,108.8	0.0	868.4	–4.1	–140.8	180.0	165.0	–13.6	33.2	52.8	39.2	–1.1	3.8
Base case 2005-05-04	–1,108.8	0.0	863.9	–0.1	–143.4	187.6	168.5	–0.4	–28.4	42.6	21.8	–0.4	3.0

6.7 Influence of the bottom boundary condition

A simulation was performed to investigate the effect of the bottom boundary condition on the near-surface water flow. This was done by using a zero-flux boundary condition at the bottom of the model, instead of the fixed head boundary condition obtained from the regional DarcyTools-model /Bosson and Berglund 2006/. The results in Figures 6-48 to 6-50 show that using a no-flux bottom boundary has small effects on the calculated hydraulic head elevations in

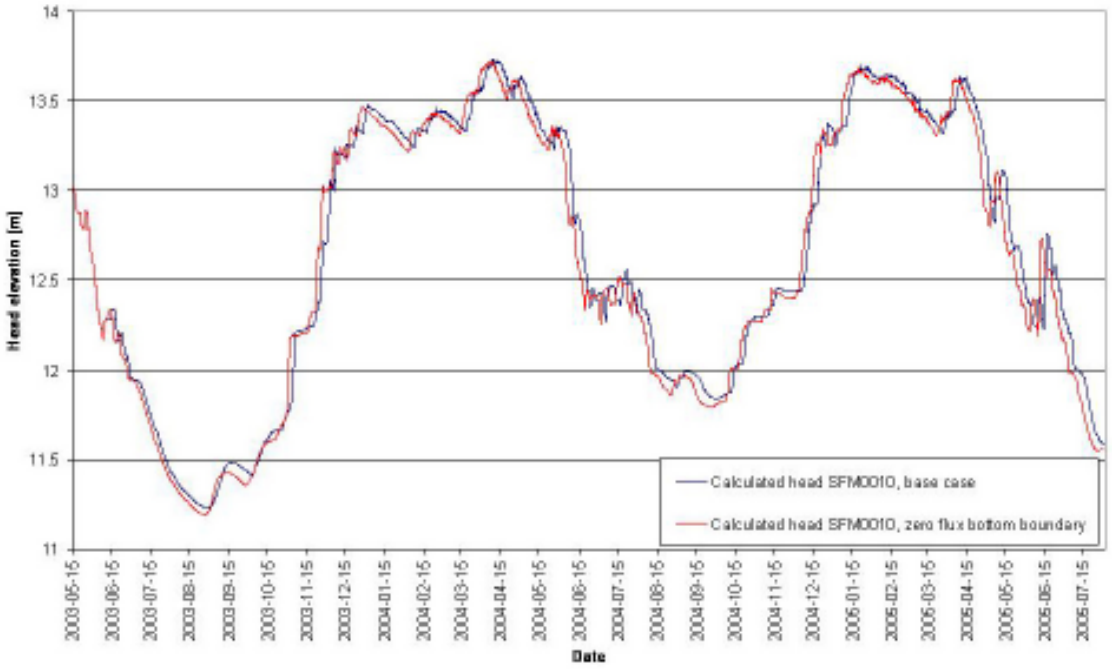

Figure 6-48. *Effects of applying a no-flux bottom boundary condition on hydraulic head elevations at SFM0010, installed along a hillside.*

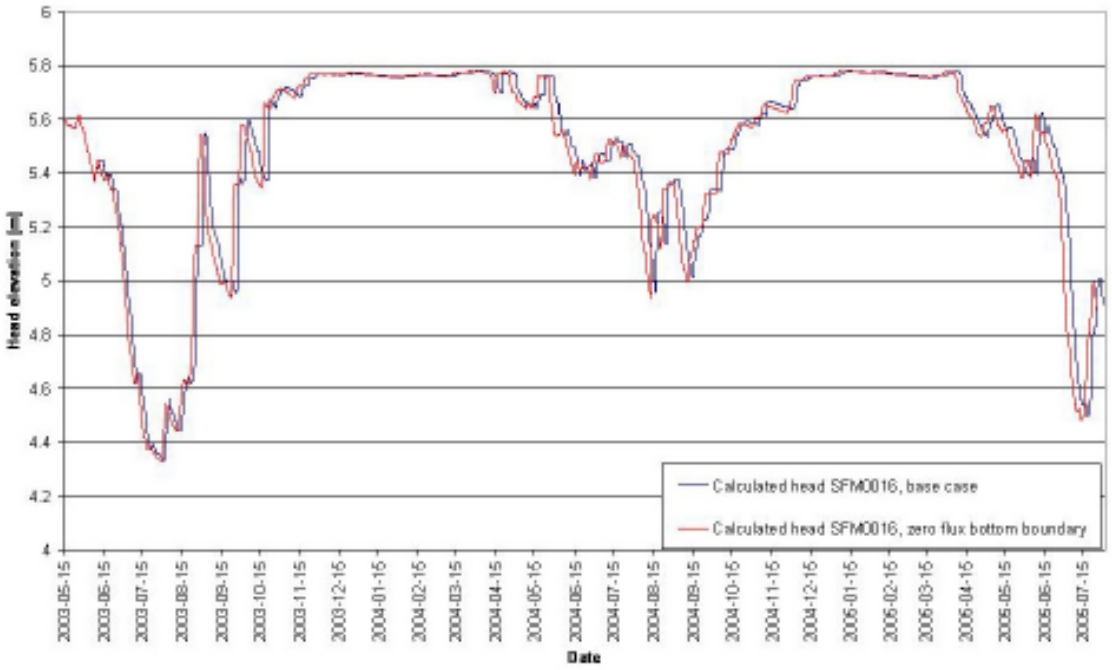

Figure 6-49. *Effects of applying a no-flux bottom boundary condition on hydraulic head elevations at SFM0016, installed along a hillside.*

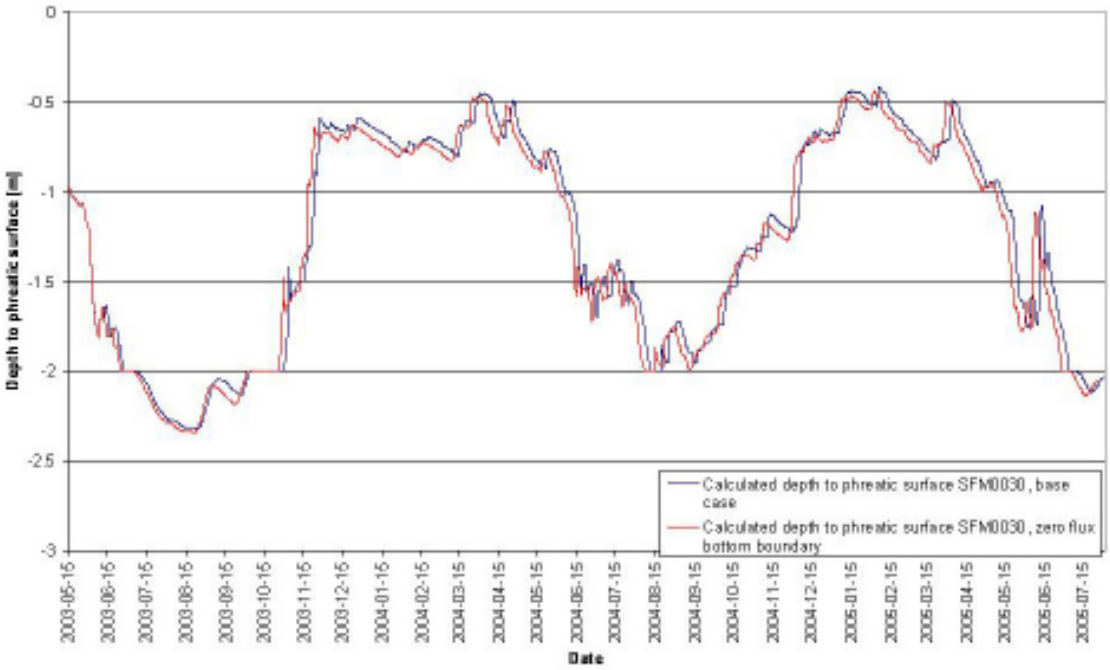

Figure 6-50. *Effects of applying a no-flux bottom boundary condition on hydraulic head elevations at SFM0030, installed in a local depression.*

specific boreholes. According to the figures, there are only minor differences between calculated hydraulic head elevations at SFM0010, SFM0016 and SFM0030 when the bottom boundary is excluded. The reason for this is that local conditions determines the extents of groundwater recharge and discharge areas within the Forsmark model domain. As an extension, not tested here, it would be interesting to evaluate how many bedrock calculation layers that can be removed before any appreciable effect can be noted on the near-surface water flow conditions.

6.8 Test of a stationary case

A simulation was made using stationary (temporally constant) meteorological input data and a stationary sea level, used as boundary condition in the MIKE 11 stream network and in the uppermost calculation layer (below the sea). These results are compared to the base case, which uses time-varying input data. In the stationary case, the daily net precipitation (1.57 mm/day) was calculated by uniformly distributing the accumulated time-varying precipitation. Likewise, the daily potential evaporation was calculated to 1.37 mm/day, and the internal boundary condition in the sea, corresponding to the annual mean, was calculated to –0.05 metre above sea level; this mean value was also used as boundary conditions for the MIKE 11 stream network.

Table 6-16 compares the total water balance from the base case and the stationary simulation case (simulation period 2003-05-15 to 2005-05-04). As can be seen in this table, the major water balance difference concerns the water exchange with the internal boundary in the sea. The stationary case results in a considerable reduction of the overland boundary in- and outflows; the net water flow between the overland component and the boundaries is c. 40% of that in the base case. The exchange between groundwater and the boundaries is also reduced when constant meteorological input data are used.

Figure 6-51 shows calculated (stationary case) and measured groundwater levels in SFM0010, SFM0015 and SFM0030. Obviously, there are no groundwater level fluctuations in the stationary case. The figures shows that there is reasonable good agreement between calculated and measured groundwater levels.

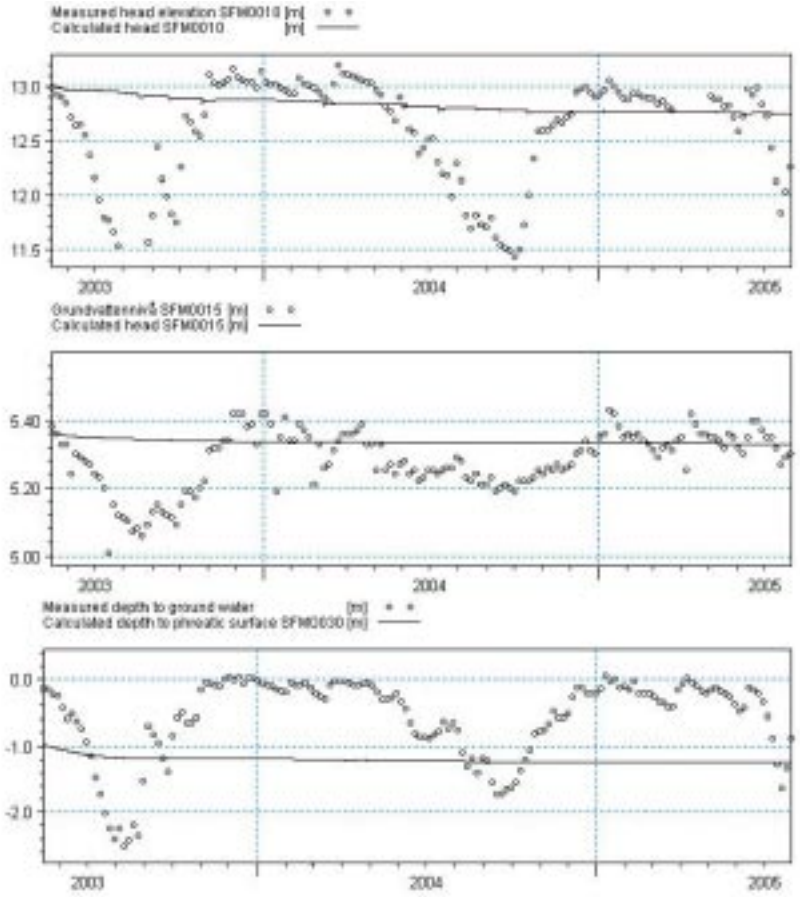

Figure 6-51. *Comparison between calculated and measured groundwater levels and groundwater depths in SFM0010, SFM0015 and SFM0030.*

Table 6-16. Comparison of the accumulated water balance (mm) between the base case and the stationary case (simulation period 2003-05-15 to 2005-05-04).

Water balance component	Base case (mm)	Constant meteorological input data (mm)
Precipitation	–1,108.8	–1,131.7
Canopy storage change	0	0.3
Evapotranspiration	863.9	988.4
OL Storage Change	–0.1	–5.4
OL Boundary Inflow	–143.4	–1.3
OL Boundary Outflow	187.6	15.9
OL to River	168.5	97.3
SubSurface Storage Change	–0.4	–4.8
SubSurface Boundary Inflow	–28.4	–19.0
SubSurface Boundary Outflow	42.6	28.4
Baseflow to River	21.8	21.1
Baseflow from River	–0.4	–0.01
Error	3.0	–10.9

7 Conclusions from the base case and the sensitivity analysis

The surface water system has a generally good agreement between measured and calculated water levels and discharges. The base case model shows a relatively good agreement in the size of peak discharges, but generally a quicker response than measured data, i.e. too fast and narrow peaks in discharge. In the model interpretation, the runoff is described as an overland flow process. In reality, parts of the runoff most likely take place in the uppermost soil, i.e. not as real surface flow. Decreasing the overland flow Manning number to unrealistically low values might be a solution to describe this phenomenon. This has however not been tested in this analysis.

There is also generally too small runoff during periods of snow and snowmelt events, which results in an underestimated total runoff. This could be a result of the correction of the precipitation data used to calculate the net precipitation. The precipitation is corrected with respect to wind on a yearly basis and is likely not corrected against type of precipitation (snow or rain). The precipitation during snow events is many times underestimated, and it is not unusual that a correction of up to 20% is applied. Focus during the initial calibration was put on the groundwater levels, but more emphasis should preferably be put on calibration of the surface water runoff in the next model version.

The results from the base case simulation show that boreholes located underneath the lakes in the area show very good agreement between simulated and observed groundwater head elevations, with two exceptions (SFM0012 and SFM0022). The groundwater elevations are strongly affected by the lake water level fluctuations, rather than the groundwater conditions affecting the water levels in the lakes. The water levels in the lakes are influenced by a large upstream area and have a significantly larger water volume affecting the local conditions than single boreholes in the groundwater. When the water levels in the lakes are resolved properly they affect and control the conditions in the groundwater. This is true if the communication between the groundwater aquifer and the water volume in the lakes is described properly but not necessarily true for boreholes located close to the lakes and near the shorelines. For SFM0012 and SFM0022, the base case showed relatively large deviations from measured data. When increasing the contact by changing the vertical hydraulic conductivity in lake sediments near these boreholes (Sens 3), a much better agreement was reached.

The results from the analysis of parameters in the saturated zone show that an increase of the horizontal hydraulic conductivities in the soil layers, $K_{h,}$ from the base case definition generally gives a better agreement between simulated and observed data. The majority of the boreholes where an increase of K_h is positive are located on local heights or hillsides in the topography. These boreholes are not exclusively located in recharge areas as they can be part of a bigger surrounding discharge area, but still be situated on a local height within the area. Around 80% of the boreholes that showed a notable improvement with an increased horizontal conductivity are located on a local height or hillside, which indicates that K_h generally should be increased under these conditions. Exceptions from this conclusion are two boreholes located underneath lakes (SFM0022 and SFM0033), also giving better results with an increased K_h.

A reduction of the horizontal conductivity in the soil layers gives a significant improvement in three boreholes (SFM0001, SFM0021 and SFM0030). These are all located in local depressions in the topography.

For the boreholes where an increase in horizontal hydraulic conductivity in the soil layers resulted in an improved agreement with observed data, a decreased vertical conductivity results in no notable changes in absolute mean errors. For boreholes where a decrease in horizontal

conductivity is positive, a reduction of vertical conductivity results in an improvement. One conclusion from this is that a vertical conductivity slightly smaller then the horizontal generally improves the results.

When combining the different parameter setups from the sensitivity simulations Sens 1 to Sens 4, around 80% of the analyzed boreholes are resolved to an error of less than 0.3 m. Five boreholes remain with major deviations from observed data. These are:

- SFM0001, which has a relatively small amplitude in observed data (around 1.5 m), but a large error throughout the sensitivity analysis. As the error decreases with a decreased hydraulic conductivity in the soil layers, it is likely that local, more extreme changes to K_h will result in a better agreement with measured data.
- SFM0018 and SFM0019, which have relatively small amplitudes in observed groundwater elevations (around 1.5 m). These boreholes are located on a hillside towards Lake Eckarfjärden and Lake Stocksjön and the interpolated topography may cause uncertainties. The error for these boreholes decreases with a more detailed model resolution and thus topography.
- SFM0021, which has a deviation between the interpolated DEM and the actual measured surface elevation at the borehole site of around one meter.
- SFM0030, which has a deviation between the interpolated DEM and the actual measured surface elevation at the borehole site of around 1.5 m, and also large amplitude in measured groundwater elevations (around 2.5 m). As the error decreases with a decreased hydraulic conductivity in the soil layers, it is likely that local, more extreme changes to K_h will result in a better agreement with measured data.
- SFM0049, which is located outside of the candidate area. The simulated head elevations are considerably higher than the observed and the borehole is quite insensitive to any changes made in the analysis. This could be an indication that there is a more permeable zone near the surface that drains the near-surface groundwater from the borehole location. Such a layer is not described in the present model.

Changes made in the local topography in Sens 5 showed relatively small changes in the calculated head elevations or depths to phreatic surfaces. The groundwater levels tend to follow the topography.

With a model resolution of 20 m instead of 40 m, the topography is more detailed as well as the soil profile definition and distribution of vegetation parameters. Of the 27 evaluated boreholes, a higher model resolution gave a positive effect in eight boreholes, a negative effect in four boreholes and very small or no effect in the remaining boreholes. This indicates that, when optimizing reasonable computational times versus model accuracy, it is not generally a benefit to increase the model resolution.

The vegetation parameters and unsaturated zone parameters were evaluated using one column model for a borehole located in a local recharge area (SFM0010), and one model in a discharge area (SFM0017). For the vegetation parameters, the root mass distribution (A_{root} and root depth) and the crop coefficient (K_c) are the most important parameters. For the unsaturated zone, the pF-curve above water contents at field capacity is the most important. Especially the given effective porosity, more or less equivalent to the specific yield (S_y), is of importance. In principle, this holds for both the studied recharge area and the discharge area, even if the results are clearly different in the two cases. The combined effect from the three most important vegetation and unsaturated zone parameters (A_{root}, K_c, and S_y) where also tested in the full model. The results from this test verified the sensitivity to these parameters.

The head elevations in lakes, such as for SFM0015, are not influenced by parameters in the unsaturated zone or vegetation parameters, as there is no unsaturated zone present and the actual evapotranspiration equals the potential evapotranspiration. They are instead affected by

the water level fluctuation in the lake and the contact between surface- and groundwater, the horizontal and vertical conductivities in the geological soil layers and the topographic position of each lake.

A general conclusion from the sensitivity analysis is that the surrounding head elevation conditions highly affect the processes near the surface, e.g. if the boreholes are located in general recharge or discharge areas. The regional catchment and the bottom layer boundary in the model have little effect on the conditions at specific boreholes, as it is the local conditions and the local catchment that defines the recharge and discharge areas within the model domain for Forsmark.

The probable variability in the analyzed parameters is quite large when looking at a local scale. When making general changes of hydraulic conductivities over whole layers, as in the sensitivity analysis, a factor of 10 can be a reasonable variability. For smaller areas, changes up to a factor of 100 or even higher are not unrealistic. For pF-curves in the unsaturated zone, there is generally a large local variation in data. The tested extremes in the sensitivity analysis most likely cover the actual variability. This also holds for the vegetation parameters, although these are more empirical and consequently not so easily determined from field surveys.

8 Proposed calibration methodology

Based on the results and findings from the initial calibration, the definition of the present base case and the sensitivity analysis, a number of steps in model calibration are suggested, according to the following:

1. Include all available field data and local knowledge of the area when evaluating model parameters and input data used in the model setup.
2. Inspect all measured calibration data carefully with respect to accuracy and validity. For instance, seek information about how reference levels from groundwater level data are obtained, and other sources to uncertainty. Eventually, divide the calibration data into data sets, characterized by different degrees of uncertainty.
3. Make a first evaluation of initial results with respect to possible errors in physical input data, such as lake thresholds, and boundary conditions such as precipitation, temperature and potential evapotranspiration.
4. Evaluate the surface runoff to the stream network to make a rough calibration of the runoff processes. Check the general water balance for the area, i.e. Precipitation – Evaporation = Runoff + Groundwater recharge – Groundwater discharge). The governing parameters are
   - Manning's number in both MIKE 11 and the overland flow component,
   - the drain parameters if the drainage option in the saturated zone is activated,
   - if river bed sediments are present, the leakage coefficient between the stream network and the saturated zone,
   - unsaturated zone parameters,
   - vegetation parameters,
   - meteorological data.
5. Characterize deviations between measured and calculated groundwater elevations to identify systematic errors in input data and parameters, such as
   - deviations in the topographical model (DEM),
   - the communication between different model components,
   - limitations in the model code, such as evapotranspiration only being calculated in the upper calculation layer of the model.
6. Characterize deviations between measured and calculated groundwater elevations to identify specific areas and parameters that need to be systematically adjusted, such as
   - the communication between different model components and layers,
   - the influence of evapotranspiration.
7. Based on the above characterization, divide the model catchment into sub areas and make a general classification of the local topographical conditions at each borehole.
8. In order to minimize deviations between calculated and measured groundwater elevations, make a parameter analysis of the governing parameters for each area. Based on the results in chapters 6 and 7, it is concluded that the parameter analysis should focus on the following parameters within each area, preferably in this order:
   - The horizontal hydraulic conductivity in the saturated zone. Results from the sensitivity analysis indicate that the horizontal conductivity generally should be increased at topographic heights and reduced at local depressions in the topography.

- The vertical hydraulic conductivity in the saturated zone. The results of the sensitivity analysis indicate that no changes should be made where the horizontal hydraulic conductivity has been increased, and that the vertical hydraulic conductivity generally should be decreased where the horizontal hydraulic conductivity has been decreased.
- The communication between groundwater and surface water, such as the vertical hydraulic conductivity of lake sediments. At locations where this communication is too small, the vertical hydraulic conductivity of clayey sediments should be increased.
- The vegetation parameters that most affect the total groundwater recharge are the root mass distribution and the crop coefficient.
- The unsaturated zone parameter that most affects the total groundwater recharge is the effective porosity, as given in the pF-curve. In addition, the shape of the pF-curve above the water content at field capacity is also of great importance.

9 References

Bosson E, Berglund S, 2006. Near-surface hydrogeological model of Forsmark. Open repository and solute transport applications – Forsmark 1.2. SKB R-06-52, Svensk Kärnbränslehantering AB.

DHI Software, 2007. MIKE SHE – User Manual. DHI Water & Environment, Hørsholm, Denmark.

Eriksson B, 1981. Den potentiella evapotranspirationen i Sverige. SMHI Rapport RMK 28 (in Swedish).

Juston J, Johansson P-O, Levén J, Tröjbom M, Follin S, 2006. Analysis of meteorological, hydrological and hydrogeological monitoring data. SKB R-06-49, Svensk Kärnbränslehantering AB.

Kristensen, K J, Jensen S E, 1975. A model for estimating actual evapotransipration from potential evapotranspiration. Royal Veterinary and Agricultural Univerisity, Nordic Hydrology 6, pp. 170–188.

Lundin L, Stendahl J, Lode E, 2005. Forsmark site investigation. Soils in two large trenches. SKB P-05-166, Svensk Kärnbränslehantering AB.

SKB, 2004. Preliminary site description. Forsmark area – version 1.1. SKB R-04-15, Svensk Kärnbränslehantering AB.

Svensson U, Kuylenstierna H-O, Ferry M, 2004. DarcyTools, Version 2.1. Concepts, methods, equations and demo simulations. SKB R-04-19, Svensk Kärnbränslehantering AB.

Werner K, Bosson E, Berglund S, 2005. Description of climate, surface hydrology, and near-surface hydrogeology. Simpevarp 1.2. SKB R-05-04, Svensk Kärnbränslehantering AB.